Proceedings of SuperB Workshop VI: New Physics at the Super Flavor Factory

Hitlin, DG; Cheng, CH; Asner, DM; Hurth, T; McElrath, B; Shindou, T; Ronga, F; Rama, M; Simi, STG; Robertson, S; Paradisi, P; Bigi, I; Stocchi, A; Viaud, B; Domingo, F; Kou, E; Morandin, M; Batignani, G; Cervelli, A; Forti, F; Neri, N; Walsh, J; Giorgi, M; Isidori, G; Lusiani, A; Bevan, A; Faccini, R; Renga, F; Polosa, A; Silvestrini, L; Virto, J; Ciuchini, M; Heinemeyer, S; Carpinelli, M; Gambino, P; Azzolini, V; Bernabeu, J; Botella, F; Branco, GC; March, NL; Vidal, FM; Oyanguren, A; Pich, A; Lozano, MAS; Vidal, J; Vives, O; Banerjee, S; Roney, JM; Gershon, T

Proceedings
of
Super$B$ Workshop VI

New Physics
at the
Super Flavor Factory

Valencia, Spain

January 7-15, 2008

Abstract

The sixth Super$B$ Workshop was convened in response to questions posed by the INFN Review Committee, evaluating the Super$B$ project at the request of INFN. The working groups addressed the capability of a high-luminosity flavor factory that can gather a data sample of 50 to 75 ab^{-1} in five years to elucidate New Physics phenomena unearthed at the LHC. This report summarizes the results of the Workshop.

D.G. Hitlin and C.H. Cheng

California Institute of Technology, Pasadena, California 91125, USA

D.M. Asner

Carleton University, Ottawa, Ontario, Canada K1S 5B6

T. Hurth and B. McElrath

CERN, CH-1211 Geneve 23, Switzerland

T. Shindou

DESY, D-22603 Hamburg, Germany

F. Ronga

ETH, CH-8093 Zurich, Switzerland

M. Rama

INFN, Laboratori Nazionali di Frascati, Frascati, Italy

S. Tosi

Università di Genova, Dipartimento di Fisica and INFN, I-16146 Genova, Italy

G. Simi

University of Maryland, College Park, Maryland 20742, USA

S. Robertson

McGill University, Montrèal, Québec, Canada H3A 2T8

P. Paradisi

Technische Universität Munchen, D-85748 Garching, Germany

I. Bigi

University of Notre Dame, Notre Dame, Indiana 46556, USA

A. Stocchi and B. Viaud

Laboratoire de lAccélèrateur Linèaire, IN2P3/CNRS et Université de Paris-Sud XI,
Centre Scientifique dOrsay, F-91898 Orsay Cedex, France

F. Domingo and E. Kou

Laboratoire de Physique Theorique, Université de Paris-Sud XI, F-91405 Orsay Cedex, France

M. Morandin

Università di Padova, Dipartimento di Fisica and INFN, I-35131 Padova, Italy

G. Batignani, A. Cervelli, F. Forti, N. Neri, and J. Walsh

Università di Pisa, Dipartimento di Fisica, Scuola Normale Superiore and INFN, I-56127 Pisa, Italy

M. Giorgi, G. Isidori, and A. Lusiani

Università di Pisa, Dipartimento di Fisica,
Scuola Normale Superiore and INFN, I-56127 Pisa, Italy
and INFN, Pisa, Italy

A. Bevan

Queen Mary, University of London, E1 4NS, United Kingdom

R. Faccini and F. Renga

Università di Roma "La Sapienza" and INFN Roma, I-00185 Roma, Italy

A. Polosa, L. Silvestrini, and J. Virto

INFN Roma, I-00185 Roma, Italy

M. Ciuchini

INFN Roma Tre, I-00146 Roma, Italy

S. Heinemeyer

Universitat de Cantabria, E-39005 Santander, Spain

M. Carpinelli

Università di Sassari and INFN, Sassari, Sardinia, Italy

P. Gambino

Universtà di Torino and INFN, I-1015 Torino, Italy

V. Azzolini, J. Bernabéu, F. Botella, G. C. Branco, N. Lopez March, F. Martinez Vidal,
A. Oyanguren, A. Pich, M. A. Sanchis Lozano, J. Vidal, and O. Vives

IFIC, Universitat de Valencia-CSIC, E-46071 Valencia, Spain

S. Banerjee and J. M. Roney

University of Victoria, Victoria, British Columbia, Canada V8W 3P6

T. Gershon

University of Warwick, Coventry, CV4 7AL, United Kingdom

Introduction

The Sixth SuperB Workshop, held at the IFIC in Valencia, Spain from January 7-15, 2008, was convened to update our understanding of the physics capabilities of the SuperB project, proposed for construction on the campus of Rome University Tor Vergata. In particular, the Workshop addressed several questions posed by members of the International Review Committee appointed by INFN to review the project. The workshop was organized into several working groups; this document comprises the reports from these groups. It is not intended as a comprehensive review of the physics capability of SuperB; rather, it should be read as a supplement to the physics section of the SuperB Conceptual Design Report (CDR)[1].

The motivation for undertaking a new generation of e^+e^- experiments is, of course, to measure effects of New Physics on the decays of heavy quarks and leptons. A detailed picture of the observed pattern of such effects will be crucial to gaining an understanding of any New Physics found at the LHC. As detailed herein, much of the study of the capability of the LHC to distinguish between, for example, models of supersymmetry breaking have emphasized information accessible at high p_T. Many of the existing constraints on models of New Physics, however, come from flavor physics. Improving limits and teasing out new effects in the flavor sector will be just as important in constraining models after New Physics has been found as it has been in the construction of viable candidate models in the years before LHC operation.

In confronting New Physics effects on the weak decays of b, c quarks and τ leptons it is crucial to have the appropriate experimental sensitivity. The experiment must measure CP asymmetries in very rare decays, rare branching fractions and interesting kinematic distributions to sufficient precision to make manifest the expected effects of New Physics, or to place constraining limits. There is a strong consensus in the community that doing so requires a data sample corresponding to an integrated luminosity of 50 to 100 ab^{-1}. There is also a consensus that a reasonable benchmark for obtaining such a data sample is of the order of five years of running. Meeting both these constraints requires a collider luminosity of 10^{36} cm^{-2}s^{-1} or more, yielding 15 ab^{-1}/Snowmass Year of 1.5×10^7 seconds. It is these boundary conditions that set the luminosity of SuperB.

Reaching this luminosity with a collider design extrapolated from PEP-II or KEKB, such as SuperKEKB, is difficult; beam currents and thus power consumption are very high, and the resulting detector backgrounds are formidable. The low emittance, crabbed waist design of SuperB provides an elegant solution to the problem; SuperB can reach unprecedented luminosity with beam currents and power consumption comparable to those at PEP-II . A test of the crabbed waist concept is underway at Frascati; it is proceeding very well, producing impressive increases in the specific luminosity at DAΦNE. More remains to be done, but the results are very encouraging.

It is important that results with sensitivity to New Physics be obtained in a timely way, engendering a "conversation" with the LHC experiments. SuperB can confidently be expected to produce a very large data sample before the end of the next decade. The more gradual SuperKEKB approach to achieving high peak luminosity cannot produce comparable data samples until close to the end of the following decade [2].

τ physics will likely assume great importance as a probe of physics beyond the Standard Model. SuperB includes in the baseline design an 85% longitudinally polarized electron beam and spin rotators to facilitate the production of polarized τ pairs. This polarization is the key to the study of the structure of lepton-flavor-violating couplings in τ decay, as well as the search for a τ EDM, or for CP violation in τ decay. SuperKEKB does not incorporate a polarized beam.

The recent observation of large $D^0\overline{D}^0$ mixing raises the exciting possibility of finding CP violation in charm decay, which would almost certainly indicate physics beyond the Standard Model. SuperB can attack this problem in a comprehensive manner, with high luminosity data sample in the $\Upsilon(4S)$ region and at the $\psi(3770)$ resonance, as the collider is designed to run at lower center-of-mass energies, at reduced luminosity. With very short duration low energy runs, a data sample an order of magnitude greater than that of the final BES-III sample can readily be obtained. SuperKEKB cannot run at low energies.

The following is a brief resumé of the capabilities of SuperB. In some instances, comparisons are made between physics results that can be obtained with the five year, 75 ab^{-1} SuperB sample and a 10 ab^{-1} sample such as could perhaps be obtained in the first five years of running of SuperKEKB. More detailed discussions will be found in the ensuing sections.

B Physics

B physics remains a primary objective of SuperB. With BABAR and Belle having clearly established the ability of the CKM phase to account for CP-violating asymmetries in tree-level $b \rightarrow c\bar{c}s$ decays, the focus shifts to the study of very rare processes. With a SUSY mass scale below 1 TeV, New Physics effects

in *CP*-violating asymmetries, in branching fractions and kinematic distributions of penguin-dominated decays and in leptonic decays can indeed be seen in the five-year Super*B* data sample.

TABLE I: Comparison of current experimental sensitivities with a 10 ab^{-1} sample and the five year Super*B* 75 ab^{-1} sample. Only a small selection of observables are shown. Quoted sensitivities are relative uncertainties if given as a percentage, and absolute uncertainties otherwise. An "X" means that the quantity is not measured at this integrated luminosity. For more details, see text and Refs. [1, 3, 4].

Mode	Sensitivity		
	Current	10 ab^{-1}	75 ab^{-1}
$\mathcal{B}(B \to X_s\gamma)$	7%	5%	3%
$A_{CP}(B \to X_s\gamma)$	0.037	0.01	0.004–0.005
$\mathcal{B}(B^+ \to \tau^+\nu)$	30%	10%	3–4%
$\mathcal{B}(B^+ \to \mu^+\nu)$	X	20%	5–6%
$\mathcal{B}(B \to X_s l^+ l^-)$	23%	15%	4–6%
$A_{\mathrm{FB}}(B \to X_s l^+ l^-)_{s_0}$	X	30%	4–6%
$\mathcal{B}(B \to K\nu\overline{\nu})$	X	X	16–20%
$S(K^0_S\pi^0\gamma)$	0.24	0.08	0.02–0.03

Table I shows a quantitative comparison of the two samples for some of the important observables that will be measured at Super*B*, including all the so-called "golden processes" of Table II (see the following section). We list below some additional comments on the entries of Table I

- The measurements of $\mathcal{B}(B \to X_s\gamma)$ and $\mathcal{B}(B^+ \to \ell^+\nu)$ are particularly important in minimal flavor violation scenarios. It is crucial to be able to search for small deviations from the Standard Model value. Therefore the improvement is sensitivity provided by Super*B* is highly significant (see Figure 5).

- A 10 ab^{-1} sample is not sufficiently large to take advantage of the theoretical cleanliness of several inclusive observables, such as the zero-crossing of the forward-backward asymmetry in $b \to s\ell^+\ell^-$. Results with 10 ab^{-1} would not match the precision from the exclusive mode $B \to K^*\mu^+\mu^-$, which will be measured by LHC*b*. Furthermore, these exclusive channel measurements will be limited by hadronic uncertainties. Super*B* can provide a much more precise and theoretically clean measurement using inclusive modes.

- Several interesting rare decay modes, such as $B \to K\nu\bar{\nu}$, cannot be observed with the statistics of 10 ab^{-1}, unless dramatic and unexpected New Physics enhancements are present. Preliminary studies are underway on several other channels

in this category, such as $B \to \gamma\gamma$ and $B \to$ invisible decays which are sensitive to New Physics models with extra-dimensions.

- Another area for comparison is the phenomenological analysis within the MSSM with generic mass insertion discussed in the Super*B* CDR. Fig. 1 shows how well the $(\delta_{13})_{LL}$ can be reconstructed at Super*B* and with 10 ab^{-1}. Improvements in lattice QCD performance, as discussed in the Appendix of the CDR, are assumed in both cases. The remarkable difference in sensitivity stems mainly from the different performance in measuring the CKM parameters $\bar{\rho}$ and $\bar{\eta}$.
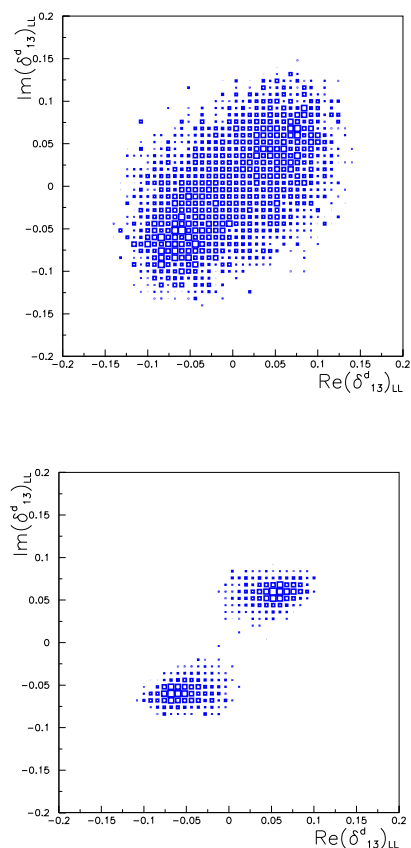

FIG. 1: Determination of the SUSY mass-insertion parameter $(\delta_{13})_{LL}$ with a 10 ab^{-1} sample (top) and with Super*B* (bottom).

Charm Physics

The influence of New Physics on the charm sector is often overlooked. Constraints on flavor-changing neutral currents from new physics in the up quark sector are much weaker than in the down quark sector. Thus

high sensitivity studies of rare charm decays offer the possibility of isolating New Physics effects in $D^0\overline{D}^0$ mixing, in CP violation and in rare decay branching fractions.

The recent observation of substantial $D^0\overline{D}^0$ mixing raises the very exciting possibility of measuring CP violation in charm decays. Many of the most sensitive measurements remain statistics limited even with Super$B$ size data samples, providing a substantial motivation for gathering 75 ab^{-1}.

In several specific cases, CP violation in mixing can be studied more precisely by taking advantage of the clean environment provided by exclusive $D^0\overline{D}^0$ production at the $\psi(3770)$ resonance. We have therefore included in the Super$B$ design the unique capability of running at this center-of mass-energy. Long data-taking runs are not required; a run of two months duration at the $\psi(3770)$ would yield a data sample an order of magnitude larger than the total BES-III sample at that energy.

Tau Physics

It is not unlikely that the most exciting results on New Physics in the flavor sector at Super$B$ will be found in τ decays. With 75 ab^{-1} Super$B$ can cover a significant portion of the parameter space of most New Physics scenarios predictions for lepton flavor violation (LFV) in tau decays.

The sensitivity in radiative processes such as $\mathcal{B}(\tau \to \mu\gamma)$ (2×10^{-9}) and in $\mathcal{B}(\tau \to \mu\mu\mu)$ decays (2×10^{-10}) gives Super$B$ a real chance to observe these LFV decays. These measurements are complementary to searches for $\mu \to e\gamma$ decay. In fact, the ratio $\mathcal{B}(\tau \to \mu\gamma)/\mathcal{B}(\mu \to e\gamma)$ is an important diagnostic of SUSY-breaking scenarios. If LFV decays such us $\tau \to \mu\gamma$ and $\tau \to \mu\mu\mu$ are found, the polarized electron beam of Super$B$ provides us with a means of determining the helicity structure of the LFV coupling, a most exciting prospect. The polarized beam also provides a novel additional handle on backgrounds to these rare processes.

The longitudinally polarized high energy ring electron beam, which is a unique feature of Super$B$, is also the key to searching for CP violation in tau production or decay. An asymmetry in production would signal a τ EDM, with a sensitivity of $\sim 10^{-19}$ ecm, while an unexpected CP-violating asymmetry in decay would be a clear signature of New Physics.

The polarized beam and the ability to procure a data sample of sufficient size to find lepton flavor-violating events, as opposed to setting limits on LFV processes are unique to Super$B$.

Spectroscopy

One of the most surprising results of the past decade has been the plethora of new states with no ready quark model explanation by the B Factories and the Tevatron. These states clearly indicate the existence of exotic combinations of quarks and gluons into hybrids, molecules or tetraquarks.

These studies, which promise to greatly enhance our understanding of the non-perturbative regime of QCD, are at an early stage. Many new states have been found. These may be combinations involving light quarks or charmed quarks, but only in the case of the $X(3872)$ have there been observations of more than a single decay channel. It is crucial to increase the available statistics by of the order of one hundred-fold in order to facilitate searches for additional decay modes. In the case of the $X(3872)$ state, for example, it is particularly critical to observe both decays to charmonium and to D or D_s^+ pairs, the latter having very small branching fractions. It is also important to provide enhanced sensitivity to search for additional states, such as the neutral partners of the $Z(4430)$.

Bottomonium studies are quite challenging, since the expected but not yet observed states are often broad and have many decay channels, thus requiring a large data sample. Leptonic decays of bottomonium states also provide, through lepton universality tests, a unique window on New Physics.

Data samples adequate for these studies, which in some cases require dedicated runs of relatively short duration, in both the 4 and 10 GeV regions, are obtainable only at Super$B$.

[1] M. Bona *et al.*, arXiv:0709.0451 [hep-ex].

[2] Y. Ohnishi, SuperKEKB Meeting, Atami, Izu, Japan, January 24-26, 2008. See also K. Kinoshita, BEACH 2008, Columbia, SC, June 23-28, 2008.

[3] T. Browder, M. Ciuchini, T. Gershon, M. Hazumi, T. Hurth, Y. Okada and A. Stocchi, JHEP **0802** (2008) 110 [arXiv:0710.3799 [hep-ph]].

[4] T. E. Browder, T. Gershon, D. Pirjol, A. Soni and J. Zupan, arXiv:0802.3201 [hep-ph].

B Physics

The physics case for Super$B$ has been discussed in some detail in the Super$B$ Conceptual Design Report (henceforth CDR) [1]. In the CDR, and in the following, we consider the discovery potential of Super$B$ in two scenarios: whether or not the LHC finds evidence for New Physics.

LHC discovers new particles

If the LHC finds physics beyond the Standard Model, the essential, and unique, role of Super$B$ will be to determine the flavor structure of the New Physics. In that sense, measurements from Super$B$ that are consistent with the Standard Model are as valuable as those that show significant deviations – in either case these measurements provide information about the New Physics flavor structure that cannot be provided by other experiments. In this context, the measurement of theoretically clean rare decays, even when found to be Standard Model-like, will yield valuable insights into the structure of New Physics models, providing information complementary to LHC results.

It is, of course, generally regarded as more valuable to find deviations from Standard Model predictions than to find a result that agrees with the Standard Model. In fact, many New Physics flavor structures do produce measurable effects. As shown in the discussion on benchmark points below, there are also scenarios in which flavor effects can be very small, and perhaps barely visible, even with Super$B$. The great precision reached at Super$B$ can still provide positive information on the underlying theory, even in a Standard Model-like flavor scenario. Indeed, we emphasize that measurement of the New Physics flavor couplings are the primary discovery goal of Super$B$; results from both LHC and Super$B$ are required to reconstruct the New Physics Lagrangian.

There is no New Physics discovery at LHC

If evidence for New Physics does not readily appear at LHC, the goal of Super$B$ would then be to emphasize measurement precision to search for deviations in flavor observables. In this scenario, finding such small effects could provide the first evidence of New Physics! The absence of knowledge about the New Physics scale from LHC would make it impossible to reconstruct the New Physics Lagrangian, but a New Physics discovery at Super$B$ would provide a solid indication that the New Physics scale is only slightly above the reach of LHC.

The chapter is organized as follows. We first present a description of work done since the writing of the CDR [1], concentrating on some particularly interesting channels that were only partially covered or not covered at all. We then update the phenomenological studies presented in the CDR, including a classification of golden modes, performance at LHC benchmark points, the impact of Super$B$ on explicit models of SUSY breaking, and a brief discussion on the interplay of flavor and high p_T physics. We concentrate on B physics at the $\Upsilon(4S)$, since we have little to add to previous studies of the potential for B_s physics at the $\Upsilon(5S)$ [2].

1. Studies of selected B decay channels

In this section we present new studies on a selected set of B meson decay channels, updating the determination of the following processes:

The CKM matrix element $|V_{ub}|$. This measurement, crucial to the model-independent determination of the CKM matrix, can only be done at an e^+e^- machine. We update the calculation of the Super$B$ reach, as suggested by the International Review Committee.

The rare branching fractions $\mathcal{B}(B \to X_s\gamma)$, $\mathcal{B}(B \to X_s\ell^+\ell^-)$. These channels were not thoroughly studied in the CDR, as they are limited by experimental and theoretical systematic uncertainties. In the CDR we concentrated on other observables, such as the photon polarization and CP and isospin asymmetries. However $\mathcal{B}(B \to X_s\gamma)$, at present one of the most powerful New Physics probes, remains a powerful constraint, even in the Minimal Flavor Violation case. We have therefore reassessed the experimental and theoretical sensitivities for these modes at Super$B$. We have also done a preliminary sensitivity study for $B \to K^{(*)}\tau^+\tau^-$.

The branching fraction $\mathcal{B}(B \to X_s\nu\overline{\nu})$. A new detailed study has been performed on this mode, evaluating the possibility of measuring the branching fraction with the full Super$B$ data sample. This information complements the measurements of $B \to X_s\gamma$ and $B \to X_s\ell^+\ell^-$ in accessing New Physics that can contribute to $\Delta B = 1$ box, photon penguin, and Z^0 penguin diagrams.

Leptonic decay modes. The precise measurement of $\mathcal{B}(B \to \ell\nu)$ is particularly interesting in New Physics scenarios with a charged Higgs at high $\tan\beta$. Following the suggestion of the IRC, we discuss possible improvements in signal efficiency and systematic

uncertainties at Super$B$. We also present a new study of radiative leptonic decays and some discuss considerations relevant to LFV modes.

Precise determination of the CKM element $|V_{ub}|$

The precise measurement of $|V_{ub}|$ is a crucial ingredient in the determination of the CKM parameters $\bar{\rho}$ and $\bar{\eta}$ in the presence of New Physics. At the time Super$B$ commences operation, LHCb will have already provided precise measurements of $\sin 2\beta$ and γ. This will allow for an improved determination of CKM parameters within the Standard Model. However, in the presence of generic New Physics contributions, this information alone is not sufficient to obtain the same precision. As precise information on CKM parameters is essential for any New Physics flavor analysis in the K and B sectors, an improved determination of $|V_{ub}|$ turns out to be quite important in New Physics searches.

The precise study of both inclusive and exclusive B semileptonic branching fractions is a unique feature of Super$B$.

Inclusive decays

The current 5–10% theoretical error on the inclusive determination of $|V_{ub}|$ is due mainly to uncertainties in the b quark mass, in weak annihilation (WA) contributions, in missing higher order perturbative corrections, and in the modeling of the shape functions.

At the time Super$B$ takes data, new calculations should decrease the perturbative error, and lattice calculations, together with improved analyses of $e^+e^- \to$ hadrons and measurements of the moments of semileptonic and radiative B decay spectra should provide better determinations of m_b; a precision of 20 MeV on m_b is possible. Weak annihilation contributions are relevant only at high q^2, and can be efficiently constrained by studying the q^2 spectrum. The shape functions can also be better-constrained by studies of the $B \to X_u \ell \nu$ spectra, but their importance will decrease as the measurements become increasingly more inclusive. A pioneering analysis in this area has recently been published by BABAR [3]. In this analysis the M_X cut is raised to values for which the shape function sensitivity becomes negligible. Such measurements are not competitive now, but the situation will be quite different at Super$B$.

As a result, we expect the theoretical uncertainty on the inclusive determination of $|V_{ub}|$ to eventually be dominated by the uncertainty in the b quark mass. In this respect, it should be stressed that in current analyses, $|V_{ub}|$ depends quite strongly on the precise value of m_b. Typically, for a cut of $M_X < 1.7$ GeV,

the relative error on V_{ub} scales as $4(\delta m_b)/m_b$. Currently, with $\delta m_b = 40$ MeV, the error induced on V_{ub} is about 3.5%. If the error on m_b were halved, $|V_{ub}|$ extracted in this way would have a parametric uncertainty below 2%. However, the presence of the M_X cut increases the sensitivity to m_b, because the distribution functions also strongly depend on m_b. Increasing the M_X cut (as mentioned above) reduces the sensitivity to m_b. Indeed, the total rate is proportional to m_b^5, and for a totally inclusive measurement one has $\delta V_{ub}/V_{ub} \simeq 2.5(\delta m_b)/m_b$. Therefore, if one could measure the total $B \to X_u \ell \nu$ rate, the uncertainty induced by $\delta m_b = 20$ MeV on $|V_{ub}|$ would be only 1%.

A promising way to deal with the large $B \to X_c \ell \nu$ backgrounds with no cut on the inclusive $B \to X_u \ell \nu$ decays phase space is to reconstruct the semileptonic decays in the recoil against the other B fully reconstructed in a hadronic final state in $e^+e^- \to \Upsilon(4S) \to B\bar{B}$ events (the so-called "hadronic tag technique"). This technique provides full knowledge of the event, including the flavor of the B, and allows the precise reconstruction of the neutrino four-momentum, significantly improving background rejection against, for example. events with several neutrinos or with one or more K_L mesons. At present, these measurements are limited by low signal efficiency, and have large statistical uncertainty. At Super$B$ however, the statistical uncertainty will be less than $\sim 1\%$. The leading systematic errors will also be reduced: those due to detector effects could reach 2% using the large data control samples available. The current analyses have uncertainties due to $B \to X_c \ell \nu$ background (branching fractions and form factors) as low as 4% – it is possible to reduce this by a factor of two. Indeed, higher statistics and improvements in the detector and analysis will yield better measurements of these quantities. Moreover, the enhanced hermeticity and superior vertexing capability of the Super$B$ detector will further improve background rejection through more precise neutrino reconstruction and the detection of the displaced D meson vertex. A total experimental uncertainty on $|V_{ub}|$ of approximately 2–3% can thus be achieved with this method.

Combined with the theoretical uncertainty discussed above, an overall precision of 3% on the determination of $|V_{ub}|$ using inclusive $B \to X_u \ell \nu$ decays at Super$B$ will be possible.

Exclusive decays

The measurement of $|V_{ub}|$ using exclusive decays is presently limited by theoretical uncertainties on the form factors (about 12%). Lattice calculations are expected to improve significantly in the next five years, mainly due to an increase of available computing power. Results from these calculations will decrease

the uncertainty to approximately 2–3% in the case of the most promising decay $B \to \pi \ell \nu$ (see the Appendix of the CDR [1]).

Using the hadronic tag approach (as in Refs. [4, 5]), the statistical uncertainty on $|V_{ub}|$ will be below 1%. This measurement being almost background-free, the systematic uncertainties are dominated by detector effects, and should be of the order of 2%. A total experimental uncertainty of 2–3% on $|V_{ub}|$ can thus be achieved, leading to an overall precision as good as 3–4%.

These figures basically confirm the sensitivities presented in the CDR for the measurement of $|V_{ub}|$.

Rare radiative decays

The branching fraction $\mathcal{B}(B \to X_s \gamma)$

The inclusive branching fraction $\mathcal{B}(B \to X_s \gamma)$ has been measured at the B factories [6, 7, 8, 10**?**]; the current experimental world average is [11]:

$$\mathcal{B}(B \to X_s \gamma)|_{E_\gamma > 1.6 \ \text{GeV}} = (3.55 \pm 0.26) \times 10^{-4} \,.$$

The 7% error on the branching fraction is a mixture of statistical, systematic and theoretical contributions, where the latter comes primarily from extrapolating the partial branching fraction, typically measured for photon energies above 1.9 GeV, down to the value of 1.6 GeV used for the theoretical prediction.

Several different experimental approaches have been pursued to make a measurement of the inclusive $B \to X_s \gamma$ branching fraction. The approach that yields the most precise measurement depends on the available statistics. Untagged inclusive analyses, in which only the high-momentum photon is reconstructed, have been carried out at B factories, but are limited by systematic errors that will make them uncompetitive in the Super$B$ era. Similarly, the semi-inclusive approach, which attempts to reconstruct as many exclusive modes as possible, and then applies a correction due to the missing rate, is already limited by the X_s fragmentation properties, *i.e.*, by uncertainty in the estimate of the fraction of the total rate that is not reconstructed. This systematic uncertainty amounts to about 15% on the branching ratio [**?**]. More detailed studies are needed to evaluate how much this systematic could be reduced with the statistics available at Super$B$.

The most promising approaches for Super$B$ are those that make use of recoil analysis, in which the "other B" in the $B\bar{B}$ event is tagged in either a semileptonic or hadronic decay. This allows backgrounds to be reduced to acceptable levels without putting constraints on the X_s system. The most recent semileptonic tag analysis [10] currently has comparable statistical and systematic uncertainties (about 8% each), but a sizable portion of the systematic uncertainty is actually statistical in nature, since it depends on the size of control samples derived from the data. The current systematic uncertainty of the hadronic tagged analysis [12] is larger, but it seems probable that refinements to this relatively new technique will be able significantly to reduce the systematic error.

With the data sample of Super$B$, all approaches will be systematics-limited. We estimate that the hadronic and semileptonic tagged analyses will be able to reduce systematic uncertainties to about 4–5%. Since the systematics are mostly uncorrelated, the combined branching fraction can be expected to have a systematic error of around 3%.

The Standard Model prediction of $\mathcal{B}(B \to X_s \gamma)$ for $E_\gamma > 1.6$ GeV is

$$\mathcal{B}(B \to X_s \gamma)|_{E_\gamma > 1.6 \ \text{GeV}} = \begin{cases} (3.15 \pm 0.23) \times 10^{-4} & [13] \\ (2.98 \pm 0.26) \times 10^{-4} & [14]. \end{cases}$$

The two predictions differ in their use of resummation of log-enhanced terms which are included in the result of [14]. There is no consensus on the consistency of the resummed result [15]. We therefore quote both predictions pending clarification. For both results, the overall uncertainty consists of non-perturbative (5%), parametric (3%), higher-order (3%) and m_c-interpolation (3%), which have been added in quadrature.

There are other perturbative NNLL corrections that are not yet included in the present NNLL estimate, but are expected to be smaller than the current uncertainty, producing a shift of the central value of about 1.6%.

While the uncertainties due to the input parameters and due to the m_c interpolation could be further reduced, the perturbative error of 3% will remain until a new major effort to compute the NNNLO is carried out. However, the theoretical prediction has now reached the non-perturbative boundaries. The largest uncertainty is presently due to nonperturbative corrections that scale with $\alpha_s \Lambda_{\text{QCD}}/m_b$. A local expansion is not possible for these contributions; it is not clear if the corresponding uncertainty of 5% (based on a simple dimensional estimate) can be reduced. Recently, a specific piece of these additional nonperturbative corrections has been estimated [16], and found to be consistent with the dimensional estimate. It is also included in the prediction of Ref. [14].

Two explicit examples should demonstrate the stringent constraints that can, with these uncertainties,

be derived from the measurement of the $B \to X_s\gamma$ branching fractions.

Fig. 2 shows the dependence of $\mathcal{B}(B \to X_s\gamma)$ on the charged Higgs mass in the 2-Higgs-doublet model (2HDM-II) [13]. The bound on $M_{H+} = 295$ GeV at

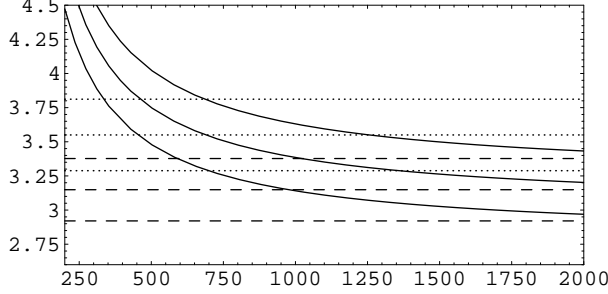FIG. 2: $\mathcal{B}(B \to X_s\gamma) \times 10^{-4}$ as a function of the charged Higgs boson mass M_{H+} (GeV) in the 2HDM II for $\tan\beta = 2$ (solid lines). Dashed and dotted lines show the Standard Model and experimental results, respectively.

95% CL, shown in Fig. 2, is currently the strongest available lower limit on the charged Higgs mass.

Similarly, the bound on the inverse compactification radius of the minimal universal extra dimension model (mACD) derived from $\mathcal{B}(B \to X_s\gamma)$ [17] is $1/R > 600$ GeV at 95% confidence level, as shown in Fig. 3.
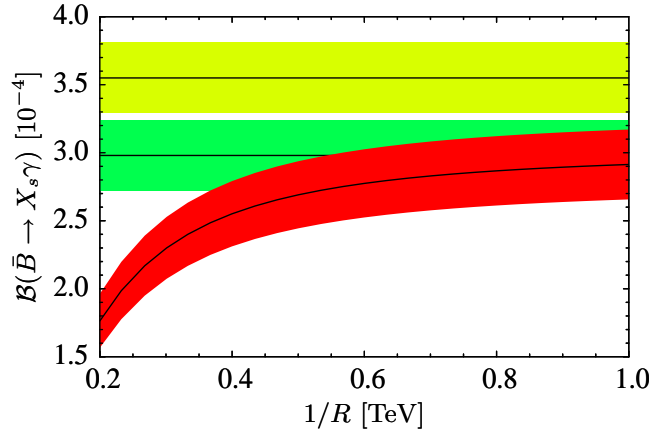

FIG. 3: Branching fraction for $E_0 = 1.6\,GeV$ as a function of $1/R$. The red (dark gray) band corresponds to the LO mUED result. The 68% CL range and central value of the experimental/Standard Model result is indicated by the yellow/green (light/medium gray) band underlying the straight solid line.

$B \to X_s\ell^+\ell^-$ *decay modes*

The decay $B \to X_s\ell^+\ell^-$ is particularly important to the Super$B$ physics programme, due to the sensi-

tivity to New Physics effects on kinematic observables, such as the dilepton invariant mass spectrum and the forward–backward asymmetry A_{FB}.

In the $B \to X_s\ell^+\ell^-$ system, one has to remove contributions from $c\bar{c}$ resonances that appear as large peaks in the dilepton invariant mass spectrum, by appropriate kinematic cuts. It is conventional to define "perturbative windows" with $s = q^2/m_b^2$ away from charmonium resonances, namely the low dilepton-mass region 1 GeV $< q^2 < 6$ GeV and the high dilepton-mass region with $q^2 > 14.4$ GeV. In these windows theoretical predictions for the invariant mass spectrum are dominated by the perturbative contributions; a theoretical precision of order 10% is, in principle, possible.

In the following, we collect the most accurate predictions for observables in $B \to X_s\mu^+\mu^-$ decay. Formulae for the electron case should be modified to take into account the experimental resolution for collinear photons.

The value of the dilepton invariant mass q_0^2, for which the differential asymmetry A_{FB} vanishes, is one of the most precise predictions in flavor physics, with a theoretical uncertainty of order 5% [18]:

$$
\begin{aligned}
(q_0^2)_{\mu\mu} &= \Big[3.50 \pm 0.10_{\text{scale}} \pm 0.002_{m_t} \pm 0.04_{m_c,C} \\
&\quad \pm 0.05_{m_b} \pm 0.03_{\alpha_s(M_Z)} \pm 0.001_{\lambda_1} \pm 0.01_{\lambda_2}\Big] \text{GeV}^2 \\
&= (3.50 \pm 0.12)\,\text{GeV}^2 .
\end{aligned} \tag{1}
$$

This accuracy cannot be reached with the analogous exclusive observable in $B \to K^*\ell^+\ell^-$, due to the unknown Λ_{QCD}/m_b corrections.

The latest update of the dilepton mass spectrum, integrated over the low and the high dilepton invariant mass region in the muonic case, leads respectively to [19]:

$$
\begin{aligned}
\mathcal{B}_{\mu\mu}^{\text{low}} &= \Big[1.59 \pm 0.08_{\text{scale}} \pm 0.06_{m_t} \pm 0.024_{C,m_c} \\
&\quad \pm 0.015_{m_b} \pm 0.02_{\alpha_s(M_Z)} \pm 0.015_{\text{CKM}} \pm 0.026_{\text{BR}_{sl}}\Big] \times 10^{-6} \\
&= (1.59 \pm 0.11) \times 10^{-6}
\end{aligned} \tag{2}
$$

and

$$
\begin{aligned}
\mathcal{B}_{\mu\mu}^{\text{high}} &= 2.40 \times 10^{-7}\Big(1 + \big[{}^{+0.01}_{-0.02}\big]_{\mu_0} + \big[{}^{+0.14}_{-0.06}\big]_{\mu_b} \pm 0.02_{m_t} \\
&\quad + \big[{}^{+0.006}_{-0.003}\big]_{C,m_c} \pm 0.05_{m_b} + \big[{}^{+0.0002}_{-0.001}\big]_{\alpha_s} \pm 0.002_{\text{CKM}} \\
&\quad \pm 0.02_{\text{BR}_{sl}} \pm 0.05_{\lambda_2} \pm 0.19_{\rho_1} \pm 0.14_{f_s} \pm 0.02_{f_u}\Big) \\
&= 2.40 \times 10^{-7}\,\big(1\,{}^{+0.29}_{-0.26}\big) .
\end{aligned} \tag{3}
$$

In the high s region, the uncertainties are larger, due to the breakdown of the heavy-mass expansion at the endpoint. However the uncertainties can be significantly reduced by considering quantities normalized

to the semileptonic $b \to u\ell\nu$ rate integrated over the same s interval [20]:

$$\mathcal{R}(s_{\min}) = \frac{\int_{s_{\min}}^{1} ds \frac{d\Gamma(B \to X_s \ell^+ \ell^-)}{ds}}{\int_{s_{\min}}^{1} ds \frac{d\Gamma(B \to X_u \ell\nu)}{ds}} . \qquad (4)$$

The numerical analysis shows that the uncertainties due $\mathcal{O}(1/m_b)$ power corrections which correspond to the parameters λ_2, ρ_1, $f_u^0 + f_s$ and $f_u^0 - f_s$ are now under control [18]:

$$\begin{aligned}
\mathcal{R}(s_{\min})_{\mu\mu}^{\text{high}} &= 2.29 \times 10^{-3} \Big(1 \pm 0.04_{\text{scale}} \pm 0.02_{m_t} \\
&\pm 0.01_{C,m_c} \pm 0.006_{m_b} \pm 0.005_{\alpha_s} \pm 0.09_{\text{CKM}} \\
&\pm 0.003_{\lambda_2} \pm 0.05_{\rho_1} \pm 0.03_{f_u^0 + f_s} \pm 0.05_{f_u^0 - f_s} \Big) \\
&= 2.29 \times 10^{-3} (1 \pm 0.13) . \qquad (5)
\end{aligned}$$

The largest remaining source of error is now $|V_{ub}|$, which will be further reduced with the precise CKM determination at Super$B$. As in the $B \to X_s\gamma$ case, additional uncertainties, such as the still unknown non-perturbative corrections that scale with $\alpha_s \Lambda_{\text{QCD}}/m_b$, are about 5%. The cuts in the hadronic invariant mass spectrum lead to additional uncertainties of order 5%, which correspond to the effects of subleading shape functions [21?].

Published analyses for $B \to X_s l^+ l^-$ [23, 24] have used a semi-inclusive approach ($X_s = 1K + n\pi, n \leq 3$). This technique is affected by large systematics arising from uncertainties on the ratio used to extrapolate from the semi-inclusive to the inclusive branching ratio. This type of analysis is expected to be systematics dominated, with statistics around 1 ab^{-1}.

With larger statistics, a fully inclusive analysis using semileptonic or hadronic tags is likely to be more sensitive. Feasibility studies for such an analysis show that about 40 signal events per ab^{-1} can be expected with a signal-to-background ratio of ~ 1.5. At Super$B$, a few percent statistical error on the inclusive branching ratio can be achieved, well below the present theoretical error (see Eqs. 2 and 3). No detailed studies are available for the systematic uncertainties, but they are likely to become dominant over experimental statistical uncertainties at this level of precision.

$B \to K^{(*)}\tau\tau$ decay modes

The branching ratio of $B \to X_s \tau^+ \tau^-$ is smaller by a factor of about 20, with respect to $B \to X_s \ell^+ \ell^-$ ($\ell = e, \mu$), in the low q^2 region, but is expected to be about 2–3×10^{-7}, comparable to $B \to X_s \ell^+ \ell^-$ (see Eq. 3), in the high q^2 region.

An inclusive experimental determination is essentially impossible, but an analysis of the exclusive decays $B \to K^{(*)}\tau\tau$ might be possible. These decays are predicted to make up 50–60% of the total inclusive rate [25]. Preliminary simulation studies using the hadronic tag technique indicate that the Standard Model branching fractions could be measurable with the full Super$B$ integrated luminosity. Other interesting measurements such as the polarization asymmetry [26] are under study.

$B \to K^{(*)}\nu\overline{\nu}$ decay modes

The rare decay $B \to K^{(*)}\nu\overline{\nu}$ is an interesting probe for New Physics in Z^0 penguins [27], such as chargino-up-squark contributions in a generic supersymmetric theory. Moreover, since only the $b \to s + \text{missing energy}$ process can be detected, the measured rate can be affected by exotic sources of missing energy, such as light dark matter [28] or "unparticle physics" [29, 30]. Notice also that New Physics effects can modify the kinematics of the decay, which implies that any selection applied on kinematical variables has an impact on the theoretical interpretation of the measured branching ratio. The best upper limit among the exclusive decay channels is $\mathcal{B}(B^+ \to K^+\nu\overline{\nu}) < 14 \times 10^{-6}$ [31], still far above the Standard Model branching fraction of 4×10^{-6} [27].

Due to the undetected neutrinos, it is not possible to reject background by means of the usual kinematical constraints, so the search for these decays must be performed using a recoil analysis.

In the $B^+ \to K^+\nu\overline{\nu}$ analysis, only one track is required on the signal side. A selection on the kaon momentum is usually applied. A final selection is applied on the extra energy E_{extra}, defined as the sum of the energies of the neutral electromagnetic calorimeter clusters that are not associated with the B_{tag} or the signal side. Current analyses employ a counting technique, but a maximum likelihood (ML) fit to the E_{extra} distribution can be used to improve performance. To be conservative, we assume the current analysis technique. From toy MC simulations, combining the results from the semileptonic and the hadronic recoil, the observation of the decay is expected with between 10 and 20 ab^{-1} with an expected error of 18%, in the most conservative scenario, at 50 ab^{-1}. The improvement in the precision as a function of luminosity is shown in Fig. 4.

In the $B^0 \to K^{*0}\nu\overline{\nu}$ analysis, the K^{*0} is reconstructed in the $K^{*0} \to K^+\pi^-$ channel, with no cut on the kinematical variables. A maximum likelihood
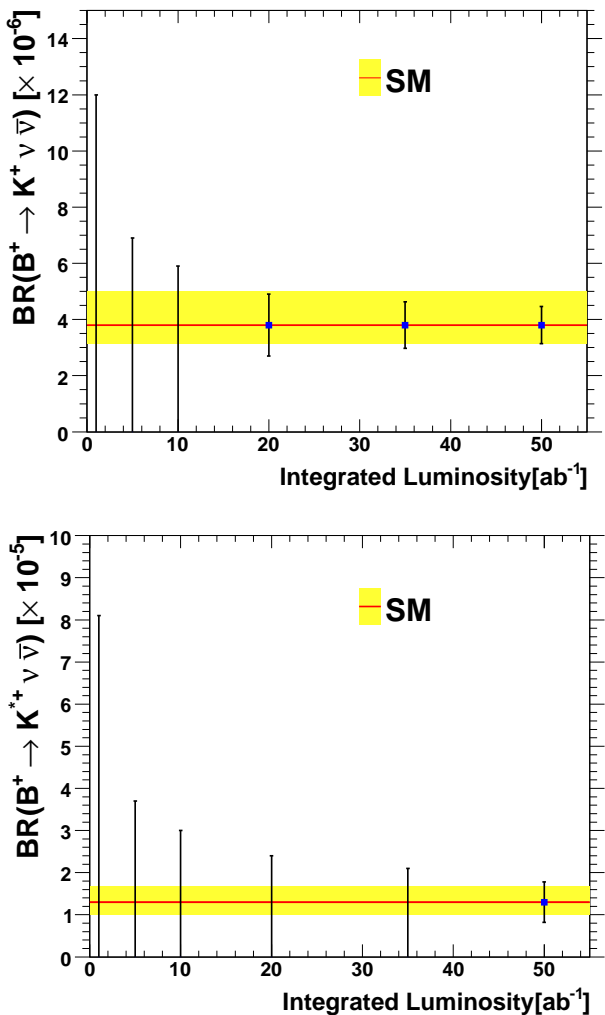
FIG. 4: Expected precision of the measurements of the branching fractions of (top) $B^+ \to K^+ \nu\bar{\nu}$ and (bottom) $B^+ \to K^{*+}\nu\bar{\nu}$ ($K^{*+} \to K_S\pi^+$) evaluated as a function of the integrated luminosity, assuming efficiencies and backgrounds as in the current *BABAR* analyses. The bands indicate the range of the Standard Model predictions.

fit is used to extract the signal yield from the $E_{\rm extra}$ distribution. Observation of this decay is expected between 10 and 20 ab^{-1} with an expected error of 20%, in the most conservative scenario, at 50 ab^{-1}.

The same approach is adopted in the $B^\pm \to K^{*\pm}\nu\bar{\nu}$ analysis, where $K^{*\pm} \to K_S^0\pi^\pm$ or $K^{*\pm} \to K^\pm\pi^0$. The observation is expected around 40 ab^{-1} with an expected error of 25%, in the most conservative scenario, at 50 ab^{-1} (see Fig. 4).

An irreducible background contribution from $B \to \tau\nu$ decays is expected in the $B \to K^{(*)\pm}\nu\bar{\nu}$ analyses. However, the effect of this background can be controlled with improvements in the analyses (such as using a maximum likelihood fit). Moreover, the

performance of the recoil technique will be improved by the improved hermeticity of the Super$B$ detector, making the cuts usually applied on the track multiplicity of the signal side more effective. Preliminary studies have shown that a 30% reduction in the background contamination with the baseline Super$B$ design is possible. For background dominated channels such as $B \to K^{(*)\pm}\nu\bar{\nu}$, a reduction in background of 30% can be shown to be roughly equivalent to an increase in statistics of $1/0.7$, *i.e.* about 40%. Therefore, such an improvement has a significant effect on the sensitivity.

If the background can be reduced sufficiently, it will be possible to do higher multiplicity studies of $b \to s\nu\bar{\nu}$ decays such as $B^+ \to K_1^+\nu\bar{\nu}$, $K_1^+ \to K^+\pi^+\pi^-$. This information could be used to make a semi-inclusive measurement of $\mathcal{B}(b \to s\nu\bar{\nu})$. Further background rejection can come from an improved vertex detector, that allows to apply vertexing requirements (poorly used now) and secondary vertex information. The semi-inclusive approximation may provide the best possible analysis of $B \to X_s\nu\bar{\nu}$ decay. Owing to the complete absence of any powerful constraint to be applied on the signal side, the fully inclusive analysis appears to be difficult in the face of large backgrounds. If a fully inclusive analysis could be performed at Super$B$, it may be possible to make a test of the theoretically clean Standard Model prediction [32]

$$\frac{\mathcal{B}(B \to X_d\nu\bar{\nu})}{\mathcal{B}(B \to X_s\nu\bar{\nu})} = \left|\frac{V_{td}}{V_{ts}}\right|^2. \qquad (6)$$

Studies of corresponding ratios using exclusive modes are less theoretically clean, however the prospects for measuring $B \to \pi\nu\bar{\nu}$ at Super$B$ look good [1].

Leptonic B decays

The branching fraction of $B \to \ell\nu$

The decays $B^\pm \to \ell^\pm\nu$ can be used to constrain the Standard Model mechanism of quark mixing. New Physics contributions can enhance the branching fractions of $B^\pm \to \ell^\pm\nu$, as described in the Super$B$ CDR [1]. Precision measurements of the branching fraction of $B^\pm \to \ell^\pm\nu$ where $\ell = e, \mu, \tau$ can be used to constrain New Physics.

Recent measurements have provided evidence for $B \to \tau\nu$ [33, 34, 35] These measurements rely on recoil analyses in which fully (partially) reconstructed B meson decays to hadronic (semileptonic) final states of the non-signal B in the event ($B_{\rm tag}$) are used to help reduce background for the partially reconstructed signal. This approach is required for the $B \to \tau\nu$ analysis, in which there are at least two missing neutrinos in the final state. For $B \to \mu\nu$ and $B \to e\nu$ [36, 37, 38],

on the other hand, the high momentum lepton alone provides a characteristic signature. Nevertheless, recoil analyses appear preferable also for these channels, due to the additional kinematic constraints and the reduction in background.

A number of possible improvements to the $B^\pm \to \ell^\pm \nu$ analyses are being explored. These include

1. All existing *BABAR* measurements rely on reconstructing B_{tag} modes with a D or D^* in the final state. However it is also possible to increase the signal efficiency by including charmonium decay modes with a J/ψ in the B_{tag} final state.

2. The B_{tag} categories all have different purities. It is a natural extension of the existing analyses to investigate the gain in precision that one can obtain by subdividing the data according to the B_{tag} purity in a multi-dimensional maximum likelihood fit, and if necessary, exclude any B_{tag} category in which systematic uncertainties are not under control. (Similar strategies have been successfully employed in time-dependent CP asymmetry measurements at the B factories.)

3. In the case of $B^\pm \to \tau^\pm \nu$, B_{sig} has contributions from several reconstructed τ decay channels that have different purities; so one should subdivide the data according to B_{tag} and B_{sig} purity.

4. Existing analyses rely heavily on a variable constructed from the sum of electromagnetic energy unassociated wither with the B_{sig} or B_{tag} to isolate signal (E_{extra}). In order to do this reliably, one has to understand, and accurately simulate, noise in the calorimeter as well as the geometric acceptance of the detector to backgrounds in which final state particles escape down the beam pipe, or into uninstrumented regions of the detector. Not only does this rely on accurate accounting of material in the inner parts of the detector, but also in the calorimeter itself, and a finely-tuned understanding of the production mechanisms for all types of B and non-B backgrounds. It is not clear if the continual use of such a variable would facilitate a precision measurement of $B^\pm \to \ell^\pm \nu$ branching fractions. It would be possible to improve control of systematic uncertainties by limiting the analysis to high purity B_{tag} samples and/or to B_{sig} channels only. During the detector R&D stage, one should also consider the effects of non-active material in the calorimeter, and material in front of the calorimeter, as it is critical that this is correctly accounted for in GEANT simulations of Super$B$.

5. The current analyses that extract the yield from a fit of the E_{extra} distribution determine the shape of the signal PDF using a control sample of semileptonic $B \to D^{(*)}\ell\nu$ decays on the recoil of B_{tag}. With Super$B$ statistics it would be possible to use hadronic B decays for the control sample, which could lead to a reduction of systematic uncertainty. This approach has been used as a systematic cross-check in one search for $B^\pm \to \tau^\pm \nu$ [38], and has also been employed by CLEO in the measurement of f_{D_s} using $D_s^+ \to \tau^+ \nu_\tau$ [39].

6. There are alternatives to the E_{extra} variable that do not rely so critically on our understanding of the detector material, acceptance, response and details of the background kinematics. Examples of such variables include the highest energy cluster unassociated with B_{sig} or B_{tag}.

7. Improvements in the detector hermeticity would, as well as increasing the signal efficiency, lead to smaller backgrounds due to particles that travel down the beam pipe. Similarly, improvements in the efficiency with which K_L mesons are detected would help to reduce the background.

The emphasis in these improvements is on increasing the signal efficiency, and on better control of systematic uncertainties associated with measuring $B^\pm \to \ell^\pm \nu$ branching fractions. It must be emphasized that, while the Standard Model expectation for the branching fraction of $B^\pm \to \mu^\pm \nu$ is significantly lower than that of $B^\pm \to \tau^\pm \nu$, the experimental signature, a high momentum muon with missing energy, is much cleaner than that of a τ lepton. Therefore, at very high luminosities, $B^\pm \to \mu^\pm \nu$ is expected to provide a more precise branching fraction measurement, as it will not be systematics limited. Measurements of $B^\pm \to \mu^\pm \nu$ and $B^\pm \to \tau^\pm \nu$ are central to the New Physics search capability of Super$B$. The phenomenological impact of these measurements is discussed in Section 2.

Radiative leptonic decays

Radiative leptonic decays, namely $B_u \to \ell\nu\gamma$, $B_{d(s)} \to \ell\ell\gamma$ and $B_{d(s)} \to \gamma\gamma$, do not contain any hadrons except the B meson. This simple observation drastically reduces theoretical uncertainties originating from the strong interaction, such as final state interactions. Super$B$ may be able to observe these extremely rare processes, due to its good efficiency for reconstruction of the radiative photon.

It has been shown that, in the Standard Model, the strong interaction factorizes at the large m_b limit, making it possible to describe these three processes in terms of an universal non-perturbative form-factor [40]. Rough estimates of the branching ratios yield $\mathcal{B}(B_u \to \ell\nu\gamma) \sim \mathcal{O}(10^{-6})$, $\mathcal{B}(B_{d(s)} \to \ell\ell\gamma) \sim \mathcal{O}(10^{-10(-9)})$ and $\mathcal{B}(B_{d(s)} \to \gamma\gamma) \sim \mathcal{O}(10^{-8(-6)})$. It should be emphasized that the helicity suppression, which diminishes the branching ratio of the pure-leptonic processes corresponding to the first two channels, $B_u \to \ell\nu$ and $B_{d(s)} \to \ell\ell$, does not occur here, due to the additional photon. As a result, one can take advantage of all three final states with $\ell = e, \mu, \tau$, which have similar decay rates.

A strategy to search for New Physics with these channels would be to first determine the form factor through the tree level $B^+ \to \ell\nu\gamma$ process [41] and then use it to extract New Physics effects from the loop level $B_{d(s)} \to \ell\ell\gamma$ and $B_{d(s)} \to \gamma\gamma$ processes. In the former, the most recent experimental results [42] are already close to the Standard Model expectation. Super$B$ can make a precise measurement of this decay; theoretical uncertainties due to the restricted phase space used in the analysis (necessary to reduce backgrounds from final state radiation photons) may then become a limiting factor. The current experimental upper limits on $B_d \to \ell\ell\gamma$ are at the 10^{-7} level [43]; since these are not background-limited, Super$B$ can improve the limits to close to the Standard Model level. Once observed, kinematical distributions in these processes provide additional New Physics sensitivity. New Physics effects on the branching ratio and the forward-backward asymmetry of the $B_{d(s)} \to \ell\ell\gamma$ process have been investigated, e.g. in [44, 45]. For example, those effects could come from an anomalous $bd(s)Z$ coupling, that could be also seen the in $B \to K^{(*)}\ell\ell$ and $B_{d(s)} \to \ell\ell$ processes.

On the other hand, the new physics effect to $B_{d(s)} \to \gamma\gamma$ process could come from two kinds of short-distance contributions: anomalous $bs\gamma$ coupling and the $bs\gamma\gamma$ coupling. In particular, the later contribution has not been explored yet and Super$B$ sensitivity will reveal these couplings for the first time. It should be noted that this contribution can be also studied in $B \to K\gamma\gamma$ [46]. Detailed investigations of the supersymmetric contributions to $B_s \to \gamma\gamma$ and $B \to X_s\gamma\gamma$ have been performed [47]. As discussed in the CDR [1], $B_s \to \gamma\gamma$ could be observed at Super$B$ after accumulating about 1 ab^{-1} at the $\Upsilon(5S)$. Extrapolating from existing upper limits on the $B_d \to \gamma\gamma$ decay [48, 49], Super$B$ could probe down to the Standard Model level of this New Physics-sensitive decay.

2. Phenomenology

Golden processes

At Super$B$, a golden channel is any channel that is very well known in the Standard Model. This includes "null tests" (observables that are zero, at least approximately, in the Standard Model) but also other channels predicted with small errors. This places more emphasis on inclusive modes than on exclusive decays. While there are probably specific channels that can be selected in charm and in τ physics, in B physics there are so many golden channels that selecting one or two risks missing the point. In addition processes that are golden (*i.e.* display a measurable deviation from Standard Model) for given New Physics scenario could be uninteresting in a different scenario. The rationale for building Super$B$ based on the New Physics-sensitivity of any individual channel can certainly be challenged – the motivation is the large range of golden channels for which Super$B$ has unsurpassed sensitivity. We will nonetheless, in response to the IRC, select some specific channels for which Super$B$ has unique potential. However, the argument given above makes it clear that golden modes are defined only in the context of a limited and non-orthogonal set of New Physics scenarios. We thus want to stress once more that one of the most sensitive searches for New Physics will be the 1% determination of CKM parameters; the possibility of performing such a precise determination in the presence of New Physics is a unique feature of Super$B$. The precision measurements required to achieve this goal are $|V_{ub}|$ and the CKM angles. In the spirit of indicating the golden modes, we select $|V_{ub}|$ and α, being β and γ precisely measured at LHCb. In the following, we denote by CKM those places in which the improvements on the CKM parameters achieved by Super$B$ are crucial to the corresponding New Physics searches. We do not include rare kaon decays in which a precise CKM measurement is also extremely important. Notice that whenever a high precision CKM determination is required, progress on Lattice QCD calculations, as discussed in the Appendix of the CDR, is needed. In Table II we show the result of our selection of golden modes in different New Physics scenarios. For each scenario, "X" marks the golden channel while "O" marks those modes which can display measurable deviation from the Standard Model.

A few comments are in order on this selection. Notice first that $\mathcal{B}(B \to X_s\gamma)$ is important in several scenarios, in particular in the MFV scenarios, and therefore we put it in the list, even though at Super$B$ it is limited by theoretical errors, unless a major breakthrough in non-perturbative calculations of power suppressed corrections is achieved. In some of the scenar-

TABLE II: Golden modes in different New Physics scenarios. A "X" indicates the golden channel of a given scenario. An "O" marks modes which are not the "golden" one of a given scenario but can still display a measurable deviation from the Standard Model. The label CKM denotes golden modes which require the high-precision determination of the CKM parameters achievable at Super$B$.

	H^+ high $\tan\beta$	Minimal FV	Non-Minimal FV (1-3)	Non-Minimal FV (2-3)	NP Z-penguins	Right-Handed currents
$\mathcal{B}(B \to X_s\gamma)$		X		O		O
$A_{CP}(B \to X_s\gamma)$				X		O
$\mathcal{B}(B \to \tau\nu)$	X-CKM					
$\mathcal{B}(B \to X_s l^+l^-)$				O	O	O
$\mathcal{B}(B \to K\nu\overline{\nu})$				O	X	
$S(K_S\pi^0\gamma)$						X
β			X-CKM			O

ios considered, of course, this list is far from complete; many other measurements are expected to show deviations from their Standard Model values. For example, in the case of non-minimal flavor violation in the transitions between third and second generations, the entire cohort of $b \to s$ penguins-dominated non-leptonic modes could show a deviation in the measured value of time-dependent CP asymmetries compared to those measured in $b \to c\bar{c}s$ transitions.

Benchmarks

The problem of defining proper benchmarks for Super$B$ has not been addressed yet. In fact benchmarks for flavor physics clearly require the specification of the New Physics flavor structure, which is not needed (at least at first approximation) for high-p_T physics. Nonetheless, stimulated by the IRC, we estimate the relevant flavor observable measured at Super$B$ within the mSUGRA models at the SPS1a, SPS4 and SPS5 benchmark points defined for the LHC in [52] . The purpose of this exercise is to evaluate the deviation from the Standard Model of flavor observables in a MFV scenario where LHC can reconstruct a large part of the SUSY spectrum. We consider a set of measurements which are likely to be affected in the MFV model under consideration.

In terms of the fundamental parameters at the high scale, the SPS considered points are defined as:

$$\text{SPS1}a: \quad m_0 = 100\text{GeV}, \quad m_{1/2} = 250\text{GeV}, \quad (7)$$
$$A_0 = -100\text{GeV}, \quad \tan\beta = 10, \quad \mu > 0$$
$$\text{SPS4}: \quad m_0 = 400\text{GeV}, \quad m_{1/2} = 300\text{GeV},$$
$$A_0 = 0, \quad \tan\beta = 50, \quad \mu > 0,$$
$$\text{SPS5}: \quad m_0 = 150\text{GeV}, \quad m_{1/2} = 300\text{GeV},$$
$$A_0 = -1000, \quad \tan\beta = 5, \quad \mu > 0.$$

Note that SPS1a, a "typical" mSUGRA scenario with intermediate $\tan\beta$, is extremely good for LHC

and indeed the most studied - the pattern of sparticle masses allows them all to be measured with very good accuracy [53]. By contrast, the relatively high squark masses and the low value of $\tan\beta$ suppress effects on flavor observables. SPS4 is an mSUGRA scenario with large $\tan\beta$. Unfortunately, no detailed studies are available at LHC for this point. Nevertheless we roughly estimated the LHC performance by studying the decay chain starting from the computed SUSY spectrum. We found a single study at SPS5 [54], a parameter configuration with relatively light stop quark and low $\tan\beta$. Here again the LHC performance in measuring the SUSY spectrum is rather good.

Based on these studies, and using the tools developed at the recent CERN-Workshop "Flavour in the LHC Era" [55] we produced the predictions presented in Table III.

The most striking feature of this result is that SPS4 is already ruled out by the present measurement of $\mathcal{B}(B \to s\gamma)$ with high significance, showing the impact of flavor observables on the SUSY parameter space even in a MFV case. Indeed, from Eqs. (1) and (1) one obtains $\text{R}^{\text{exp}}(B \to X_s\gamma) = 1.13 \pm 0.12$. In the absence of a detailed analysis, we have not attempted an estimate of the errors associated with the predictions of Table III at SPS4. Nevertheless, even assuming an error of 50%, much larger than the other points, $\text{R}(B \to X_s\gamma)=0.25$ at SPS4 is more than 5σ away from the present experimental value. SPS5 is marginally compatible with present measurement of $\mathcal{B}(B \to s\gamma)$. Clearly this point will produced a measurable effect on $\mathcal{B}(B \to s\gamma)$ at Super$B$. Considering these results, it is not surprising that the recent MSSM analysis in [55] found that the best fit to present data, using $\mathcal{B}(B \to s\gamma)$ among the constraints, resembles SPS1a.

SPS1a is clearly the least favorable point from the flavor point of view. However, even here Super$B$ could see a definite pattern of 1-2 σ deviations from the Standard Model in $\mathcal{R}(B \to \tau\nu)$, $\mathcal{R}(b \to s\gamma)$

TABLE III: Predictions of flavor observables based on expected measurements from LHC in mSUGRA at SPS1a, SPS4, SPS5 benchmark points. Quantities denoted $\mathcal{R}$ are the ratios of the branching fractions to their Standard Model values. Quoted uncertainties (when available) come from the errors on the measurement of the New Physics parameters at LHC. Uncertainties on the Standard Model predictions of flavor observables are not included. For the SPS4 benchmark point the sensitivity study at LHC are not available.

	SPS1a	SPS4	SPS5
$\mathcal{R}(B \to X_s\gamma)$	0.919 ± 0.038	0.248	0.848 ± 0.081
$\mathcal{R}(B \to \tau\nu)$	0.968 ± 0.007	0.436	0.997 ± 0.003
$\mathcal{R}(B \to X_s l^+l^-)$	0.916 ± 0.004	0.917	0.995 ± 0.002
$\mathcal{R}(B \to K\nu\overline{\nu})$	0.967 ± 0.001	0.972	0.994 ± 0.001
$\mathcal{B}(B_d \to \mu^+\mu^-)/10^{-10}$	1.631 ± 0.038	16.9	1.979 ± 0.012
$\mathcal{R}(\Delta m_s)$	1.050 ± 0.001	1.029	1.029 ± 0.001
$\mathcal{B}(B_s \to \mu^+\mu^-)/10^{-9}$	2.824 ± 0.063	29.3	3.427 ± 0.018
$\mathcal{R}(K \to \pi^0\nu\overline{\nu})$	0.973 ± 0.001	0.977	0.994 ± 0.001
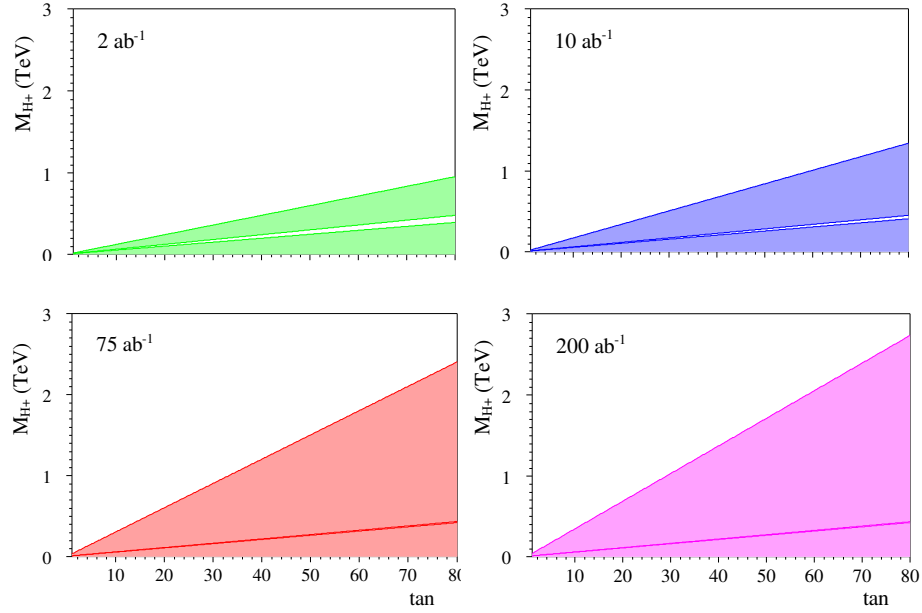
FIG. 5: Exclusion regions in the $m(H^+)$–$\tan\beta$ plane arising from the combinations of the measurement of $\mathcal{B}(B \to \tau\nu)$ and $\mathcal{B}(B \to \mu\nu)$ using 2 ab^{-1} (top left), 10 ab^{-1} (top right) 75 ab^{-1} (bottom left) and 200 ab^{-1} (bottom right). We assume that the result is consistent with the Standard Model.
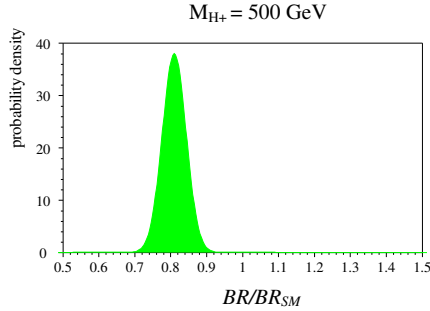
FIG. 6: Distribution of $R = \mathcal{B}(B \to \ell\nu)/\mathcal{B}_{SM}(B \to \ell\nu)$ in 2HDM, using $m(H^+)$=500GeV and $\tan\beta$=30 as it would be measured in 5 years at Super$B$.

and $\mathcal{R}(B \to X_s l^+ l^-)$, although this does depend, to some extent, on improvements in theory. In any case, Super$B$ flavor measurements are required to establish that the New Physics flavor couplings are small as predicted by mSUGRA, since LHC alone cannot establish which model is behind the measured SUSY spectrum.

One of the lessons of this exercise is that the benchmarks for flavor physics, if needed, should mainly address the problem of defining a "typical" non-minimal flavor structure with an economical number of parameters. A possible way to further investigate is using models of SUSY-breaking as discussed below.

Update on the $B \to \ell\nu$ predictions

We update in this section the analysis of the decay $B \to \ell\nu$ in the 2HDM. The case of SUSY, discussed in the CDR, is very similar.

Figure 5 shows a comparison of the exclusion plot in the $m(H^+)$–$\tan\beta$ plane coming from a measurement of $\mathcal{B}(B \to \tau\nu)$ with different data samples, 2 ab^{-1}, 10 ab^{-1}, 75 ab^{-1} and 200 ab^{-1}, assuming that the result is consistent with the Standard Model.

Note that moving from 10 ab^{-1} to 75 ab^{-1} the channel $B \to \mu\nu$ begins to give a significant contribution to the average, and the scale is then larger than the naive statistical gain. With further increases in the integrated luminosity beyond 75 ab^{-1}, $B \to \tau\nu$ become systematics-dominated but $B \to \mu\nu$ still scales with statistics.

To give an example of a positive signal as seen at Super$B$, Figure 6 shows the deviation of $\mathcal{B}(B \to \ell\nu)$ with respect to its Standard Model value computed in the 2HDM for $m(H^+)$=500GeV and $\tan\beta$=30 as it would be measured with a sample of 75 ab^{-}1. It's clear that the deviation is established with very high significance.

SUSY-breaking models

Within supersymmetric extensions of the Standard Model, the flavor structure is directly linked to the crucial question of the supersymmetry-breaking mechanism. Indeed, the bulk of soft SUSY-breaking terms is given by the sfermion bilinear and trilinear couplings, which are matrices in flavor space. Thus, once some SUSY particles have been found, the measurement of the flavor sector can provide important information for distinguishing among models of supersymmetry. This is a manifestation of the complementary nature of flavor physics and collider physics. At the LHC direct searches for supersymmetric particles are essential in establishing the existence of new physics. On the other hand, there are a variety of possibilities for the origin
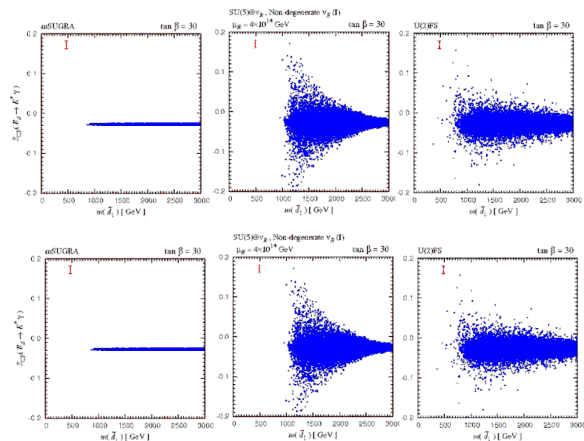
FIG. 7: Time-dependent CP asymmetry of $B \to K_s\pi^0\gamma$ and the difference between the time-dependent asymmetries of $B \to \phi K_S$ and $B \to J/\psi\,K_S$ modes for three SUSY breaking scenarios: mSUGRA(left), SU(5) SUSY GUT with right-handed neutrinos in non-degenerate case (middle), and MSSM with U(2) flavor symmetry (right). The Super$B$ sensitivities are also shown.

of SUSY breaking and of flavor structures within supersymmetry. Flavor physics provides an unique tool with which fundamental questions, such as how supersymmetry is broken, can be addressed.

A comprehensive analysis of the flavor patterns generated in SUSY models with different SUSY-breaking sector has been recently presented in Ref. [56]. The models under study are mSUGRA, MSSM with U(2) flavor symmetry, MSSM with right-handed neutrinos, and SU(5) SUSY-GUT with right-handed neutrinos. Different scenarios for the neutrino mass spectrum and Yukawa couplings have also been considered. For our purpose, it is sufficient to consider a few examples. We refer the reader to the original publication for all the details.
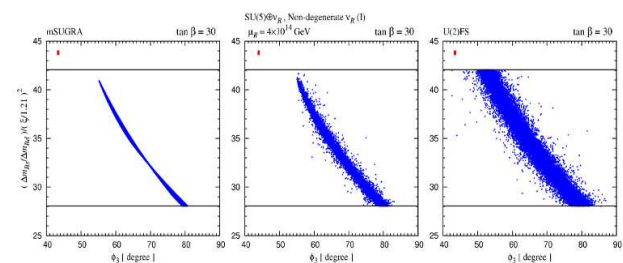
FIG. 8: Correlation of $\Delta m_s/\Delta m_d$ and γ (ϕ_3) for three SUSY breaking scenarios: mSUGRA(left), SU(5) SUSY GUT with right-handed neutrinos in non-degenerate case (middle), and MSSM with U(2) flavor symmetry (right).

Figs. 7–8 from Ref. [56] are examples of the power of Super$B$ in discriminating different SUSY-breaking scenarios. Additional information can certainly be obtained from a systematic study of correlations among flavor observables. It is interesting to notice that the plot in Fig. 8 calls for a determination of γ (ϕ_3) with a sub-degree precision, which could be obtained at Super$B$ with 100 ab^{-1}.

3. Interplay of flavor and high p_T physics

In this section we want to report some result of the recent workshops "Flavour in the LHC era" [57, 58, 59] from the perspective of Super$B$.

We have already commented on the complementarity of the physics goals of flavor and high p_T physics, which are both necessary to identify the structure of the New Physics models.

Three analyses out of these reports should demonstrate the importance of the interplay in our future new physics search:

In the context of this workshop the study of several SUSY-breaking models, along the same lines of the previous section, have been presented to show the capability of combined flavor and high p_T data in identifying the SUSY-breaking mechanism.

Another study that started at the workshop concerns the effects of flavor violation on direct searches at LHC, which are often not fully taken into account. It has been shown that flavor violation could, in some cases, change the decay chains used at LHC to reconstruct the New Physics mass spectrum, possibly making the analysis more involved [57, 60].

The workshop result most relevant to Super$B$ physics comes from a first attempt at combining of flavor and high p_T physics on the same New Physics parameter space. Based on existing flavor physics and high-energy computer codes, a so-called master tool was developed which combines calculations from both low-energy and electroweak observables in one common code. The details of the analysis presented at the workshop can be found in [58].

The complementarity of flavor physics and high p_T physics is shown in Figure 9. It is clearly demonstrated that, without the inclusion of both the flavor and electroweak constraints, the parameters $\tan\beta$ and M_A are much less well-determined. It can be seen, as well, that LHC mainly constrains the mass, whereas flavor physics constrains the flavor coupling (*i.e.* the $\tan\beta$-enhanced Yukawa coupling). Even in a model such as CMSSM with only a few New Physics parameters, both constraints are required to effectively bound the parameter space.
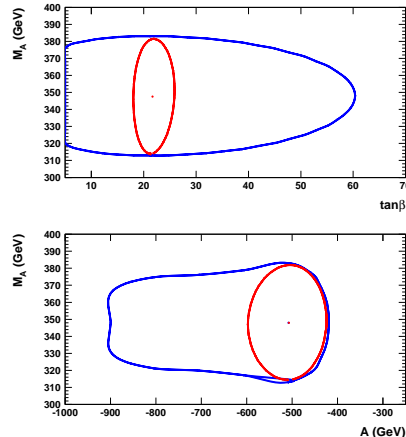
FIG. 9: The red (clear) contour corresponds to the LHC scenario that includes the low-energy and electroweak constraints, while the blue (darker) contour makes the same assumptions about the assumed LHC discoveries, but does not include any external constraints.

A working group on the "Interplay between high-p_T and flavor physics" has been set up [61]; the first meeting was held at CERN in December 2007 [62].

[1] M. Bona *et al.*, arXiv:0709.0451 [hep-ex].
[2] E. Baracchini *et al.*, JHEP **0708** (2007) 005 [arXiv:hep-ph/0703258].
[3] B. Aubert *et al.* [*BABAR* Collaboration], Phys. Rev. Lett. **96** (2006) 221801 [arXiv:hep-ex/0601046].
[4] B. Aubert *et al.* [*BABAR* Collaboration], Phys. Rev. Lett. **97** (2006) 211801 [arXiv:hep-ex/0607089].
[5] K. Abe *et al.* [Belle Collaboration], arXiv:hep-ex/0610054.
[6] S. Chen *et al.* [CLEO Collaboration], Phys. Rev. Lett. **87** (2001) 251807 [arXiv:hep-ex/0108032].
[7] K. Abe *et al.* [Belle Collaboration], Phys. Lett. B **511** (2001) 151 [arXiv:hep-ex/0103042].
[8] P. Koppenburg *et al.* [Belle Collaboration], Phys. Rev. Lett. **93** (2004) 061803 [arXiv:hep-ex/0403004].
[9] B. Aubert *et al.* [BABAR Collaboration], Phys. Rev. D **72** (2005) 052004 [arXiv:hep-ex/0508004].
[10] B. Aubert *et al.* [*BABAR* Collaboration], Phys. Rev. Lett. **97** (2006) 171803 [arXiv:hep-ex/0607071].
[11] E. Barberio *et al.* [Heavy Flavor Averaging Group (HFAG)], arXiv:hep-ex/0603003.
[12] B. Aubert *et al.* [BABAR Collaboration], Phys. Rev. D **77** (2008) 051103 [arXiv:0711.4889 [hep-ex]].
[13] M. Misiak *et al.*, Phys. Rev. Lett. **98** (2007) 022002 [arXiv:hep-ph/0609232].
[14] T. Becher and M. Neubert, Phys. Rev. Lett. **98** (2007) 022003 [arXiv:hep-ph/0610067].
[15] http://www.theorie.physik.uni-muenchen.de/lsfritzsch/albufeira/Talks/albufeiramm.pdf

[16] S. J. Lee, M. Neubert and G. Paz, Phys. Rev. D **75** (2007) 114005 [arXiv:hep-ph/0609224].

[17] U. Haisch and A. Weiler, Phys. Rev. D **76** (2007) 034014 [arXiv:hep-ph/0703064].

[18] T. Huber, T. Hurth and E. Lunghi, arXiv:0712.3009 [hep-ph].

[19] T. Huber, E. Lunghi, M. Misiak and D. Wyler, Nucl. Phys. B **740** (2006) 105 [arXiv:hep-ph/0512066].

[20] Z. Ligeti and F. J. Tackmann, Phys. Lett. B **653**, 404 (2007) [arXiv:0707.1694 [hep-ph]].

[21] K. S. M. Lee and I. W. Stewart, Phys. Rev. D **74** (2006) 014005 [arXiv:hep-ph/0511334].

[22] K. S. M. Lee, Z. Ligeti, I. W. Stewart and F. J. Tackmann, Phys. Rev. D **74** (2006) 011501 [arXiv:hep-ph/0512191].

[23] B. Aubert *et al.* [*BABAR* Collaboration], Phys. Rev. Lett. **93** (2004) 081802 [arXiv:hep-ex/0404006].

[24] M. Iwasaki *et al.* [Belle Collaboration], Phys. Rev. D **72** (2005) 092005 [arXiv:hep-ex/0503044].

[25] D. S. Du, C. Liu and D. X. Zhang, Phys. Lett. B **317** (1993) 179.

[26] J. L. Hewett, Phys. Rev. D **53** (1996) 4964 [arXiv:hep-ph/9506289].

[27] G. Buchalla, G. Hiller and G. Isidori, Phys. Rev. D **63** (2001) 014015 [arXiv:hep-ph/0006136].

[28] C. Bird, P. Jackson, R. Kowalewski and M. Pospelov, Phys. Rev. Lett. **93** (2004) 201803 [arXiv:hep-ph/0401195].

[29] H. Georgi, Phys. Rev. Lett. **98** (2007) 221601 [arXiv:hep-ph/0703260].

[30] T. M. Aliev, A. S. Cornell and N. Gaur, JHEP **0707** (2007) 072 [arXiv:0705.4542 [hep-ph]].

[31] K. F. Chen *et al.* [Belle Collaboration], Phys. Rev. Lett. **99** (2007) 221802 [arXiv:0707.0138 [hep-ex]].

[32] A. J. Buras, P. Gambino, M. Gorbahn, S. Jager and L. Silvestrini, Phys. Lett. B **500** (2001) 161 [arXiv:hep-ph/0007085].

[33] K. Ikado *et al.*, Phys. Rev. Lett. **97** (2006) 251802 [arXiv:hep-ex/0604018].

[34] B. Aubert *et al.* [*BABAR* Collaboration], Phys. Rev. D **76** (2007) 052002 [arXiv:0705.1820 [hep-ex]].

[35] B. Aubert *et al.* [*BABAR* Collaboration], Phys. Rev. D **77** (2008) 011107 [arXiv:0708.2260 [hep-ex]].

[36] N. Satoyama *et al.* [Belle Collaboration], Phys. Lett. B **647** (2007) 67 [arXiv:hep-ex/0611045].

[37] B. Aubert *et al.* [*BABAR* Collaboration], Phys. Rev. Lett. **92** (2004) 221803 [arXiv:hep-ex/0401002].

[38] B. Aubert *et al.* [*BABAR* Collaboration], arXiv:hep-ex/0607110.

[39] K.M. Ecklund *et al.* [CLEO Collaboration], arXiv:0712.1175 [hep-ex].

[40] S. Descotes-Genon and C. T. Sachrajda, Phys. Lett. B **557** (2003) 213 [arXiv:hep-ph/0212162].

[41] G. P. Korchemsky, D. Pirjol and T. M. Yan, Phys. Rev. D **61** (2000) 114510 [arXiv:hep-ph/9911427].

[42] B. Aubert *et al.* [*BABAR* Collaboration], arXiv:0704.1478 [hep-ex].

[43] B. Aubert *et al.* [*BABAR* Collaboration], arXiv:hep-ex/0607058.

[44] U. O. Yilmaz, B. B. Sirvanli and G. Turan, Nucl. Phys. B **692** (2004) 249 [arXiv:hep-ph/0407006].

[45] S. R. Choudhury, A. S. Cornell, N. Gaur and G. C. Joshi, Int. J. Mod. Phys. A **21** (2006) 2617 [arXiv:hep-ph/0504193].

[46] G. Hiller and A. S. Safir, JHEP **0502** (2005) 011 [arXiv:hep-ph/0411344].

[47] S. Bertolini and J. Matias, Phys. Rev. D **57** (1998) 4197 [arXiv:hep-ph/9709330].

[48] B. Aubert *et al.* [*BABAR* Collaboration], Phys. Rev. Lett. **87** (2001) 241803 [arXiv:hep-ex/0107068].

[49] K. Abe *et al.* [Belle Collaboration], Phys. Rev. D **73** (2006) 051107 [arXiv:hep-ex/0507036].

[50] T. Browder, M. Ciuchini, T. Gershon, M. Hazumi, T. Hurth, Y. Okada and A. Stocchi, JHEP **0802** (2008) 110 [arXiv:0710.3799 [hep-ph]].

[51] T. E. Browder, T. Gershon, D. Pirjol, A. Soni and J. Zupan, arXiv:0802.3201 [hep-ph].

[52] B. C. Allanach *et al.*, arXiv:hep-ph/0202233.

[53] G. Weiglein *et al.* [LHC/LC Study Group], Phys. Rept. **426** (2006) 47 [arXiv:hep-ph/0410364].

[54] I. Borjanovic, J. Krstic and D. Popovic, Czech. J. Phys. **55** (2005) B793.

[55] O. Buchmueller *et al.*, Phys. Lett. B **657** (2007) 87 [arXiv:0707.3447 [hep-ph]].

[56] T. Goto, Y. Okada, T. Shindou and M. Tanaka, Phys. Rev. D **77** (2008) 095010, arXiv:0711.2935 [hep-ph].

[57] F. del Aguila *et al.*, arXiv:0801.1800 [hep-ph].

[58] G. Buchalla *et al.*, arXiv:0801.1833 [hep-ph].

[59] M. Raidal *et al.*, arXiv:0801.1826 [hep-ph].

[60] T. Hurth and W. Porod, Eur. Phys. J. C **33** (2004) S764 [arXiv:hep-ph/0311075].

[61] https://twiki.cern.ch/twiki/bin/view/Main/ColliderAndFlavour

[62] http://indico.cern.ch/conferenceOtherViews.py?view=standard&confId=22180

Charm Physics

New Physics, in general, generates flavor-changing neutral currents (FCNC). Those could be much less suppressed in the up-type than the down-type quark sectors. Among the up-type quarks, only charm allows the *full* range of probes for FCNC, and thus New Physics, in oscillation phenomena, in particular those involving CP violation. The Standard Model makes nontrivial predictions for CP violation in charm transitions: *direct* CP violation should occur only in Cabibbo-suppressed modes at an observable level $\sim \mathcal{O}(10^{-3})$.

The recent evidence for $D^0\overline{D}^0$ oscillations – with x_D, $y_D \simeq 0.005$–0.01 – does not prove the presence of New Physics. However it greatly widens the stage on which CP violation can appear as a manifestation of New Physics. Within the Standard Model, time dependent CP asymmetries could reach the 10^{-5} [10^{-4}] level in Cabibbo-allowed and once [doubly]-suppressed modes, whereas New Physics could enhance these asymmetries by almost three orders of magnitude. A search for New Physics should then aim at sensitivity levels of $\mathcal{O}(10^{-3})$ or better and $\mathcal{O}(10^{-2})$ or better in Cabibbo-allowed or once-suppressed nonleptonic channels and in doubly Cabibbo-suppressed or wrong-sign semileptonic modes, respectively. Signals for New Physics might actually be clearer in D than in B decays: for while *conventional* New Physics scenarios tend to create larger effects in the latter than the former, those signals must also contend with a much larger Standard Model "background" in the latter than the former.

These searches can be done at the $\Upsilon(4S)$ using D^* tagging and tracking of the D production and decay vertices. Relatively short runs in the charm threshold region can provide unique and important information on strong phases needed for a proper interpretation of results obtained in $\Upsilon(4S)$ runs. They might reveal significantly enhanced effects that can be seen only in $e^+e^- \to D^0\overline{D}^0$ exclusive production.

1. New Physics in charm decays: mainly CP violation

The landscape

New Physics in general generates flavor changing neutral currents (FCNC). The Standard Model had to be crafted carefully to suppress them in the strangeness sector down to the observed level. Those FCNC could actually be much less suppressed in the up-type than the down-type quark sectors. Among the up-type quarks, only charm allows the *full* range of probes for FCNC, and thus, New Physics in oscillation phenomena, in particular those involving CP violation: (i) Top quarks decay before they can hadronize; without top hadrons T^0 oscillations cannot occur. Furthermore the sheer size of phase space in top decays greatly reduces the coherence between different amplitudes needed to make direct CP violation observable. (ii) Hadrons built with u and $\bar{u}$ quarks, like the π^0 and η, are their own antiparticle; thus there can be no $\pi^0 - \pi^0$ etc. oscillations as a matter of principle. They also decay very rapidly. In addition, they possess so few decay channels that CPT invariance largely rules out CP asymmetries in their decays.

Strong evidence for $D^0\overline{D}^0$ oscillations has been recently found [1]. The most recent averages for the mixing parameters are

$$x_D \equiv \frac{\Delta M_D}{\overline{\Gamma}_D} = 0.0097^{+0.0027}_{-0.0029} \,, \qquad (8)$$

$$y_D \equiv \frac{\Delta \Gamma_D}{2\overline{\Gamma}_D} = 0.0078^{+0.0018}_{-0.0019} \,. \qquad (9)$$

According to our present understanding – or lack thereof – these quantities could be produced by Standard Model dynamics, yet x_D could still harbour substantial contributions from New Physics. It will require a theoretical breakthrough to resolve this ambiguity in the interpretation of the data.

We will be on much firmer ground in interpreting CP asymmetries. For on one hand, $D^0\overline{D}^0$ oscillations greatly widen the stage on which CP violation can appear as a manifestation of New Physics; on the other hand, the Standard Model makes nontrivial predictions for CP violation in charm transitions. In CKM dynamics there is a weak phase in $\Delta C = 1$ transitions entering (in the Wolfenstein representation) through V_{cs}, yet it is highly diluted:

$$V_{cs} \simeq 1 - \frac{1}{2}\lambda^2 - i\eta A^2 \lambda^4 \simeq 0.97 - 6\cdot 10^{-4}i \,. \qquad (10)$$

Furthermore two different, yet coherent, amplitudes must contribute to the same channel to produce a direct CP asymmetry. Within the Standard Model this can happen at an observable level only in Cabibbo-suppressed modes – even in these channels, CP asymmetries can be no more than $\mathcal{O}(10^{-3})$. This means that any observation of direct CP violation in Cabibbo-allowed or doubly-suppressed channel establishes the intervention of New Physics. The only exception to this general rule is provided by modes like $D^\pm \to K_S \pi^\pm$, where one becomes sensitive to (i) the interference between $D^+ \to \bar{K}^0 \pi^+$ and $D^+ \to K^0 \pi^+$ and (ii) the slight CP impurity in the K_S state. The

latter effect dominates, inducing a CP asymmetry of $3.3 \cdot 10^{-3}$.

With x_D, $y_D \sim 0.005 - 0.01$ the possibilities for CP asymmetries proliferate. In addition to the aforementioned direct CP violation one can encounter *time dependent CP* asymmetries. The latter can be induced by CP violation in $\Delta C = 2$ dynamics, or even by CP-conserving contributions to the latter that can make the weak phase in a $\Delta C = 1$ amplitude observable. In both cases an educated Standard Model guess points to time-dependent CP asymmetries of order $10^{-3} \sim x_D \sim 10^{-5}$.

The menu

There are three classes of CP asymmetries:

1. Direct CP violation can lead to a difference in the rates for $D \rightarrow f$ and $\bar{D} \rightarrow \bar{f}$:

$$|A_f| \equiv |A(D \rightarrow f)| \neq |\bar{A}_{\bar{f}}| \equiv |A(\bar{D} \rightarrow \bar{f})| . \quad (11)$$

Strong phase shifts due to final state interactions, are required to produce such asymmetries in partial widths. Since charm decays proceed in an environment populated by many resonances, this requirement will not, in general, represent a limiting factor; it might make, however, the interpretation of signals a more complex task.

2. Indirect CP violation – *i.e.*, that which occurs only in $\Delta C = 2$ transitions. One measure for it is provided by

$$|q/p| \sim 1 + \frac{\Delta\Gamma_D}{\Delta M_D}\sin\phi_{\text{weak}} \neq 1 . \quad (12)$$

The same educated Standard Model guess mentioned above points to $|1-|q/p|| \sim \text{several}\times 10^{-4}$. One should note here that the factor $\Delta\Gamma_D/\Delta M_D$ apparently is close to unity and thus provides no suppression to this observable, unlike the case of B^0 mesons. Thus one has practically undiluted access to a weak phase due to the intervention of New Physics in $D^0\overline{D}^0$ oscillations. As discussed below, such an asymmetry can be searched for cleanly in semileptonic decays of neutral D mesons. While we already know the ratio of wrong-sign leptons is small, their CP asymmetry could conceivably be as large as several percent! While the rate of wrong-sign leptons oscillates with time, the CP asymmetry does not.

3. CP violation in the interference between mixing and decay: In qualitative analogy to $B_d \rightarrow J/\psi K_S^0$, a time-dependent CP asymmetry can arise due to an interference between an oscillation and decay amplitude:

$$\phi_f = \arg\left(\frac{q}{p}\frac{\bar{A}_{\bar{f}}}{A_f}\right) \neq 0 . \quad (13)$$

A CP asymmetry generated by $\phi_f \neq 0$ is also proportional to $\sin\Delta M_D t \simeq x_D(t/\tau_D)$ and thus effectively bounded by x_D; *i.e.*, the present lack of a signal for a time-dependent CP asymmetry in $D^0 \rightarrow K^+K^-$ on about the 1% level is not telling at all, in view of $x_D \leq 1\%$. Yet any improvement in experimental sensitivity could reveal a genuine signal.

Searching for CP violation in charm decays is not a "wild goose chase". We know that baryogenesis requires the presence of CP-violating New Physics. Signals for such New Physics might actually be clearer in D than in B decays: for while *conventional* New Physics scenarios tend to create larger effects in the latter than the former, those signals would also have to contend with a much larger Standard Model "background" in the latter than the former; *i.e.*, the theoretical "signal-to-noise" ratio could be better in charm decays.

The required searches can be undertaken very profitably in runs at the $\Upsilon(4S)$ by tagging the D^0 flavor at production time using $D^{*+} \rightarrow D^0\pi^+$ decays and reconstructing the proper decay time and its error. This is done by tracking the D production and decay vertices with constraints provided by the position and size of the tight e^+e^- interaction region. Relatively short runs in the charm threshold region, *e.g.*, $\psi(3770)$, can provide unique and important information on strong phases needed for a proper interpretation of results obtained in $\Upsilon(4S)$ runs. In the latter D^0 flavor tagging exploits the quantum correlations at $\psi(3770)$; the poor proper time resolution (about the D^0 lifetime) will make time-dependent measurements challenging.

In summary: Comprehensive and precise studies of CP invariance in charm decays provide sensitive probes for the presence of New Physics.

- 'Comprehensive' means that one analyses nonleptonic as well as semileptonic channels on all Cabibbo levels in as many modes as possible; *i.e.*, including final states containing neutrals.

- 'Precise' means that one achieves sensitivity levels of 10^{-3} or better.

Charm decays provide another highly promising avenue towards finding CP violation, namely in final state distributions, rather than in partial widths considered so far. This issue will be addressed separately below.

Side remarks on rare decays

The obvious motivation for measuring the branching fractions for $D^+/D_s^+ \to \mu^+\nu$, $\tau^+\nu$ decays is to extract the decay constants f_D and f_{D_s} in order to compare them with lattice QCD calculations and, hopefully, to validate these calculations with high accuracy. A more ambitious goal is to probe for contributions from a charged Higgs field, as an indication of New Physics.

The mode $D^0 \to \mu^+\mu^-$ arises within the Standard Model mainly through a two photon intermediate state – $D^0 \to \gamma^*\gamma^* \to \mu^+\mu^-$ – and can reach the 10^{-12} level. With the present experimental upper bound of 1.3×10^{-6} there is a search window for New Physics of six orders of magnitude. Multi-Higgs models or SUSY models with R parity breaking could conceivably induce a signal in a range as "large" as few$\times 10^{-8}$ and 10^{-6}, respectively.

Channels such as $D \to \gamma h$, l^+l^-h, $l^+l^-h_1h_2$, with h denoting a hadron, receive relatively sizable contributions within the Standard Model from long distance dynamics. Thus a search for New Physics contributions are not very promising there, unless one can measure precisely the lepton spectra in the final states.

One can probe a rather exotic variant of New Physics by searching for two-body modes $D^+ \to K^+/\pi^+ f$; the charge neutral f denotes a 'familon', which could arise as the Nambu-Goldstone boson resulting from the spontaneous breakdown of a global family symmetry. It has been searched for in K^+ and B^+ decays, but apparently not yet in D^+ decays.

2. $D^0\overline{D}^0$ mixing at $\Upsilon(4S)$ and $\psi(3770)$ energies

The parameters describing charm mixing can be measured in time-dependent studies of D mesons or with time-integrated observables of D mesons produced coherently near charm threshold.

The time-dependent $D^0\overline{D}^0$ mixing formalism and a summary of recent experimental results can be found in Ref. [2]. Many different charm decay modes can be used to search for charm mixing.

- The appearance of "wrong-sign" kaons in semileptonic decays would provide direct evidence for $D^0\overline{D}^0$ oscillations (or another process of beyond Standard Model origin).

- The most precise limits are obtained by exploiting the time-dependence of D decays produced in e^+e^- collision near 10 GeV.

  – The wrong-sign hadronic decay $D^0 \to K^+\pi^-$ is sensitive to linear combinations of the mass and lifetime differences, denoted x'^2 and y'. The relation of these parameters to x_D and y_D is controlled by a strong phase difference $\delta_{K\pi}$.

  – Direct measurements of x_D and y_D independent of unknown strong interaction phases can also be made using time-dependent studies of amplitudes present in multi-body decays of the D^0, for example, $D^0 \to K_S^0\pi^+\pi^-$.

  – Direct evidence of y_D can also appear through lifetime differences between decays to CP eigenstates. The measured quantity in this case y_{CP}, is equivalent to y_D in the absence of CP violation.

- Another approach is to study quantum correlations near charm threshold [3] in $e^+e^- \to D^0\overline{D}^0(\pi^0)$ and $e^+e^- \to D^0\overline{D}^0\gamma(\pi^0)$ decays, which yield C-odd and C-even $D^0\overline{D}^0$ pairs, respectively. Taken together, the time-integrated decay rate to semileptonic, $K\pi$, and CP eigenstates provide sensitivity to x_D, y_D, and $\cos\delta_{K\pi}$.

Several recent results provide evidence that charm mixing is at the upper end of the range of Standard Model predictions.

BABAR [4] and CDF [5] find evidence for oscillations in $D^0 \to K^+\pi^-$, with 3.9σ ($\Delta\mathrm{Log}\mathcal{L}$) and 3.8σ (Bayesian), respectively. The most precise measurement is from Belle which excludes $x'^2 = y' = 0$ at 2.1σ [6] (Feldman-Cousins).

Belle [7] and BABAR [8] see 3.2σ and 3σ effects, respectively, for y_{CP} in $D^0 \to K^+K^-$. The most precise measurement of y_D is in $D^0 \to K_S^0\pi^+\pi^-$ from Belle [9] and is only 1.2σ significant. From the same analysis, Belle also reports a 2.4σ significant result for x_D. The current situation would greatly benefit from more precise knowledge of the strong phase difference δ; this would allow one to unfold x_D and y_D from the $D^0 \to K^+\pi^-$ measurements of x'^2 and y', and directly compare them to the $D^0 \to K_S^0\pi^+\pi^-$ results.

All mixing measurements can be combined to obtain world average (WA) values for x and y. The Heavy Flavor Averaging Group (HFAG) has done such a combination [10, 11]. The resulting 1σ-5σ contours are shown in Fig. 10 and Fig. 11. The fits exclude the no-mixing point ($x = y = 0$) at 6.7σ for both the no CP violation scenario and the case allowing for CP violation. One-dimensional likelihood functions for parameters are obtained by allowing, for any value of the parameter, all other fit parameters to take their preferred values. The resulting likelihood functions give central values, 68.3% C.L. intervals, and 95% C.L. intervals as listed in Table IV.

From the results of the HFAG averaging, we can conclude the following:

- The experimental data consistently indicates that D^0 mesons undergo mixing. The effect is presumably dominated by long-distance processes, and unless $|x| \gg |y|$, it may be difficult to identify New Physics from mixing alone.

- Since y_{CP} is positive, the CP-even state is shorter-lived, as in the K^0-$\overline{K}^0$ system. However, since x appears to be positive, the CP-even state is heavier, unlike in the K^0-$\overline{K}^0$ system.

- There is no evidence yet for CP violation in the D^0-$\overline{D}^0$ system.

TABLE IV: HFAG Charm Mixing Averages.

Fit	Parameter	HFAG Average	95% C.L. Interval
CPV	$x(\%)$	$0.97^{+0.27}_{-0.29}$	(0.39:1.48)
	$y(\%)$	$0.78^{+0.18}_{-0.19}$	(0.41:1.13)
	$R_D(\%)$	0.335 ± 0.009	(0.316:0.353)
	$\delta_{K\pi}(°)$	$21.9^{+11.5}_{-12.5}$	(-6.3:44.6)
	$\delta_{K\pi\pi^0}(°)$	$32.4^{+25.1}_{-25.8}$	(-20.3:82.7)
	$A_D(\%)$	-2.2 ± 2.5	(-7.10:2.67)
	$|q/p|$	$0.86^{+0.18}_{-0.15}$	(0.59:1.23)
	$\phi(°)$	$-9.6^{+8.3}_{-9.5}$	(-30.3:6.5)
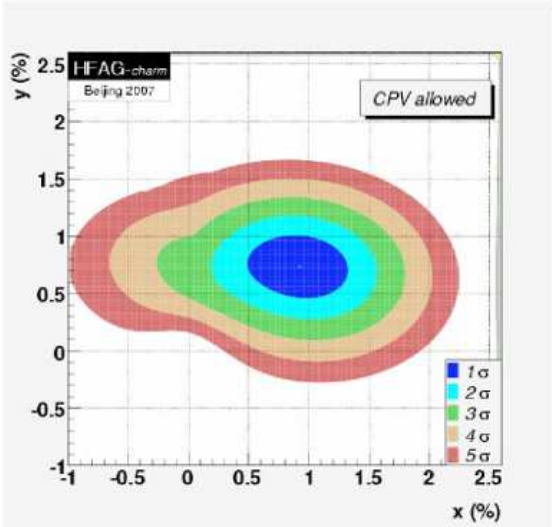
FIG. 10: Two-dimensional 1σ-5σ contours for (x, y), obtained from a global fit to the measured observables for x, y, $|q/p|$, Arg(q/p), $\delta_{K\pi}$, $\delta_{K\pi\pi^0}$, and R_D from measurements of $D^0 \to K^+\ell\nu$, $D^0 \to h^+h^-$, $D^0 \to K^+\pi^-$, $D^0 \to K^+\pi^-\pi^0$, $D^0 \to K^+\pi^-\pi^+\pi^-$, and $D^0 \to K^0_S\pi^+\pi^-$ decays, and double-tagged branching fractions measured at the $\psi(3770)$ resonance (from HFAG [12]).
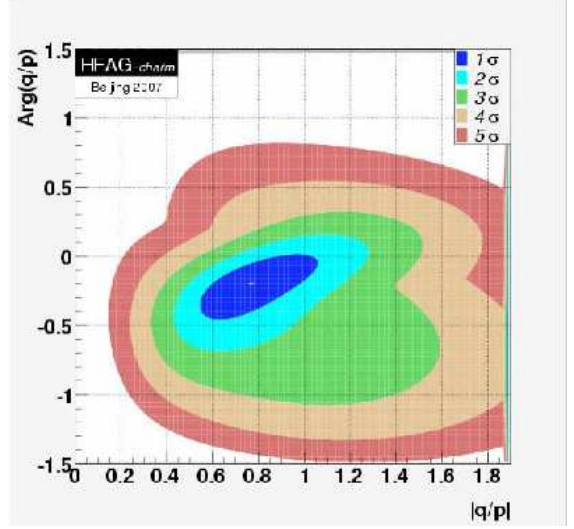
FIG. 11: Two-dimensional 1σ-5σ contours for $(|q/p|, \text{Arg}(q/p))$, obtained from a global fit to the measured observables for x, y, $|q/p|$, Arg(q/p), $\delta_{K\pi}$, $\delta_{K\pi\pi^0}$, and R_D from measurements of $D^0 \to K^+\ell\nu$, $D^0 \to h^+h^-$, $D^0 \to K^+\pi^-$, $D^0 \to K^+\pi^-\pi^0$, $D^0 \to K^+\pi^-\pi^+\pi^-$, and $D^0 \to K^0_S\pi^+\pi^-$ decays, and double-tagged branching fractions measured at the $\psi(3770)$ resonance (from HFAG [12]).

The interpretation of the new results in terms of New Physics is inconclusive. It is not yet clear whether the effect is caused by $x_D \neq 0$ or $y_D \neq 0$ or both, although the latter is favored, as shown in Table IV. Furthermore, there is no single 5σ observation of charm mixing nor is one anticipated from the current B Factories. This situation will be remedied by results anticipated from Super$B$. Table V shows the sensitivity to mixing in $D^0 \to K^+\pi^-$, K^+K^-, and $K^0_S\pi^+\pi^-$ channels from the $\Upsilon(4S)$ data is in excess of 5σ if the lifetime and mass differences in the D^0 system lie at the upper end of the range of Standard Model predictions.

Table V also shows the sensitivity to mixing from two months of running at charm threshold. The sensitivity to the mixing parameters is comparable to five years at $\Upsilon(4S)$, with different sources of systematic uncertainties. The $\psi(3770)$ data provides unique sensitivity to $\cos \delta_{K\pi}$. Although $\cos \delta_{K\pi}$ can be determined from a global fit to $\Upsilon(4S)$ results, the direct measurement from $\psi(3770)$ data allow y' and x'^2 determined from $D^0 \to K^+\pi^-$ to contribute to the precision determination of x and y.

Although the D mesons from $\psi(3770)$ decay are produced nearly at rest in the center-of-mass frame, the asymmetric e^+e^- collisions make time-dependent mixing analyses possible. However, since the production rate of charm during threshold running and $\Upsilon(4S)$ running is comparable, the statistical power of the time-dependent analyses near threshold is small.

TABLE V: Expected precision (σ) on the measured quantities using methods described in the text for Super$B$ with an integrated luminosity of 75 ab^{-1} at Super$B$ at 10 GeV, 300 fb^{-1} ($\sim$ two months) running at charm threshold with Super$B$, and LHCb with 10 fb^{-1}[13].

Mode	Observable	$\Upsilon(4S)$ (75 ab^{-1})	$\psi(3770)$ (300 fb^{-1})	LHCb (10 fb^{-1})
$D^0 \to K^+\pi^-$	x'^2	3×10^{-5}		6×10^{-5}
	y'	7×10^{-4}		9×10^{-4}
$D^0 \to K^+K^-$	y_{CP}	5×10^{-4}		5×10^{-4}
$D^0 \to K_S^0\pi^+\pi^-$	x	4.9×10^{-4}		
	y	3.5×10^{-4}		
	$|q/p|$	3×10^{-2}		
	ϕ	$2°$		
$\psi(3770) \to D^0\overline{D}^0$	x^2		$(1-2) \times 10^{-5}$	
	y		$(1-2) \times 10^{-3}$	
	$\cos\delta$		$(0.01-0.02)$	

A serious limitation in the interpretation of charm oscillations in terms of New Physics is the theoretical uncertainty on the Standard Model prediction. However, the recent evidence for oscillations opens the window to searches for CP asymmetries that do provide unequivocal New Physics signals. The sensitivity to these New Physics signals is shown in Fig. 12.
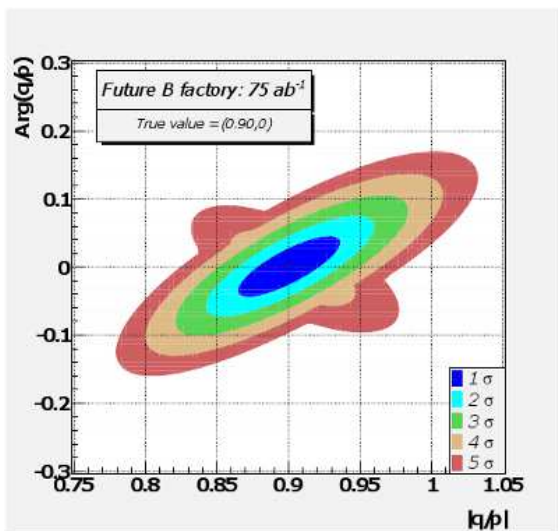
FIG. 12: Projected two-dimensional 1σ-5σ contours with 75 ab^{-1} for ($|q/p|$, Arg(q/p)), obtained from a global fit to the observables for x, y, $|q/p|$, Arg(q/p), $\delta_{K\pi}$, $\delta_{K\pi\pi^0}$, and R_D from the sensitivity estimates in Table V. A "true value" of $|q/p| = 0.90$, Arg(q/p) $= 0$ is assumed.

3. CP violation

Direct CP violation

Searches for CP violation in $\Delta C = 1$ transitions can be performed by measuring asymmetries in the partial widths or in final state distributions.

Golden modes are the Cabibbo-suppressed decays $D^0 \to h^+h^-$, $h = K, \pi$, and the doubly Cabibbo-suppressed decay $D^0 \to K^+\pi^-$. These studies can be performed either time-integrated or by analyzing the time dependence of the D^0 and $\overline{D}^0$ decay rates, although in both cases time-integrated asymmetries are measured. Data at the $\Upsilon(4S)$ provides the largest data sample with excellent purities (as large as $\sim 99\%$). The contamination from $B\overline{B}$ decays can be virtually eliminated by imposing a 2.5 GeV/c cut on the D momentum in the center-of-mass frame, which preserves more than 85% of signal events.

The most precise analysis to date [14] compares time-integrated $D^0 \to h^+h^-$ and $\overline{D}^0 \to h^+h^-$ rates, $a_{CP}^{hh} = [N_{D^0} - N_{\overline{D}^0}]/[N_{D^0} + N_{\overline{D}^0}]$, where N_{D^0} ($N_{\overline{D}^0}$) is the number of D^0 ($\overline{D}^0$) mesons decaying into h^+h^- final state. In this construction, all CP violation contributions, direct and indirect are present. Direct CP violation in one or both modes would be signaled by a non-vanishing difference between the asymmetries for $D^0 \to K^+K^-$ and $D^0 \to \pi^+\pi^-$, $a_{CP}^{KK} \neq a_{CP}^{\pi\pi}$. There are two main experimental challenges in these measurements. Firstly, the experimental asymmetry in D^0 flavor tagging. This asymmetry is measured by determining the relative detection efficiency for soft pions in data, using the Cabibbo-allowed decay $D^0 \to K^-\pi^-$ with (tagged) and without (non-tagged) soft-pion flavor tagging, as a function of the pion-momentum and the polar angle in the lab frame. For the azimuthal de-

pendence, an integrated scale factor is sufficient, since charm production is uniform in azimuth. Since the reconstructed modes are CP-even, this is the only detector asymmetry. Secondly, the forward-backward (FB) asymmetry in $c\bar{c}$ production at $\Upsilon(4S)$, a consequence of the γ/Z^0 interference and higher order QED corrections (both at the percent level at this energy), coupled with the asymmetric acceptance of the detector, which produces a difference in the number of reconstructed D^0 and $\bar{D}^0$ events. This effect is directly measured by determining the number of D^0 and $\overline{D}^0$ events (after soft pion asymmetry correction) as a function of $\cos\theta_D^{CM}$ and decomposing these events into even (representing the CP asymmetry and independent of $|\cos\theta_D^{CM}|$) and odd (representing the FB production asymmetry) parts. The associated systematic uncertainties are therefore not a limiting factor, and are mostly statistical in nature. Other potential sources of uncertainty are highly suppressed because the final states are reconstructed identically for D^0 and $\bar{D}^0$. With a SuperB data sample of 75 ab^{-1}, sensitivities at 3×10^{-4} and 4×10^{-4} level, for a_{CP}^{KK} and $a_{CP}^{\pi\pi}$ respectively, are foreseen.

A time-dependent D-mixing analysis of DCS (wrong sign) $D^0 \to K^+\pi^-$ and $\overline{D}^0 \to K^-\pi^+$ decays can be used to separate the contributions of DCS decays from $D^0\overline{D}^0$ mixing, separately for D^0 and $\overline{D}^0$. A direct CP asymmetry can then be constructed from the difference of DCS D^0 and $\overline{D}^0$ decays, $A_D = (R_{D^0} - R_{\overline{D}^0})/(R_{D^0} + R_{\overline{D}^0})$, where $R_{D^0}(R_{\overline{D}^0})$ is the D^0 ($\overline{D}^0$) DCS rate. The main experimental difficulties in this analysis are accurate proper time reconstruction and calibration, together with asymmetry in the D^0 flavor tagging and the modeling of the differences between K^+ and K^- absorption in the detector. At SuperB, the much smaller luminous region and the significantly enhanced vertexing capabilities provide proper time significances at the 10σ level (3-4 times better than in BABAR [15], with decay length resolution of about 80 μm, $\sim 3\sigma$), significantly reducing the systematic uncertainties associated with the modeling of the long decay time component and possible biases. Systematic uncertainties related to the asymmetry in the soft-pion tagging can be keep under control using a similar procedure to that outlined above. Corrections due to the FB production asymmetry and kaon hadronic interactions can be performed relying mainly on data, through untagged $D^0 \to K^-\pi^+$ and $\overline{D}^0 \to K^+\pi^-$ decays measured as a function of $\cos\theta_D^{CM}$. Scaling the statistical uncertainty from the BABAR analysis to 75 ab^{-1} we obtain a sensitivity on A_D of 4×10^{-3}. To reach or improve this sensitivity level, systematic uncertainties, currently 15×10^{-3}, will have to be reduced by a factor of five or better, which is feasible since the uncertainty of the systematic corrections scale with the size of the data sample.

For asymmetries in final state distributions, the simplest way is to compare CP conjugate Dalitz plots for 3-body decays. Different regions of the Dalitz plot may exhibit CP asymmetries of varying signs that largely cancel out when one integrates over the entire phase space, therefore subdomains of the Dalitz plot could contain significantly larger CP asymmetries than the whole phase space. Since understanding the dynamics is not an easy goal to achieve, one could try up to four strategies, three of which are model-independent. First, quantify differences between the D^0 and $\overline{D}^0$ Dalitz plots in two dimensions. Secondly, look for differences in the angular moments of D^0 and $\overline{D}^0$ intensity distributions. Thirdly, in a model-dependent approach, look for CP asymmetries in the amplitudes describing intermediate states in the D^0 and $\overline{D}^0$ decays. Finally, look for the phase-space integrated asymmetry. Asymmetries in the D^0 flavor assignment and FB production asymmetries only affect the last method, and can be kept under control, as discussed above. From the pioneering BABAR analysis using $D^0 \to \pi^-\pi^+\pi^0$ and $D^0 \to K^-K^+\pi^0$ [16], sensitivities at 3×10^{-4} and 9×10^{-4} level, respectively, are anticipated.

For more complex final states other probes have to be employed. A golden example is discussed below.

Indirect CP violation at the $\Upsilon(4S)$ and $\psi(3770)$

CP violation in mixing can be investigated from the data taken at the $\Upsilon(4S)$ and at the $\psi(3770)$ resonances in semi-leptonic transitions. In both cases one measures an asymmetry from events in which the D^0 or $\bar{D}^0$, previously flavor tagged, has oscillated (signaled as a wrong sign decay),

$$a_{SL} = \frac{N^{--}(t) - N^{++}(t)}{N^{--}(t) + N^{++}(t)} = \frac{|q|^4 - |p|^4}{|q|^4 + |p|^4} , \qquad (14)$$

where N^{--} (N^{--}) represents the number of $D^0 \to \ell^-\nu X$ ($\overline{D}^0 \to \ell^+\nu X$) decays when the other D meson was tagged as D^0 ($\overline{D}^0$) at production time. Data at the $\psi(3770)$ benefit from a very clean environment with almost no background. Several decay channels can be exclusively reconstructed to increase the asymmetry sensitivity. Considering the D^0 and $\bar{D}^0$ both decaying into $K^-\pi^+$, $K^-\pi^+\pi^0$, $K^-\pi^+\pi^+\pi^-$, $K^-e^+\nu$, $K^-\mu^+\nu$, $K^{*-}e^+\nu$, $K^{*-}\mu^+\nu$, $K^{*-}e^+\nu$, $\pi^-e^+\nu$, $\pi^-\mu^+\nu$, K^-K^+ and $\pi^-\pi^+$, and using recent results for the $D^0\overline{D}^0$ mixing parameters x and y [1], a sensitivity to CP violation of 2.5% in one month of running at threshold is expected. The quantum correlation ensures that the same-sign combinations can only be due to mixing; thus hadronic modes can be treated like the semileptonic decays (no DCS contribution). Control

of systematic uncertainties is expected at the percent level, dominated by channels with π^0 and ν particles [17, 18]. Missing mass techniques with full reconstruction of $\psi(3770) \to D\bar{D}$ events, omitting one of the product particles, can be used to evaluate the accuracy in the reconstruction. Large control samples of decay channels with unequivocal particle content like $D^0 \to K_s^0 \pi^+ \pi^-$ and $D^+ \to K^- \pi^+ \pi^+$ will reduce the uncertainty on PID efficiencies. Other sources of systematic uncertainties will also benefit from the precise measurement of the beam energy and improved detector performance.

At the $\Upsilon(4S)$, the soft pion coming from D^* decays $(D^{*+} \to D^0 \pi^+)$ can be used to tag the flavor of the D^0. The measurement of wrong sign leptons in semileptonic decays then provides a clear signature of a mixed event. Data are taken from the continuum. Background events from B decays can be reduced by imposing a 2.5 GeV/c cut on the D momentum. With this method, the statistical sensitivity in the decay asymmetries would reach the 1% level in one year of data taking. Systematic uncertainties are foreseen to arise from the control of backgrounds and PID management (mainly lepton identification), which will benefit from the vertex capabilities to suppress the background and large control samples to study the PID.

*CP*V in the interference of mixing and decay

CP violation in the interplay of $\Delta C = 1, 2$ dynamics can be searched for through time-dependent analyses of $D^0 \to K^+ K^-$ and $D^0 \to \pi^+ \pi^-$ decays. CP violation and $D^0\overline{D}^0$ mixing alter the decay time distribution of D^0 and $\overline{D}^0$ mesons that decay into final states of specific CP, and a time-dependent analysis of the tagged D^0 and $\overline{D}^0$ intensities allows a measurement of the ϕ_f. To a good approximation, these decay time distributions can be treated as exponential, with effective lifetimes τ_{hh}^+ and τ_{hh}^-.

The effective lifetimes can be combined into the quantities y_{CP} and ΔY:

$$y_{CP} = \frac{\tau_{K\pi}}{\langle \tau_{hh} \rangle} - 1 \;, \quad \Delta Y = \frac{\tau_{K\pi}}{\langle \tau_{hh} \rangle} A_\tau \;,$$

where $\langle \tau_{hh} \rangle = (\tau_{hh}^+ + \tau_{hh}^-)/2$ and $A_\tau = (\tau_{hh}^+ - \tau_{hh}^-)/(\tau_{hh}^+ + \tau_{hh}^-)$. The golden mode is $D^0 \to K^+ K^-$, since the combinatorial background is $\sim 10 \times$ smaller than in the $\pi^+ \pi^-$ channel, and the selected sample is $\sim 2 \times$ larger. $D^0 \to K_s^0 \phi$ instead has a large ($\sim 10\%$) contribution from S wave, so it is better analyzed using the Dalitz plot technique (see Sec. 4).

The Super$B$ sensitivity to y_{CP} and ΔY in the KK and $\pi\pi$ modes can be extrapolated from the current *BABAR* analysis [14], assuming that the systematic errors can be kept under control. Provided that CP vi-

olation in mixing is small, the sensitivity to the CP-violating phase is dominated by the first term in the expression for y_{CP} and ΔY.

$$2y_{CP} = (|q/p| + |p/q|)y \cos\phi - (|q/p| - |p/q|)x \sin\phi,$$
$$2\Delta Y = (|q/p| - |p/q|)y \cos\phi - (|q/p| + |p/q|)x \sin\phi,$$

therefore we can estimate the sensitivity as $\delta(\cos\phi) \simeq \delta(y_{CP})/y \simeq 3 \times 10^{-4}/y$, $\delta(\sin\phi) \simeq \delta(\Delta Y)/x \simeq 3 \times 10^{-4}/x$.

Most of the systematic errors affecting the signal cancel in the lifetime ratio. The errors associated with the background are unrelated between D^0 and $\overline{D}^0$ and do not cancel; however they do improve with statistics. In addition, the superior resolution of the vertex detector will further reduce the systematic errors associated with the position measurement. We therefore expect that the systematic errors can be kept under control.

One underlying assumption in the recent *BABAR* analysis [14] is that the resolution bias is the same for all the channels ($K\pi$, KK, $\pi\pi$) and does not depend on the polar angle θ. This could introduce a bias in the measurements, because of the different polar angle acceptance in the various channels. With a higher statistics sample, however, this systematic effect can be overcome by splitting the sample into polar angle (or other variable) intervals. The production asymmetry is not important with *BABAR* statistics, but could become significant at sensitivities of the order of few $\times 10^{-4}$. However this can be handled using control samples, such as the untagged D^0, which have about 5 times more events (assuming D^0 and D^* have the same asymmetry), as discussed in Sec. 3.

T odd correlations

All CP asymmetries observed so far have surfaced in partial widths – with one notable exception: the forward-backward asymmetry $\langle A \rangle$ in the $\pi^+ \pi^-$ and $e^+ e^-$ planes in $K_L \to \pi^+ \pi^- e^+ e^-$. $\langle A \rangle \simeq 14\%$ had been predicted – and confirmed by experiment – as being driven by the indirect CP impurity $|\eta_{+-}| \simeq 0.23\%$. The reason for this magnification by two orders of magnitude is well understood: $\langle A \rangle$ is induced by the interference between a CP-violating and a CP-conserving amplitude, both of which are suppressed, albeit for different reasons. This explains why the enhancement of the CP asymmetry comes at the expense of the branching ratio, which is about $3 \cdot 10^{-7}$; *i.e.*, one has traded branching fraction for the size of the asymmetry.

It is possible that a similar effect and enhancement occurs in the analogous mode $D_L \to K^+ K^- \mu^+ \mu^-$, where D_L denotes the "long-lived" neutral D meson. This mode can be studied uniquely at Super$B$ operating at the $\psi(3770)$ by CP-tagging the other neutral D

meson produced as a "short-lived" D_S:

$$e^+e^- \to \gamma^* \to D^0\overline{D}^0 \to [K^+K^-]_D D_L \quad (15)$$

There is a more general lesson from the $K_L^0 \to \pi^+\pi^- e^+e^-$ example, namely that CP violation could surface in an enhanced fashion in multi-body final states. This could turn an apparent vice in charm decays – the preponderance of multi-body final states – into a virtue. This issue will be addressed in detail in Sec. 4.

These considerations also apply to four-body modes, although less experience with such studies has been accumulated so far. Some intriguing pilot studies have been performed on a comparison of $D^0 \to f$ and $\overline{D}^0 \to f$, $f = K^+K^-\pi^+\pi^-$ channels. Denoting by ϕ the angle between the $\pi^+\pi^-$ and K^+K^- planes, one has

$$\frac{d\Gamma}{d\phi}(D^0 \to f) = \Gamma_1\cos^2\phi + \Gamma_2\sin^2\phi + \Gamma_3\cos\phi\sin\phi \ , \tag{16}$$

$$\frac{d\Gamma}{d\phi}(\overline{D}^0 \to f) = \overline{\Gamma}_1\cos^2\phi + \overline{\Gamma}_2\sin^2\phi - \overline{\Gamma}_3\cos\phi\sin\phi \ . \tag{17}$$

Upon integrating over ϕ, the Γ_3 and $\overline{\Gamma}_3$ terms cancel; $(\Gamma_1, \Gamma_2) \neq (\overline{\Gamma}_1, \overline{\Gamma}_2)$ thus represents a CP asymmetry in the partial widths. The Γ_3 and $\overline{\Gamma}_3$ terms can be projected out by integrating over two quadrants:

$$\langle A \rangle = \frac{\int_0^{\pi/2} d\phi \frac{d\Gamma}{d\phi} - \int_{\pi/2}^{\pi} d\phi \frac{d\Gamma}{d\phi}}{\int_0^{\pi} d\phi \frac{d\Gamma}{d\phi}} = \frac{2\Gamma_3}{\pi(\Gamma_1 + \Gamma_2)} \ , \tag{18}$$

$$\langle \overline{A} \rangle = \frac{\int_0^{\pi/2} d\phi \frac{d\overline{\Gamma}}{d\phi} - \int_{\pi/2}^{\pi} d\phi \frac{d\overline{\Gamma}}{d\phi}}{\int_0^{\pi} d\phi \frac{d\overline{\Gamma}}{d\phi}} = \frac{2\overline{\Gamma}_3}{\pi(\overline{\Gamma}_1 + \overline{\Gamma}_2)} \ . \tag{19}$$

While Γ_3 and $\overline{\Gamma}_3$ represent T-odd moments, they do not necessarily signal T violation, since they could be induced by strong final state interactions. Yet

$$\Gamma_3 \neq \overline{\Gamma}_3 \implies CP \text{ violation.} \tag{20}$$

Such an analysis is theoretically clean, since the dependence on the angle ϕ is specifically predicted, which in turn allows cross checks to control experimental systematics.

Alternatively, one can define another T-odd correlation among the pion and kaon momenta, namely $C_T \equiv \vec{p}_{K^+} \cdot (\vec{p}_{\pi^+} \times \vec{p}_{\pi^-})$ for D^0 and $\overline{C}_T \equiv \vec{p}_{K^-} \cdot (\vec{p}_{\pi^-} \times \vec{p}_{\pi^+})$ for $\overline{D}^0$. Similar to the previous case one has: $C_T \neq -\overline{C}_T \implies CP$ violation. One can then construct T-odd moments

$$A_T = \frac{\Gamma(C_T > 0) - \Gamma(C_T < 0)}{\Gamma(C_T > 0) + \Gamma(C_T < 0)} \ , \tag{21}$$

$$\overline{A}_T = \frac{\Gamma(\overline{C}_T > 0) - \Gamma(\overline{C}_T < 0)}{\Gamma(\overline{C}_T > 0) + \Gamma(\overline{C}_T < 0)} \ , \tag{22}$$

and therefore

$$A_{\mathcal{T}} = \frac{1}{2}(A_T - \overline{A}_T) \neq 0 \implies CP \text{ violation.} \tag{23}$$

A preliminary study based on 380 fb^{-1} of BABAR data suggests a sensitivity of 5.3×10^{-3} in $A_{\mathcal{T}}$ that would extrapolate to 4×10^{-4} for 75 ab^{-1}. With such a sample one can analyze even time slices of $A_{\mathcal{T}}$. These are very promising sensitivities.

Similar CP studies can be performed for other four-body modes, and one can also compare Y_L^0 moments and even full amplitude analyses.

Charm baryon decays

Charm baryons decays are sensitive only to direct CP violation. Longitudinally polarized beams – motivated mainly by CP studies in τ production and decays – provide an intriguing handle for CP studies in charm baryon decays, since charm baryons would be produced with a net longitudinal polarization that would allow the formation of novel CP-odd correlations with the momenta of the particles in the final state. The control of the sign of longitudinal polarization provides an excellent handle on systematics.

4. Mixing and *CP*V in 3-body decays

A Dalitz plot analysis of $D^0 \to K_S^0\pi^+\pi^-$ events provides a golden method for studying mixing and CP violation in mixing/decay/interference. If Dalitz plot model systematics can be kept under control, direct CP-violation can also be investigated. Present BABAR data [19] show that at the $\Upsilon(4S)$, signal events from the decay chain $D^{*+} \to D^0\pi^+$ with $D^0 \to K_S^0\pi^+\pi^-$ can be selected at a rate close to $1000/\text{fb}^{-1}$ with a purity of 97.0%, and a mistag probability of 0.1%. K_S^0 are reconstructed in the $\pi^+\pi^-$ final state; a requirement that the K_S^0 proper time be $\leq 8\tau_S$ allows us to reduce K_L^0 contamination to a level of 10^{-5}. Reconstructing the $D^0 \to K_S^0\pi^+\pi^-$ decay vertex, the D^0 proper time (τ_D) can be measured with an average error of ± 0.2 ps in BABAR and ± 0.1 ps at SuperB, to be compared with the D^0 lifetime of 0.4 ps.

We use the invariant mass of $K\pi$ pairs: $m_+^2 = m^2(K_S^0, \pi^+)$ and $m_-^2 = m^2(K_S^0, \pi^-)$, and we define the following Dalitz plot amplitudes (f_D) and probabilities (p_D), which also depend on t:

$$p_D(m_+^2, m_-^2, t) \equiv |f_D(m_+^2, m_-^2, t)|^2 \quad D^0\text{tag} \tag{24}$$

$$\overline{p}_D(m_+^2, m_-^2, t) \equiv |\overline{f}_D(m_+^2, m_-^2, t)|^2 \quad \overline{D}^0\text{tag} \tag{25}$$

The signatures for interesting processes are the following ones:

- Mixing without *CP* violation

$$p_D(m_+^2, m_-^2, t) = \overline{p}_D(m_-^2, m_+^2, t) \quad \forall \, t \quad \text{but} \quad (26)$$
$$p_D(m_+^2, m_-^2, 0) \neq p_D(m_+^2, m_-^2, t) \quad (27)$$

- *CP* violation in mixing

$$p_D(m_+^2, m_-^2, 0) = \overline{p}_D(m_-^2, m_+^2, 0) \quad \text{and} \quad (28)$$
$$p_D(m_+^2, m_-^2, t) \neq \overline{p}_D(m_-^2, m_+^2, t) \quad (29)$$

- Direct *CP* violation

$$p_D(m_+^2, m_-^2, 0) \neq \overline{p}_D(m_-^2, m_+^2, 0) \quad (30)$$

and the quantities, to be measured, that enter in the previous Dalitz plot distribution functions, are: x, y (mixing parameters), $|q/p|$ or $\epsilon = \frac{1-|q/p|}{1+|q/p|}$ and $\phi = \arg(\frac{q\bar{A}_f}{pA_f})$ (*CP*-violation parameters).

x, y, ϵ and ϕ can be extracted in a Dalitz model-dependent analysis with the isobar or K-matrix approach, using global fits. Examples are described in references [19, 20]. For the model-dependent approach, we conservatively estimate the Super$B$ sensitivity at 75 ab^{-1} by extrapolating from the current analyses. Statistical errors can be scaled with the square root of luminosity. The result exceeds the desired goal of 10^{-3}, a level not reachable by BES-III. The second source is from systematic errors due to the experiment. They are mainly due to background parametrization, efficiency variation over the Dalitz plot, experimental resolution biases on Dalitz plot variables, decay time parametrization, and mistag fractions. Background parametrization is checked with sidebands (according to the Monte Carlo, the background does not peak in the D^0 mass signal region), and scales with statistics. Efficiency variation studied with Monte Carlo events scales with the Monte Carlo statistics. Biases on Dalitz plot variable mass resolution are negligible. Decay time parametrization improves with the size of the data sample and due to the time resolution at Super$B$. Mistag fractions can be checked with other final D states; their contribution is negligible. It is thus plausible that the errors arising from experimental sources can be scale with statistics as well, but we prefer to be conservative, and evaluate these systematic errors using an additional safety factor of two. These errors are shown in Table VI; we can see that they are smaller than the statistical errors.

The last, but not the least important, source of systematic errors, is the model used, typically isobar or K-matrix models or a partial-wave analysis. Uncertainties arise from radius parameters, masses and widths of the resonances, and the choice of resonances included in the fit. Recent results from CLEO and Belle [9, 20] have, however, demonstrated that the

TABLE VI: Current Belle errors with 0.54 ab^{-1} on relevant mixing and *CP* violation parameters.

Par.	Stat.	Exp. Syst.	Model Syst.	Total
x (10^{-4})	30.0	8.0	12.0	33.3
y (10^{-4})	24.0	10.0	7.0	26.9
ϵ (10^{-4})	15.0	2.5	4.0	15.7
ϕ (deg)	17.0	4.0	3.0	17.7

TABLE VII: Super$B$ errors with 75 ab^{-1} on relevant mixing and *CP* violation parameters.

Par.	Stat.	Exp. Syst.	Model Syst.	Total
x (10^{-4})	2.5	1.4	4.0	4.9
y (10^{-4})	2.0	1.7	2.3	3.5
ϵ (10^{-4})	1.3	0.4	1.3	1.9
ϕ (deg)	1.4	0.7	1.0	1.9

mixing and *CP* violation parameters are not very sensitive to Dalitz model variations. The sensitivity to models will be checked using two model independent approaches:

- With a very large data sample, a partial-wave analysis is capable to determine the amplitude and phase variation over the phase space directly from data.

- Data collected at charm threshold will make the $D^0\overline{D}^0$ relative phase accessible [21].

Even if it is extremely difficult to make predictions on the Dalitz model systematics at Super$B$, it is reasonable to assume that these will be substantially reduced with respect to the present errors from Belle [9]. By comparing the CLEO analysis based on 9.0 fb^{-1} with the Belle analysis based on 540 fb^{-1}, we realize an improvement of the Dalitz model systematic error of more than a factor of four on average. This improvement is mainly due to the fact that the larger statistics data sample allows a better determination of the Dalitz model parameters. Contemplating a factor of three improvement for the model error at Super$B$ seems conservative, since it does not take into account the benefits of partial-wave analysis, and the use of data collected at charm threshold. Sensitivity predictions for mixing and *CP* violation parameters at Super$B$ are shown in Table VII.

[1] Heavy Flavor Averaging Group (E. Barberio *et al.*), [arXiv:hep-ex/0603003]. Updates and plots: http://www.slac.stanford.edu/xorg/hfag.
[2] D. M. Asner, to appear in the Review of Particle Physics.

[3] D. M. Asner and W. M. Sun, Phys. Rev. D **73**, 034024 (2006) [arXiv:hep-ph/0507238].

[4] B. Aubert *et al.* [*BABAR* Collaboration], Phys. Rev. Lett. **98**, 211802 (2007) [arXiv:hep-ex/0703020].

[5] T. Aaltonen *et al.* [CDF Collaboration], Phys. Rev. Lett. **100**, 121802 (2008) [arXiv:0712.1567 [hep-ex]].

[6] L. M. Zhang *et al.* [Belle Collaboration], Phys. Rev. Lett. **96**, 151801 (2006) [arXiv:hep-ex/0601029].

[7] M. Staric *et al.* [Belle Collaboration], Phys. Rev. Lett. **98**, 211803 (2007) [arXiv:hep-ex/0703036].

[8] B. Aubert *et al.* [*BABAR* Collaboration], arXiv:0712.2249 [hep-ex] - submitted to Phys. Rev. D.

[9] K. Abe *et al.* [Belle Collaboration], Phys. Rev. Lett. **99**, 131803 (2007) [arXiv:0704.1000 [hep-ex]].

[10] A. J. Schwartz, *Proceedings of 5th Flavor Physics and CP Violation Conference (FPCP 2007), Bled, Slovenia, 12-16 May 2007, pp 024* [arXiv:0708.4225 [hep-ex]].

[11] A. J. Schwartz, *Proceedings of the BES-Belle-CLEO-BABAR Workshop on Charm Physics, IHEP, Beijing, 26-27 November 2007.* [arXiv:0803.0082 [hep-ex]].

[12] Heavy Flavor Averaging Group (HFAG)-charm subgroup http://www.slac.stanford.edu/xorg/hfag/charm/.

[13] P. Spradlin, Proceedings of the Innternation Workshop on Charm Physics (Charm 2007), Ithaca, New York, p.40. [arXiv:0711.1661 [hep-ex]].

[14] B. Aubert *et al.* [*BABAR* Collaboration], Phys. Rev. Lett. **100**, 061803 (2008) [arXiv:0709.2715 [hep-ex]].

[15] B. Aubert *et al.* [*BABAR* Collaboration], Phys. Rev. Lett. **98**, 211802 (2007) [arXiv:hep-ex/0703020].

[16] B. Aubert *et al.* [*BABAR* Collaboration], submitted to Phys. Rev. Lett. [arXiv:0802.4035].

[17] Q. He *et al.* [CLEO Collaboration], Phys. Rev. Lett. **95**, 121801 (2005), Erratum-ibid. **96**, 199903 (2006) [arXiv:hep-ex/0504003].

[18] T. E. Coan *et al.* (CLEO Collaboration) Phys. Rev. Lett. **95**, 181802 (2005) [arXiv:hep-ex/0506052].

[19] B. Aubert *et al.* [*BABAR* Collaboration], Phys. Rev. Lett. **95**, 121802 (2005) [arXiv:hep-ex/0504039].

[20] D. M. Asner *et al.* [CLEO Collaboration], Phys. Rev. D **72**, 012001 (2005) [arXiv:hep-ex/0503045].

[21] E. White and Q. He [CLEO Collaboration], arXiv:0711.2285 [hep-ex].

Tau Physics

Searches for lepton flavor violation in tau decays constitute one of the most theoretically and experimentally clean and powerful probes to extend our knowledge in particle physics. In this specific area, $SuperB$ has clear advantages over the LHC experiments and SuperKEKB, and it is complementary to muon LFV searches. Experimental investigations on CP violation in tau decay and on the tau EDM and $g-2$ provide $SuperB$ with additional experimentally clean tools to shed light on unexplored territories, with the ability to test some specific New Physics scenarios. Furthermore, precise tests of lepton universality can reveal new phenomena, although attaining the required precision is challenging, $SuperB$ is once again the best-positioned project, due to its very high luminosity.

With an integrated luminosity of $75\,\mathrm{ab}^{-1}$, $SuperB$ will be able to explore a significant portion of the parameter space of most New Physics scenarios by searching for LFV in tau decays. While the MEG experiment [1] will search for $\mu \to e\gamma$ with great sensitivity, $SuperB$ will uniquely explore transitions between the third and first or second generations, providing crucial information to determine the specific New Physics model that produces LFV. The LHC experiments are, in general, not competitive in LFV searches; SuperKEKB, with $10\,\mathrm{ab}^{-1}$, will also be able to explore LFV in tau decay, but with a sensitivity that does not challenge the majority of New Physics models. $SuperB$ has the advantage of higher luminosity, which increases its tau LFV sensitivity by a factor 2.7 in the worst hypothesis of background-dominated analyses, even assuming no improvement in analysis techniques. For analyses which are background-free, $SuperB$ will have a sensitivity at least 7.5 times better, and will also profit from reduced machine background. Furthermore, $SuperB$ can have a 85% linearly polarized electron beam, which will produce tau leptons with known and well-defined polarization that can be exploited either to improve the selection of LFV final states, given a specific LFV interaction, or to better determine the features of the LFV interaction, once they are found.

Experimental studies on CP violation in tau decay and on the tau EDM and $g-2$ are especially clean tools, because they rely on measurement of asymmetries with relatively small systematic uncertainties from the experiment. The beam polarization also improves the experimental sensitivity for tau EDM and $g-2$ determinations, by allowing measurements of the polarization of a single tau, rather than measurements of correlations between two taus produced in the same events. with this technique, $SuperB$ can test whether supersymmetry is a viable explanation for the present discrepancy on the muon $g-2$. Although the most plausible New Physics models constrained with the available experimental results predict CP violation in tau decay and the tau EDM in a range that is not measurable, $SuperB$ can test specific models that enhance those effects to measurable levels.

1. Lepton Flavor Violation

Predictions from New Physics models

In the following, we discuss the size of τ LFV effects on decays and correlations that are expected in supersymmetric extensions of the Standard Model and, in particular, in the so-called constrained MSSM, The flavor-conserving phenomenology of this framework is characterized by five parameters: $M_{1/2}$, M_0, A_0, $\tan\beta$, sgn μ. We will discuss a subset of the "Snowmass Points and Slopes" (SPS) [2], listed in Table VIII, in this five-dimensional parameter space to illustrate the main distinctive features of the model as they relate to lepton flavor violation.

Specifying one such point is sufficient to determine the phenomenology of the model relevant for the LHC, but it is not sufficient to unambiguously compute LFV rates. The amount of flavor-violation is controlled by other parameters, which play no role in high-p_T physics. Nonetheless, specifying the flavor-conserving parameters allows us to simplify the description of LFV decays and, in particular, to establish clear correlations among different processes.

TABLE VIII: Values of $M_{1/2}$, M_0, A_0, $\tan\beta$, and sign of μ for the SPS points considered in the analysis.

SPS	$M_{1/2}$ (GeV)	M_0 (GeV)	A_0 (GeV)	$\tan\beta$	μ
1 a	250	100	-100	10	> 0
1 b	400	200	0	30	> 0
2	300	1450	0	10	> 0
3	400	90	0	10	> 0
4	300	400	0	50	> 0
5	300	150	-1000	5	> 0

At all the SPS points, LFV decays are dominated by the contribution of dipole-type effective operators of the form $(\bar{l}_i \sigma_{\mu\nu} l_j F^{\mu\nu})$. Defining $\mathcal{R}^{(a)}_{(b)} = \mathcal{B}(\tau \to a)/\mathcal{B}(\tau \to b)$, The dipole dominance allows us to establish the following relations,

$$\mathcal{R}^{(\mu ee)}_{(\mu\gamma)} \approx 1.0 \times 10^{-2} \ \to \ \mathcal{B}(\tau \to \mu e^+ e^-) < 5 \times 10^{-10}$$

$$\mathcal{R}^{(\mu\rho^0)}_{(\mu\gamma)} \approx 2.5 \times 10^{-3} \rightarrow \mathcal{B}(\tau \rightarrow \mu\rho^0) < 10^{-10}$$

$$\mathcal{R}^{(3\mu)}_{(\mu\gamma)} \approx 2.2 \times 10^{-3} \rightarrow \mathcal{B}(\tau \rightarrow 3\mu) < 10^{-10}$$

$$\mathcal{R}^{(\mu\eta)}_{(\mu\gamma)} < 10^{-3} \rightarrow \mathcal{B}(\tau \rightarrow \mu\eta) < 5 \times 10^{-11},$$

where the bounds correspond to the present limit $\mathcal{B}(\tau \rightarrow \mu\gamma) < 4.5 \times 10^{-8}$. Similar relations hold for $\tau \rightarrow e$ transitions. As a result, in such a framework only $\tau \rightarrow \mu\gamma$ and $\tau \rightarrow e\gamma$ decays are within experimental reach.

To estimate the overall scale of $\tau \rightarrow (\mu, e)\gamma$ rates, we must specify the value of the LFV couplings, since they are not determined by the SPS conditions. In the mass-insertion and leading-log approximation, assuming that the leading LFV couplings appear in the left-handed slepton sector, we can write

$$\frac{\mathcal{B}(l_j \rightarrow l_i\gamma)}{\mathcal{B}(l_j \rightarrow l_i\bar{\nu}_i\nu_j)} \approx \frac{\alpha^3}{G_F^2} \frac{\left|\left(m^2_{\tilde{L}}\right)_{ji}\right|^2}{M_S^8} \tan^2\beta, \quad (31)$$

where, to a good approximation, $M_S^8 \simeq 0.5 M_0^2 M_{1/2}^2 \times (M_0^2 + 0.6 M_{1/2}^2)^2$. In a Grand Unified Theory (GUT) with heavy right-handed neutrinos, the off-diagonal entries of the slepton mass matrix $m^2_{\tilde{L}}$ are likely to be dominated by the flavor mixing in the (s)neutrino sector. These terms can be expressed as

$$\left(m^2_{\tilde{L}}\right)_{ji} \approx -\frac{6M_0^2 + 2A_0^2}{16\pi^2} \delta_{ij}, \quad (32)$$

where $\delta_{ij} = \left(Y_\nu^\dagger Y_\nu\right)_{ji} \log(M_{GUT}/M_R)$ in terms of the neutrino Yukawa couplings (Y_ν), the average heavy right-handed neutrino mass (M_R) and the GUT scale $(M_{GUT} \sim 10^{15}$–10^{16} GeV). Given the large phenomenological value of the 2–3 mixing in the neutrino sector (and the corresponding suppression of the 1–3 mixing) we expect $|\delta_{32}| \gg |\delta_{31}|$ hence $\mathcal{B}(\tau \rightarrow \mu\gamma) \gg \mathcal{B}(\tau \rightarrow e\gamma)$. For sufficiently heavy right-handed neutrinos, the normalization of Y_ν is such that $\mathcal{B}(\tau \rightarrow \mu\gamma)$ can reach values in the 10^{-9} range. In particular, $\mathcal{B}(\tau \rightarrow \mu\gamma) \gtrsim 10^{-9}$ if at least one heavy right-handed neutrino has a mass around or above 10^{13} GeV (in SPS 4) or 10^{14} GeV (in SPS 1a,1b,2,3,5).

A key issue that must be addressed is the role of $\mathcal{B}(\mu \rightarrow e\gamma)$ in constraining the LFV couplings and, more generally, the correlations between $\mathcal{B}(\tau \rightarrow (\mu, e)\gamma)$ and $\mathcal{B}(\mu \rightarrow e\gamma)$ in this framework. An extensive analysis of such questions has been presented in Ref. [3, 4], under the hypothesis of a hierarchical spectrum for the heavy right-handed neutrinos.

The overall structure of the $\mathcal{B}(\tau \rightarrow \mu\gamma)$ vs. $\mathcal{B}(\mu \rightarrow e\gamma)$ correlation in SPS 1a is shown in Fig. 13. As anticipated, $\mathcal{B}(\tau \rightarrow \mu\gamma) \sim 10^{-9}$ requires a heavy right-handed neutrino around or above 10^{14} GeV. This possibility is not excluded by $\mathcal{B}(\mu \rightarrow e\gamma)$ only if the 1–3

mixing in the lepton sector (the θ_{13} angle of the neutrino mixing matrix) is sufficiently small. This is a general feature, valid at all SPS points, as illustrated in Fig. 14. In Table IX we show the predictions for $\mathcal{B}(\tau \rightarrow \mu\gamma)$ and $\mathcal{B}(\tau \rightarrow 3\mu)$ corresponding to the neutrino mass parameters chosen in Fig. 14 (in particular $M_{N_3} = 10^{14}$ GeV), for the various SPS points. Note that this case contains points that are within the SuperB sensitivity range, yet are not excluded by $\mathcal{B}(\mu \rightarrow e\gamma)$ (as illustrated in Fig. 14).
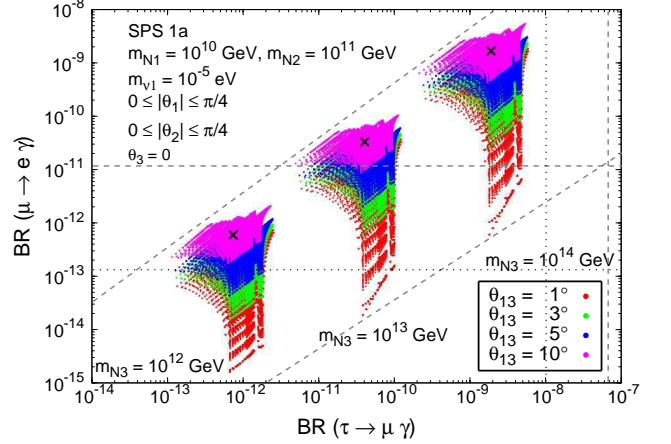
FIG. 13: $\mathcal{B}(\tau \rightarrow \mu\gamma)$ vs. $\mathcal{B}(\mu \rightarrow e\gamma)$ in SPS 1a, for three reference values of the heavy right-handed neutrino mass and several values of θ_{13}. The horizontal dashed (dotted) line denotes the present experimental bound (future sensitivity) on $\mathcal{B}(\mu \rightarrow e\gamma)$. All other relevant parameters are set to the values specified in Ref. [3].
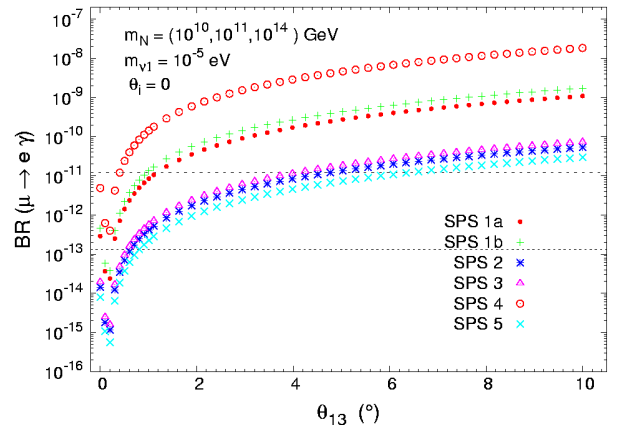
FIG. 14: $\mathcal{B}(\mu \rightarrow e\gamma)$ as a function of θ_{13} (in degrees) for various SPS points. The dashed (dotted) horizontal line denotes the present experimental bound (future sensitivity). All other relevant parameters are set to the values specified in Ref. [3].

TABLE IX: Predictions for $\mathcal{B}(\tau \to \mu\gamma)$ and $\mathcal{B}(\tau \to 3\mu)$ corresponding to the SPS points. The values of m_{N_i} and m_{ν_1} are as specified in Fig. 14 [3].

SPS	1 a	1 b	2	3	4	5
$\mathcal{B}(\tau \to \mu\gamma) \times 10^{-9}$	4.2	7.9	0.18	0.26	97	0.019
$\mathcal{B}(\tau \to 3\mu) \times 10^{-12}$	9.4	18	0.41	0.59	220	0.043

LFV in the NUHM scenario

At large $\tan\beta$ and not too heavy Higgs masses, another class of LFV interactions is relevant, the effective coupling between a μ–τ pair and the heavy (scalar and pseudoscalar) Higgs bosons. This coupling can overcome the constraints on $\mathcal{B}(\tau \to \mu\mu\mu)$ and $\mathcal{B}(\tau \to \mu\eta)$ dictated by $\mathcal{B}(\tau \to \mu\gamma)$ in the dipole-dominance scenario. Such a configuration cannot be realized in the CMSSM, but it could be realized in the so-called NUHM SUSY scenario, which is also theoretically well-motivated and rather general. In such a framework, there are specific regions of the parameter space in which $\tau \to \mu\eta$ could have a branching ratio in the 10^{-9}–10^{-10} range, comparable or even slightly larger than $\mathcal{B}(\tau \to \mu\gamma)$ [5].

Finally, in more exotic New Physics frameworks, such as SUSY without R parity, Little Higgs Models with T parity (LHT) or Z' models with non-vanishing LFV couplings ($Z'\ell_i\ell_j$), the $\tau \to \mu\mu\mu$ rate could be as large as, or even larger than $\tau \to \mu\gamma$ (see *e.g.*, [6]). In this respect, an improvement of $\mathcal{B}(\tau \to \mu\mu\mu)$ at the 10^{-10} level would be interesting even with $\mathcal{B}(\tau \to \mu\gamma) \lesssim 10^{-9}$.

Super$B$ experimental reach

SuperB experimental reach

A sensitive search for lepton flavor-violating τ decays at Super$B$ requires signal to be selected with as high an efficiency as possible, while allowing minimal, and preferably zero, background. A candidate $e^+e^- \to \tau^+\tau^-$ events obtained from an initial screening selection is divided into hemispheres in the center-of-mass frame, each containing the decay products of one τ lepton. Unlike Standard Model τ decays, which contain at least one neutrino, the decay products from a LFV decay have a combined energy in the center-of-mass frame equal to $\sqrt{s}/2$ and a mass equal to that of the τ. A requirement on the two dimensional signal region in the $E_{\ell X}$–$M_{\ell X}$ plane therefore provides a powerful tool to reject backgrounds, which arise from well-understood Standard Model $\tau$ decays. Consequently, residual background rates and distributions are reliably estimated from Monte Carlo simulations and validated using quantitative comparisons with data as various selection requirements are applied. Global event properties and an explicit identification of the non-signal τ decay can be applied to suppress non-τ backgrounds with only marginal loss of efficiency.

The considerable experience developed in searching for these decays in the ~ 0.5 ab^{-1} data set at *BABAR* enables us confidently to estimate background levels to be expected with 75 ab^{-1} for selection strategies similar to those of the existing experiments. These lead us to classify the LFV decay modes into two categories for the purposes of estimating the experimental τ LFV discovery reach of Super$B$: (i) modes having "irreducible backgrounds" and (ii) modes that do not have irreducible backgrounds. For luminosities of 10^{36} cm^{-2}s^{-1}, $\tau^\pm \to \ell^\pm\gamma$ decays fall into category (i), whereas $\tau \to \ell\ell\ell$ and $\tau^\pm \to \ell^\pm h^0$ generally fall into category (ii), where ℓ is either a muon or electron and h^0 is a hadronic system. The hadronic system may be identified as a pseudoscalar or vector meson (π^0, η, η', K^0_S, ω, ϕ, K^* *etc.*) or a non-resonant system of two pions, two kaons or a pion and kaon.

The category (ii) decay modes have the property that with perfect particle identification no known process or combination of processes can mimic the signal at rates relevant to Super$B$. The challenge in searching for these decays is thus to remove all non-τ backgrounds and to provide as powerful a particle identification as possible. For category (i) modes, however, even with perfect particle identification, there exist backgrounds that limit the discovery sensitivity. In fact, there are no $\tau^\pm \to \ell^\pm\gamma$ Standard Model processes expected at these luminosities, but there are combinations of processes that can mimic this signal, even with perfect measurements. In the case of $\tau^\pm \to \mu^\pm\gamma$ for example, the irreducible background arises from events having a $\tau \to \mu\nu\bar{\nu}$ decay and a γ from initial state radiation (ISR) in which the photon combines with the muon to form a candidate that accidentally falls into the signal region in the $E_{\ell X}$–$M_{\ell X}$ plane. At sufficiently high rates, $\tau \to \ell\pi^0$ and $\tau \to \ell\eta$ ($\eta \to \gamma\gamma$) searches will suffer the same problems when two hard ISR photons accidentally reconstruct to a π^0 or η mass, but the rate for two hard-photon ISR emission will be roughly 100 times lower than the rate for a signal hard photon emission and lower still when requiring a $\gamma\gamma$ mass to match that of a π^0 or η. Consequently, this is not expected to be an issue at Super$B$ luminosities. Similarly, $\tau \to ee^+e^-$ and $\tau \to \mu e^+e^-$ can, in principle, suffer a background from $\tau \to \ell\nu\bar{\nu}e^+e^-$ events where the ISR photon undergoes internal pair production. Such background events are expected to start to just become measurable for luminosities roughly 100 times higher than current experiments, and so might just begin to impact the experimental bounds placed on those modes at Super$B$.

The experimental reach is expressed here in terms of "the expected 90% CL upper limit" assuming no signal, as well as in terms of a 4σ discovery branching fraction in the presence of projected backgrounds. In the absence of signal, for large numbers of background events $N_{\rm bkd}$, the 90% CL upper limit for the number of signal events can be given as $N_{90}^{UL} \sim 1.64\sqrt{N_{\rm bkg}}$, whereas for small $N_{\rm bkg}$ a value for N_{90}^{UL} is obtained using the method described in [7], which gives, for $N_{\rm bkg} \sim 0$, $N_{90}^{UL} \sim 2.4$. If a signal is determined from counting events within a signal region rather than from a fit, the 90% CL branching ratio upper limit is:

$$B_{90}^{UL} = \frac{N_{90}^{UL}}{2N_{\tau\tau}\epsilon} = \frac{N_{90}^{UL}}{2\mathcal{L}\sigma_{\tau\tau}\epsilon}, \qquad (33)$$

where $N_{\tau\tau} = \mathcal{L}\sigma_{\tau\tau}$ is the number of τ-pairs produced in e^+e^- collisions; $\mathcal{L}$ is the integrated luminosity, $\sigma_{\tau\tau}$=0.919 nb [8] is the τ-pair production cross section, and ϵ is the signal efficiency.

The $\tau^\pm \to \mu^\pm\gamma$ projected sensitivity is based on the published BABAR analysis [9], but incorporating changes designed for a very high luminosity data set and using the improved muon particle identification efficiencies that became available with a hardware upgrade to the BABAR muon system. The published analysis explicitly identifies the non-signal τ decays as specific Standard Model decay modes. In the published analysis, this set of tag modes includes $\tau \to \mu\nu\bar{\nu}$, which has a disproportionate amount of μ-pair background compared to the other tag modes. For SuperB luminosities it would appear that a more optimal analysis would not include this mode. The consequence is that the efficiency for a 2σ signal ellipse region suffers a decrease from dropping the μ-tag, but increases from the other improvements to both the analysis and the hardware, so that the net efficiency is 7.4%. The background levels for 75 ab^{-1} are projected from the Monte Carlo to be 200 ± 50 events from the $\tau \to \mu\nu\bar{\nu}(\gamma)$ irreducible background. This leads to an expected 90%CL upper limit of 2.3×10^{-9} and 4σ discovery reach of 5.6×10^{-9}. It is important to note that further improvements can be obtained using the SuperB polarized electron beam. For a 100% polarized electron beam, the polar angles of the signal decay products provide additional background suppression, as is evident from Figure 15. The "irreducible background" would be cut by 70% for a 39% loss in signal efficiency. This would result in approximately a 10% improvement in the sensitivity: an expected upper limit of 2.1×10^{-9} and 4σ discovery level of 5.0×10^{-9}. However, by far the most important aspect of having the polarization is the possibility to determine the helicity structure of the LFV coupling from the final state momenta distributions (see for instance Ref.[10] for the $\tau \to \mu\mu\mu$ process). Note that for a data sample of 15 ab^{-1} using a machine with no polarization, the

same analysis and detector can be expected to yield an expected upper limit of 5.2×10^{-9} with a discovery potential of 1.3×10^{-8}. Similar analyses can be expected to yield comparable sensitivities for the $\tau^\pm \to e^\pm\gamma$ LFV decay mode, based on the published BABAR analysis [11].

The situation for the other LFV decays, $\tau \to \ell_1\ell_2\ell_3$ and $\tau \to \ell h$, is different, as these modes do not suffer the problem of accidental photons with which the $\tau^\pm \to \ell^\pm\gamma$ searches must contend. In these cases, one can project sensitivities assuming $N_{\rm bkg}$ comparable to backgrounds in existing analyses for approximately the same efficiencies. For illustrative purposes, we demonstrate how this is accomplished for the $\tau^\pm \to \mu^\pm\mu^+\mu^-$ based on modifications to the published BABAR analysis [12]. The published analysis managed to suppress the backgrounds for the data set without explicitly identifying the Standard Model τ decays for the non-signal τ and using the loosest muon identification algorithms.
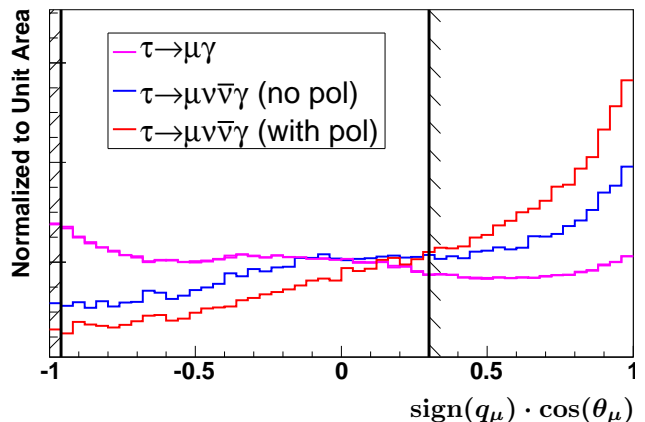
FIG. 15: Distribution of the cosine of the signal-side muon multiplied by the muon charge for signal and background events with and without electron beam polarization in the $\tau^\pm \to \mu^\pm\gamma$ search analysis at SuperB.

Table X summarizes the sensitivities for various LFV decays.

TABLE X: Expected 90% CL upper limits and 4σ discovery reach on $\tau^\pm \to \mu^\pm\gamma$ and $\tau^\pm \to \mu^\pm\mu^+\mu^-$ LFV decays with 75 ab^{-1} with a polarized electron beam.

Process	Expected 90%CL upper limited	4σ Discovery Reach
$\mathcal{B}(\tau \to \mu\,\gamma)$	2×10^{-9}	5×10^{-9}
$\mathcal{B}(\tau \to \mu\,\mu\,\mu)$	2×10^{-10}	8.8×10^{-10}

2. Lepton universality

Tree-level Higgs exchanges in supersymmetric new physics models can induce modifications of lepton universality of order 0.1% [13], smaller but close to the present experimental accuracy of $\approx$ 0.2% [14]. As discussed in Ref. [15], Super$B$ can probably measure lepton universality to 0.1% or better. However the measurement is limited by experimental systematic uncertainties on the measurement of the tau leptonic branching fractions and the tau lifetime, as the modest progress provided by the existing B Factories also confirms [16]. Therefore it cannot be advocated that the Super$B$ advantages in terms of luminosity are crucial and necessary for the advancement of this particular sector, although large statistical samples will be an advantage to reduce experimental systematic uncertainties.

3. Tau CPV, EDM and $g-2$

Predictions from New Physics models

CP violation and T-odd observables in tau decay

CP violation in the quark sector has been observed both in the K and in the B systems; the experimental results are thus far fully explained by the complex phase of the CKM matrix. On the contrary, CP violation in the lepton sector has yet not been observed. Within the Standard Model, CP-violating effects in charged-lepton decays are predicted to be vanishingly small. For instance, the CP asymmetry rate of $\tau^{\pm} \rightarrow K^{\pm}\pi^0\nu$ is estimated to be of order $\mathcal{O}(10^{-12})$ [17]. Evidence for CP violation in tau decay would therefore be a clear signal of New Physics. In one instance, the $\tau^{\pm} \rightarrow K_S\pi^{\pm}\nu$ rate asymmetry, a small CP asymmetry of 3.3×10^{-3} is induced by the known CP-violating phase of the $K^0\overline{K}^0$ mixing amplitude [18]. This asymmetry is known to 2% precision. Thus, this mode can serve as a calibration, and in addition, any deviation from the expected asymmetry would be a sign of New Physics.

Most of the known New Physics models cannot generate observable CP-violating effects in τ decays (see *e.g.*, [6]). The only known exceptions are R parity-violating supersymmetry [19] or specific non-supersymmetric multi-Higgs models. In such a framework, the CP asymmetries of various τ-decay channels can be enhanced up to the 10^{-1} level, without conflicting with other observables, and saturating the experimental limits obtained by CLEO [20]. Similar comments also apply to T-odd CP-violating asymmetries in the angular distribution of τ decays.

Tau electric dipole moment

In natural SUSY frameworks, lepton EDMs (d_ℓ) scale linearly with the lepton mass. As a result, the existing limits on the electron EDM generally preclude any visible effect in the τ and μ cases. In multi-Higgs models, however, EDMs scale with the cube of the lepton masses [21], d_τ can thus be substantially enhanced. However, in this case the electron and muon EDMs receive sizable two-loop effects via Barr-Zee diagrams, which again scale linearly with the lepton masses. As a result, one can derive an approximate bound $d_\tau \lesssim 0.1 \times (m_\tau/m_\mu)^3(m_\mu/m_e)d_e$ which is still very strong. From the present experimental upper bound on the electron EDM, $d_e \lesssim 10^{-27}e$ cm, it follows that $d_\tau \lesssim 10^{-22}e$ cm.

Tau $g-2$

The Standard Model prediction for the muon anomalous magnetic moment is not in perfect agreement with recent experimental results. In particular, $\Delta a_\mu = a_\mu^{\mathrm{exp}} - a_\mu^{\mathrm{SM}} \approx (3\pm1)\times10^{-9}$. Within the MSSM, this discrepancy can naturally be accommodated, provided $\tan\beta \gtrsim 10$ and $\mu > 0$.

A measurement of the τ anomalous magnetic moment could be very useful to confirm or disprove the interpretation of Δa_μ as due to New Physics contributions. The natural scaling of heavy-particle effects on lepton magnetic dipole moments, implies $\Delta a_\tau/\Delta a_\mu \sim m_\tau^2/m_\mu^2$. Thus, if we interpret the present muon discrepancy $\Delta a_\mu = a_\mu^{\mathrm{exp}} - a_\mu^{\mathrm{SM}} \approx (3\pm1)\times10^{-9}$ as a signal of New Physics, we should expect $\Delta a_\tau \approx 10^{-6}$.

In the supersymmetric case, such an estimate holds for all the SPS points (see Table XI) and, more generally, in the limit of almost degenerate slepton masses. If $m_{\tilde\nu_\tau}^2 << m_{\tilde\nu_\mu}^2$ (as happens, for instance, in the so-called effective-SUSY scenario), Δa_τ could be enhanced up to the 10^{-5} level.

TABLE XI: Values of Δa_μ and Δa_τ for various SPS points.

SPS	1a	1b	2	3	4	5
$\Delta a_\mu \times 10^{-9}$	3.1	3.2	1.6	1.4	4.8	1.1
$\Delta a_\tau \times 10^{-6}$	0.9	0.9	0.5	0.4	1.4	0.3

Super$B$ experimental reach

CP violation and T-odd observables in tau decay

A first search for CP violation in tau decay has been conducted by the CLEO collaboration [20], looking

for a tau-charge-dependent asymmetry of the angular distribution of the hadronic system produced in $\tau \to K_S \pi \nu$. In multi-Higgs doublet New Physics, the CP-violating asymmetry arises from the Higgs coupling and the interference between S wave scalar exchange and P wave vector exchange. The Cabibbo-suppressed decay mode into $K_S \pi \nu$ has a larger mass-dependent Higgs coupling; the events in the sidebands of the K_S mass distributions can thus be used to calibrate the detector response. With a data sample of $13.3\,\text{fb}^{-1}$ (12.2×10^6 tau pairs), the mean of the optimal asymmetry observable is $\langle \xi \rangle = (-2.0 \pm 1.8) \times 10^{-3}$. As the above measurement relies on detector calibration with side-band events, it is conceivable that Super$B$ with $75\,\text{ab}^{-1}$ would not be limited by systematics and would therefore reach an experimental resolution $\Delta \langle \xi \rangle \approx 2.4 \times 10^{-5}$.

Tau electric dipole moment

The tau electric dipole moment (EDM) influences both the angular distributions and the polarization of the tau produced in $e^+ e^-$ annihilation. With a polarized beam, it is possible to construct observables from the angular distribution of the products of a single tau decay that unambiguously discriminate between the contribution due to the tau EDM and other effects [22, 23]. Recent work has provided an estimate of the Super$B$ upper limit sensitivity for the real part of the tau EDM $|\text{Re}\{d_\tau^\gamma\}| \leq 7.2 \times 10^{-20}\,e\,\text{cm}$ with $75\,\text{ab}^{-1}$ [22]. The result assumes a 100% polarized electron beam colliding with unpolarized positrons at the $\Upsilon(4S)$ peak, no uncertainty on the polarization, and perfect reconstruction of the tau decays $\tau \to \pi\nu$. Studies have been done assuming more realistic conditions:

- an electron beam with a linear polarization of $80\% \pm 1\%$;

- 80% geometric acceptance;

- track reconstruction efficiency $97.5\% \pm 0.1\%$ (similarly to what has been achieved in LEP analyses [24] and *BABAR* ISR analyses [25].

The process $e^+ e^- \to \tau^+ \tau^-$ is simulated with the KK generator [26] and the Tauola package for tau decay [26]; the simulation includes the complete spin correlation density matrix of the initial-state beams and the final state tau leptons. Tau EDM effects are simulated by weighting the tau decay product angular distributions. The studies are not complete, and do not yet include uncertainties in reconstructing the tau direction. The preliminary indications are that the tau EDM experimental resolution is $\approx 10 \times 10^{-20} e\,\text{cm}$, corresponding to an angular asymmetry of 3×10^{-5}; the

uncertainties in track reconstruction give a $\approx 1 \times 10^{-20}$ systematic contribution. Asymmetries proportional to the tau EDM depend on events that go into the same detector regions but arise from tau leptons produced at different angles, minimizing the impact of efficiency uncertainties. It must be added that all the hadronic tau channels have at least theoretically the same statistical power as the $\tau \to \pi\nu$ mode in measuring the tau polarization [27], and can therefore be used to improve the experimental resolution.

A search for the tau EDM with unpolarized beams has been completed at Belle [28]. In this case, one must measure correlations of the angular distributions of both tau leptons in the same events, thereby losing in both reconstruction efficiency and statistical precision. The analysis shows the impact of inefficiency and uncertainties in the tau direction reconstruction, and also demonstrates that all tau decays, including leptonic decays with two neutrinos, provide statistically useful information for measurement of the tau EDM. With $29.5\,\text{fb}^{-1}$ of data, the experimental resolution on the real and imaginary parts of the tau EDM is $[0.9-1.7] \times 10^{-17}\,e\,\text{cm}$, including systematic effects. An optimistic extrapolation to Super$B$ at $75\,\text{ab}^{-1}$, assuming systematic effects can be reduced according to statistics, corresponds to an experimental resolution of $[17-34] \times 10^{-20}$.

Tau g−2

In a manner similar to an EDM, the tau anomalous moment $(g-2)$ influences both the angular distribution and the polarization of the tau produced in $e^+ e^-$ annihilation. Polarized beams allow the measurement of the real part of the $g-2$ form factor by statistically measuring the tau polarization with the angular distributions of its decay products. Bernabéu *et al.* [29] estimate that Super$B$ with $75\,\text{ab}^{-1}$ will measure the real and imaginary part of the g–2 form factor at the $\Upsilon(4S)$ with a resolution in the range $[0.75-1.7] \times 10^{-6}$. Two measurements of the real part of g–2 are proposed, one fitting the polar angle distribution of the tau leptons, and one based on the measurement of the tau transverse and longitudinal polarization from the angular distribution of its decay products. All events with tau leptons decaying either in $\pi\nu$ or $\rho\nu$ are considered, but no detector effects are accounted for. For the tau polarization measurements, electron beams with perfectly known 100% polarization are assumed. Studies simulating more realistic experimental conditions are ongoing. While the polar angle distribution measurement will conceivably suffer from uncertainties in the tau direction reconstruction, the preliminary results on the tau EDM measurement, mentioned above, indicate that asymmetries measuring the tau polarization are

least affected by reconstruction systematics. Transposing the preliminary results obtained with simulations for the tau EDM to the real part of the $g-2$ form factor, one can estimate that $a_\mu = (g - 2)/2$ can be measured with a statistical error of 2.4×10^{-6}, with systematic effects from reconstruction uncertainties one order of magnitude lower.

[1] M. Grassi (MEG Collaboration), Nucl. Phys. Proc. Suppl. **149**, 369 (2005).

[2] B. C. Allanach et al. (2002), hep-ph/0202233.

[3] S. Antusch, E. Arganda, M. J. Herrero, and A. M. Teixeira, JHEP **11**, 090 (2006), hep-ph/0607263.

[4] E. Arganda and M. J. Herrero, Phys. Rev. **D73**, 055003 (2006), hep-ph/0510405.

[5] P. Paradisi, JHEP **02**, 050 (2006), hep-ph/0508054.

[6] M. Raidal et al. (2008), arXiv:0801.1826 [hep-ph].

[7] R. D. Cousins and V. L. Highland, Nucl. Instrum. Meth. **A320**, 331 (1992).

[8] S. Banerjee, B. Pietrzyk, J. M. Roney, and Z. Was, Phys. Rev. D (in press) (2007), arXiv:0706.3235 [hep-ph], arXiv:0706.3235 [hep-ph].

[9] B. Aubert et al. (*BABAR* Collaboration), Phys. Rev. Lett. **95**, 041802 (2005), hep-ex/0502032.

[10] A. Matsuzaki and A. I. Sanda, Phys. Rev. **D77**, 073003 (2008), 0711.0792.

[11] B. Aubert et al. (*BABAR* Collaboration), Phys. Rev. Lett. **96**, 041801 (2006), hep-ex/0508012.

[12] B. Aubert et al. (*BABAR* Collaboration), Phys. Rev. Lett. **99**, 251803 (2007), arXiv:0708.3650 [hep-ex].

[13] P. Krawczyk and S. Pokorski, Phys. Rev. Lett. **60**, 182 (1988).

[14] A. Pich, Int. J. Mod. Phys. **A21**, 5652 (2006), hep-ph/0609138.

[15] M. Bona et al. (2007), arXiv:0709.0451 [hep-ex].

[16] A. Lusiani, PoS(KAON)054 (2007), arXiv:0709.1599 [hep-ex].

[17] D. Delepine, G. Lopez Castro, and L. T. Lopez Lozano, Phys. Rev. **D72**, 033009 (2005), hep-ph/0503090.

[18] I. I. Bigi and A. I. Sanda, Phys. Lett. **B625**, 47 (2005), hep-ph/0506037.

[19] D. Delepine, G. Faisel, and S. Khalil, Phys. Rev. **D77**, 016003 (2008), arXiv:0710.1441 [hep-ph].

[20] G. Bonvicini et al. (CLEO Collaboration), Phys. Rev. Lett. **88**, 111803 (2002), hep-ex/0111095.

[21] V. D. Barger, A. K. Das, and C. Kao, Phys. Rev. **D55**, 7099 (1997), hep-ph/9611344.

[22] G. A. Gonzalez-Sprinberg, J. Bernabéu, and J. Vidal (2007), arXiv:0707.1658 [hep-ph].

[23] J. Bernabéu, G. A. Gonzalez-Sprinberg, and J. Vidal, Nucl. Phys. **B763**, 283 (2007), hep-ph/0610135.

[24] S. Schael et al. (ALEPH), Phys. Rept. **421**, 191 (2005), hep-ex/0506072.

[25] M. Davier (2007), private communication.

[26] S. Jadach, B. F. L. Ward, and Z. Was, Comput. Phys. Commun. **130**, 260 (2000), hep-ph/9912214.

[27] J. H. Kuhn, Phys. Rev. **D52**, 3128 (1995), hep-ph/9505303.

[28] K. Inami et al. (Belle), Phys. Lett. **B551**, 16 (2003), hep-ex/0210066.

[29] J. Bernabéu, G. A. Gonzalez-Sprinberg, J. Papavassiliou, and J. Vidal, Nucl. Phys. **B790**, 160 (2008), arXiv:0707.2496 [hep-ph].

Spectroscopy and the Decays of Quarkonia

Although the Standard Model is well-established, QCD, the fundamental theory of strong interactions, provides a quantitative comprehension only of phenomena at very high energy scales, where perturbation theory is effective due to asymptotic freedom. The description of hadron dynamics below the QCD dimensional transmutation scale is therefore far from being under full theoretical control.

Systems that include heavy quark-antiquark pairs (quarkonia) are a unique and, in fact, ideal laboratory for probing both the high energy regimes of QCD, where an expansion in terms of the coupling constant is possible, and the low energy regimes, where nonperturbative effects dominate. For this reason, quarkonia have been studied for decades in great detail. The detailed level of understanding of the quarkonia mass spectra is such that a particle mimicking quarkonium properties, but not fitting any quarkonium level, is most likely to be considered to be of a different nature.

In particular, in the past few years the B Factories and the Tevatron have provided evidence for states that do not admit the conventional mesonic interpretation and that instead could be made of a larger number of constituents (see Sec. 2). While this possibility has been considered since the beginning of the quark model [1], the actual identification of such states would represent a major revolution in our understanding of elementary particles. It would also imply the existence of a large number of additional states that have not yet been observed.

Finally, the study of the strong bound states could be of relevance to understanding the Higgs boson, if it turns out to be itself a bound state, as predicted by several technicolor models (with or without extra dimensions) [2].

The most likely possible states beyond the mesons and the baryons are:

- **hybrids:** bound states of a quark-antiquark pair and a number of constituent gluons. The lowest-lying state is expected to have quantum numbers $J^{PC} = 0^{+-}$. Since a quarkonium state cannot have these quantum numbers (see below), this a unique signature for hybrids. An additional signature is the preference for a hybrid to decay into quarkonium and a state that can be pro-

duced by the excited gluons (*e.g.*, $\pi^+\pi^-$ pairs); see *e.g.*, Ref. [3].

- **molecules:** bound states of two mesons, usually represented as $[Q\bar{q}][q'\bar{Q}]$, where Q is the heavy quark. The system would be stable if the binding energy were to set the mass of the states below the sum of the two meson masses. While this could be the case for when $Q = b$, this does not apply for $Q = c$, the case for which most of the current experimental data exist. In this case, the two mesons can be bound by pion exchange. This means that only states decaying strongly into pions can bind with other mesons (*e.g.*, there could be D^*D states), but that the bound state could decay into its constituents [4].

- **tetraquarks:** a bound quark pair, neutralizing its color with a bound antiquark pair, usually represented as $[Qq][\bar{q'}\bar{Q}]$. A full nonet of states is predicted for each spin-parity, *i.e.*, a large number of states are expected. There is no need for these states to be close to any threshold [5].

In addition, before the panorama of states is fully clarified, there is always the lurking possibility that some of the observed states are misinterpretations of threshold effects: a given amplitude might be enhanced when new hadronic final states become energetically possible, even in the absence of resonances.

While there are now several good experimental candidates for unconventional states, the overall picture is not complete and needs confirmation, as well as discrimination between the alternative explanations. A much larger dataset than is currently available is needed, at several energies, to pursue this program; this capability is uniquely within the reach of Super$B$.

Finally, bottomonium decays also allow direct searches for physics beyond the Standard Model in regions of the parameters space that have not been reached by LEP.

1. Light meson spectroscopy

The problem of the interpretation of the light scalar mesons, namely f_0, a_0, κ, σ, is one of the oldest problems in hadronic physics [6]. For many years the question of the existence of the σ meson as a resonance in $\pi\pi$ scattering has been debated [7]; only recently has a thorough analysis of $\pi\pi$ scattering amplitudes shown that the $\sigma(500)$ and $\kappa(800)$ can be considered to be proper resonances [8].

Reconsideration of the σ was triggered by the E791 analysis of $D \to 3\pi$ data [9]; a number of papers have commented on those results, *e.g.*, Ref. [10]. The role of the scalar mesons in several exclusive B decays could

be rather relevant: for example, in the perspective of a high precision measurement of the α angle at the SuperB factory, the hadronic contributions, like the one of the isoscalar σ in $B \to rho\pi$, must be properly controlled [11]. Also diverse studies on light and heavy scalar mesons could be performed analyzing the Dalitz plots of exclusive decays like $B \to KKK$ and $B \to K\pi\pi$. In this respect, having sufficient statistics to clearly assess the presence of a scalar $\kappa(800)$ resonance, would certainly be a major result for hadron spectroscopy.

Beyond the "taxonomic" interest in the classification of scalar mesons, the idea that these mesons could play a key role in our understanding of aspects of non-perturbative QCD has been raised; see, for example, the interesting paper, Ref. [12].

In what follows we would like to underscore the latter point by observing that:

- Light scalar mesons are most likely the lightest particles with an *exotic* structure, *i.e.*, they cannot be classified as $q\bar{q}$ mesons.

- Their dynamics is tightly connected with instanton physics. Recent discussions have shown that instanton effects facilitate the creation of a consistent model for the description of light scalar meson dynamics, under the hypothesis that these particles are diquark-antidiquark mesons.

Therefore, new modes of aggregation of quark matter could be established by the experimental/theoretical investigation of these particles, further expanding the role of instantons in hadronic physics.

The idea of four-quark mesons dates back to the pioneering papers by Jaffe [13], while the discussion of exotic mesons and hadrons in terms of diquarks was introduced in Ref. [14] and then extended in Ref. [15] to the scalar meson sector.

In the following, we will assume that the scalar mesons below 1 GeV are indeed bound states of a spin 0 diquark and an anti-diquark (we will often call this a tetraquark). A spin 0 diquark field can be written as:

$$\mathfrak{q}_{i\alpha} = \epsilon_{ijk}\epsilon_{\alpha\beta\gamma}\bar{q}_C^{j\beta}\gamma_5 q^{k\gamma}, \qquad (34)$$

where Latin indices label flavor and Greek letters label color. The color is saturated, as in a standard $q\bar{q}$ meson: $\mathfrak{q}^{\alpha}\bar{\mathfrak{q}}_{\alpha}$. Therefore, since a spin zero diquark is in a $\bar{\mathbf{3}}$-flavor representation, nonets of $\mathfrak{q}\bar{\mathfrak{q}}$ states are allowed (crypto-exotic states). The sub-GeV scalar mesons most likely represent the lowest tetraquark nonet.

The $\mathfrak{q}\bar{\mathfrak{q}}$ model of light-scalars is very effective at explaining the most striking feature of these particles, namely their inverted pattern, with respect to

that of ordinary $q\bar{q}$ mesons, in the mass-versus-I_3 diagram [13], as shown in Fig. 16.

FIG. 16: Vector mesons ($q\bar{q}$ states) and the sub-GeV scalar mesons in the $I_3 - m$ plane.

Such a pattern is not explained in a $q\bar{q}$ model, in which, for example, the $f_0(980)$ would be an $s\bar{s}$ state [10] while the $I = 1$, $a_0(980)$, would be a $u\bar{u} + d\bar{d}$ state. If this were the case, the degeneracy of the two particles appears rather unnatural.

Besides a correct description of the mass-I_3 pattern, the tetraquark model offers the possibility of explaining the decay rates of scalars at a level never reached by standard $q\bar{q}$ descriptions. The effective decay Lagrangian into two pseudoscalar mesons, *e.g.*, $\sigma \to \pi\pi$, is written as:

$$\mathcal{L}_{\text{exch.}} = c_f S_j^i \epsilon^{jtu} \epsilon_{irs} \partial_\mu \Pi_t^r \partial^\mu \Pi_u^s, \qquad (35)$$

where i, j are the flavor labels of $\mathfrak{q}^i$ and $\bar{\mathfrak{q}}^j$, while r, s, t, u are the flavor labels of the quarks $\bar{q}^t, \bar{q}^u$ and q^r, q^s. c_f is the effective coupling weighting this interaction term and S, Π are the scalar and pseudoscalar matrices. This Lagrangian describes the quark exchange amplitude for the quarks to tunnel out of their diquark shells to form ordinary mesons [15]. Such a mechanism is an alternative to the color string breaking $\mathfrak{q}$ 〰〰〰 $q\bar{q}$ 〰〰〰 $\bar{\mathfrak{q}}$ $\to B\bar{B}$, *i.e.*, a baryon-antibaryon decay, which is phase-space forbidden to sub-GeV scalar mesons.

The main problem with eq. (35) is that it is not able to describe the decay $f_0 \to \pi\pi$, since $f_0 = (\mathfrak{q}^2\bar{\mathfrak{q}}^2 + \mathfrak{q}^1\bar{\mathfrak{q}}^1)/\sqrt{2}$, being $1, 2, 3$ the u, d, s flavors so that, see equation (34), $\mathfrak{q}^1 = [ds]$ and $\mathfrak{q}^2 = [su]$. An annihilation diagram would be needed to replace the s quarks, inducing a small rate that does not match the observation.

Alternatively, one can suppose the mixing between the two isoscalars f_0 and σ is at work, the σ component ($\mathfrak{q}^3\bar{\mathfrak{q}}^3$) providing the $\pi\pi$ decay. However, as discussed in [16], such mixing is expected to be too small, $< 5°$, to account for the structure of the inverted mass pattern (a precise determination of the κ mass would be crucial to fix this point).

A solution that improves the overall agreement with data of all light scalar mesons decay rates has been found [16]. In low energy QCD, instantons generate a

quark interaction term that can be written as:

$$\mathcal{L}_I = \det(\bar{q}_L^i q_R^j), \qquad (36)$$

$i, j = 1, 2, 3$ being flavor indices. Such a left-right mixing interaction is screened at high energies, the instanton action scaling as $S \sim \exp(-8\pi^2/g^2)$. In addition to the quark-exchange diagrams, described at the effective theory level by the Lagrangian of eq. (35), (see Fig. 17 (a)), there are also contributions such as those in Fig. 17 (b) [17].
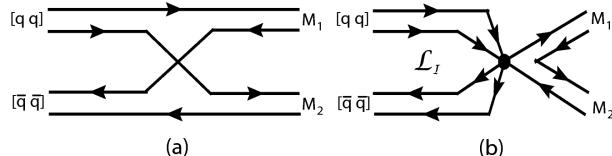

FIG. 17: Decay of a tetraquark scalar meson S in two $q\bar{q}$ mesons $M_1 M_2$: (a) quark rearrangement (b) instanton-induced process.

The quark-level instanton interaction, Fig. 17(b), reflects into an effective meson interaction of the kind:

$$\mathcal{L}_I = c_I \mathrm{Tr}(\mathbf{S} \times (\partial \mathbf{\Pi})^2), \qquad (37)$$

c_I being an effective coupling as c_f in (35). Assuming that the low energy dynamics of light scalar mesons is described by:

$$\mathcal{L} = \mathcal{L}_{\mathrm{exch.}} + \mathcal{L}_I, \qquad (38)$$

one can reach a remarkably satisfying description of light meson decays [16]. Namely:

- Such a good description of decays is possible *only* if the assumption is made that sub-GeV light scalars are diquark-antidiquark mesons (see Table XII). In the $q\bar{q}$ hypothesis, the agreement of $a_0 \to \pi^0 \eta$ with data appears very poor.

- The inverted mass spectrum of super-GeV scalar mesons can be explained by assuming that they form the lightest $q\bar{q}$ scalar multiplet, deformed in the mass-I_3 pattern by mixing with the lowest exotic multiplet of sub-GeV scalar mesons (see Fig. 18 [16]).

One of the isoscalars in the decuplet in Fig. 18 is likely to be the lowest *glueball*; there are arguments favoring the $f_0(1500)$ as the most probable glueball candidate.

We quote a table from [16] describing at what level one can fit the decays of the lightest scalar mesons in a diquark-antidiquark picture:

A relative of the lowest lying scalar mesons may have been found very recently by *BABAR*: the $Y(2175)$, a particle first observed in the decay $Y \to \phi f_0(980)$ [19].
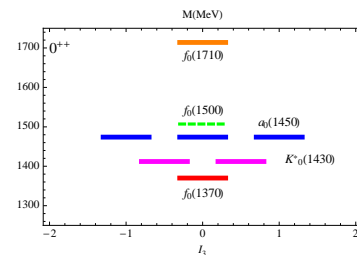

FIG. 18: Super-GeV scalar mesons in the $I_3 - m$ plane.

TABLE XII: Numerical results, amplitudes in GeV. Second and third columns: results obtained with a decay Lagrangian including or not including instanton effects, respectively (Labels I and no-I mean that we add or do not add the instanton contribution.). No $f_0 - \sigma$ mixing is assumed in this table. Fourth column: best fit, see text, with instanton effects included. Fifth column: predictions for a $q\bar{q}$ picture of the light scalars. The $\eta - \eta'$ singlet-octet mixing angle assumed: $\phi_{PS} = -22°$ [18]. Data for σ and κ decays are from [8], the reported amplitudes correspond to: $\Gamma_{\mathrm{tot}}(\sigma) = 272 \pm 6$, $\Gamma_{\mathrm{tot}}(\kappa) = 557 \pm 24$.

Proc.	$\mathcal{A}_{\mathrm{th}}([qq][\bar{q}\bar{q}])$			$\mathcal{A}_{\mathrm{th}}(q\bar{q})$	$\mathcal{A}_{\mathrm{expt}}$
	I	no-I	best fit	I	
$\sigma(\pi^+\pi^-)$	input	input	1.7	input	2.27(0.03)
$\kappa^+(K^0\pi^+)$	5.0	5.5	3.6	4.4	5.2(0.1)
$f_0(\pi^+\pi^-)$	input	**0**	1.6	input	1.4(0.6)
$f_0(K^+K^-)$	4.8	4.5	3.8	4.4	3.8(1.1)
$a_0(\pi^0\eta)$	4.5	5.4	3.0	8.9	2.8(0.1)
$a_0(K^+K^-)$	3.4	3.7	2.4	3.0	2.16(0.04)

This object could be a radial excitation of the lowest lying scalar mesons, of the kind $\mathfrak{q}^1\bar{\mathfrak{q}}^1 + \mathfrak{q}^2\bar{\mathfrak{q}}^2$ and could strikingly manifest all the three tetraquark decay mechanisms: the instanton ($Y \to \phi(1020)f_0(980)$), the quark rearrangement ($Y \to KK^*$), and the string breaking ($Y \to KK^*$) mechanisms. It is to be noted that only the first decay mode has been observed; there are only hints of the other two.

We tend to exclude the possibility of a $Y(2175)$ built as $\mathfrak{q}^3\bar{\mathfrak{q}}^3$ because, though it would contain four s quarks as the observed final state, it would involve spin 1 diquarks, because of Fermi statistics. Spin 1 diquarks are thought to be energetically disfavoured, but, worse, they are in the $\mathbf{6_f}$ representation, thus requiring a large number of exotic particles: $\mathbf{6} \otimes \bar{\mathbf{6}} = \mathbf{1} \oplus \mathbf{8} \oplus \mathbf{27}$. The search for other decay mechanisms would be quite crucial to test this hypothesis.

Searches of radially excited partners of the scalar mesons in the high statistics data samples from a SuperB factory, would deeply improve the comprehension of the tetraquark picture. To give an example, consider that predictions of lighter partners of the $Y(2175)$, to be found in ISR, are at hand. Are the good, spin zero, diquarks the only relevant building blocks, or bad, spin

one, diquarks are also effective degrees of freedom to describe states at higher mass than the standard scalar nonets? It is decisive to understand to what extent the actual models for multiquark particles are predictive.

2. Charmonium

In the past few years the B Factories have observed several states with clear $c\bar{c}$ content, which do not behave like standard mesons, and that are therefore an indication of new spectroscopy.

The $X(3872)$ was the first state found that did not easily fit into charmonium spectroscopy. It was initially observed decaying into $J/\psi\pi^+\pi^-$ with a mass just beyond the open charm threshold [20]. The $\pi^+\pi^-$ invariant mass distribution, the observation of the $X \to J/\psi\gamma$ and the full angular analysis from CDF [21] and Belle [22] favor the assignment of $J^{PC} = 1^{++}$ for this state, and of $B \to J/\psi\rho$ as its dominant decay. There are therefore several indications that this is not a charmonium state: the mass assignment does not match any prediction of long-verified potential models (see Fig. 19); the dominant decay would be isospin-violating; and the state is relatively narrow (less than a few MeV) despite that fact that its mass is above threshold for the production of two charmed mesons.
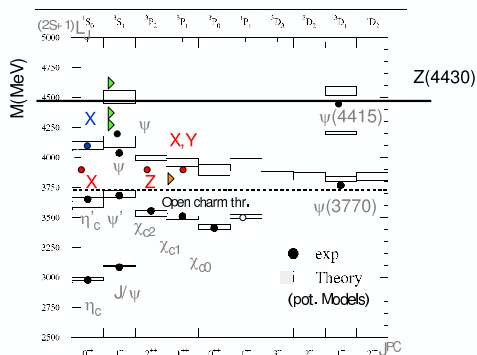

FIG. 19: Measured masses of the newly observed states, positioned in the spectroscopy according to their most likely quantum numbers. The charged state ($Z(4430)$) clearly has no C quantum number.

Another aspect of interest of the $X(3872)$ are the measurements of its mass, the most recent of which is Ref. [23]: there is an indication that there are two different particles, one decaying into $J/\psi\pi\pi$ and one into $D^{*0}D^0$, their masses differing by about 4.5 standard deviations. This observation makes the $X(3872)$ a good tetraquark candidate: di-quarks with an heavy meson are, in fact, flavor-triplets, and therefore pairs give rise to the same nonet structure as conventional mesons. There should therefore be two states with

$S = I_3 = 0$ very close in mass [5]. Without this evidence, the closeness to the $D^0 D^{*0}$ threshold suggests the hypothesis that this is a molecule composed of these two mesons.

Furthermore, the B Factories investigate a large range of masses for particles with $J^{PC} = 1^{--}$ by looking for events where the initial state radiation brings the e^+e^- center-of-mass energy down to the particle's mass. While in principle only particles already observed in $R = \sigma_{had}/\sigma_{\mu\mu}$ scans could be produced, the high luminosity has allowed the observation of several new particles: the $Y(4260) \to J/\psi\pi^+\pi^-$ [24], the $Y(4350)$ [25] and the $Y(4660)$ [26], both observed in their decay to $\psi(2S)\pi\pi$.

The invariant mass of the two pions in these decays is a critical observable in discerning the nature of these particles, which are unlikely to be charmonium, since their masses are above the open-charm threshold, yet they are relatively narrow. Furthermore, their decays to two charmed mesons have not yet been observed, the most stringent limit being [27] $\mathcal{B}(Y(4260) \to D\bar{D})/\mathcal{B}(Y(4260) \to J/\psi\pi^+\pi^-) < 1.0@$ 90% confidence level.

Figure 20 shows the di-pion invariant mass spectra for all regions in which new resonances have been observed. There is some indication that only the $Y(4660)$ has a well-defined intermediate state (most likely an f_0), while others have a more complex structure.

These observations make the $Y(4260)$ a good hybrid candidate, and the $Y(4350)$ and $Y(4660)$ good candidates for $[cd][\bar{c}\bar{d}]$ and $[cs][\bar{c}\bar{s}]$ tetraquarks, respectively. The latter would, in fact, prefer to decay into an f_0, while the mass difference between the two states is consistent with the hypothesis that the two belong to the same nonet.

The turning point in the query for states beyond charmonium was therefore the observation by the Belle Collaboration of a charged state decaying into $\psi(2S)\pi^\pm$ [28]. Figure 21 shows the fit to the $\psi(2S)\pi$ invariant mass distribution in $B \to \psi(2S)\pi K$ decays, returning a mass $M = 4433 \pm 4\text{MeV}/c^2$ and a width $\Gamma = 44^{+17}_{-13}$ MeV.

In terms of quarks, such a state must contain a c and a $\bar{c}$, but given its charge it must also contain at least a u and a $\bar{d}$. The only open options are the tetraquark, the molecule or threshold effects. The latter two options are viable due to the closeness of the $D_1 D^*$ threshold.

Finding the corresponding neutral state, observing a decay mode of the same state, or at least having a confirmation of its existence, are critical before a complete picture can be drawn.

There are several reasons why a run at fifty to one hundred times the existing integrated luminosity is critical to convert these of hints into a complete, solid picture:
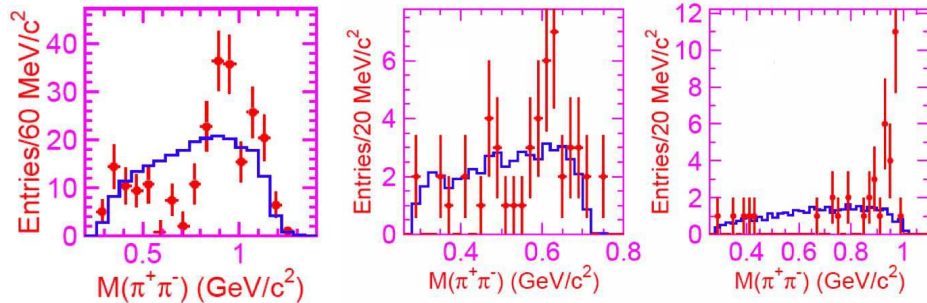
FIG. 20: Di-pion invariant mass distribution in $Y(4260) \rightarrow J/\psi\,\pi^+\pi^-$ (left), $Y(4350) \rightarrow \psi(2S)\pi^+\pi^-$ (center), and $Y(4660) \rightarrow \psi(2S)\pi^+\pi^-$ (right) decays.
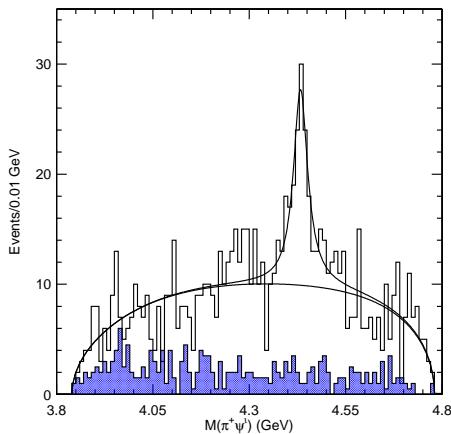

FIG. 21: The $\psi(2S)\pi$ invariant mass distribution in $B \rightarrow \psi(2S)\pi K$ decays.

- all the new states, apart from the $X(3872)$, have been observed in only a single decay channel, with significance that are barely above 5σ. a hundredfold increase in statistics would allow searches in several other modes. It is in particular critical to observe both the decay to charmonium and to D-meson pairs and/or D_s meson pairs. Since the branching fraction of observable final states for the D and especially for the D_s mesons are particularly low, current experiments do not have the sensitivity to observe all the decays.

- the models predict several other states, such as the neutral partners of the $Z(4430)$ and the nonet partners, for instance $[cd][\bar{c}\bar{s}]$ candidates decaying into a charmonium state and a kaon, at a significantly lower rate (see *e.g.*, Ref. [29])

than the observed modes. Furthermore , several of these states decay into particles (in particular neutral pions and kaons) that have a low detection efficiency.

3. Bottomonium

Exotic states with two bottom quarks, analogous to those with two charm quarks, could also exist. In this respect, bottomonium spectroscopy is a very good testbench for speculations advanced to explain the charmonium states. On the other side, searching for new bottomonium states is more challenging, since they tend to be broader and there are more possible decay channels. This explains why there are still eight unobserved states with masses below open bottomonium threshold.

Among the known states, there is already one with unusual behavior: there has been a recent observation [30] of an anomalous enhancement, by two orders of magnitude, of the rate of $\Upsilon(5S)$ decays to the $\Upsilon(1S)$ or a $\Upsilon(2S)$ and two pions. This indicates that either the $\Upsilon(5S)$ itself or a state very close by in mass has a decay mechanism that enhances the amplitudes for these processes.

In order to understand whether the exotic state coincides with the $\Upsilon(5S)$) or not, a high luminosity (at least 20 fb^{-1} per point to have a 10% error) scan of the resonance region is needed.

In any case, the presence of two decay channels to other bottomonium states excludes the possibility of this state being a molecular aggregate, but all other models are possible, and would predict a large variety of not yet observed states.

As an example, one can estimate possible resonant states with the tetraquark model, by assuming that the masses of states with two b quarks can be obtained from one with two c quarks by adding the mass difference between the $\Upsilon(1S))$ and the J/ψ. Under this assumption, which works approximately for the known bottomonium states, we could expect three nonets that could be produced by the $\Upsilon(3S)$ and decaying into $\Upsilon(1S)$ and pions. Assuming that the production and decay rates of these new states are comparable to the charmonium states, and assuming a data sample of $\Upsilon(3S)$ events comparable in size to the current $\Upsilon(4S)$ sample is needed to clarify the picture, we would need about 10^9 $\Upsilon(3S)$ mesons, corresponding to an integrated luminosity of 0.3 ab^{-1}.

As already mentioned, searching for bottomonium-like states would require higher statistics than the corresponding charmonium ones; this therefore represents an even stronger case for Super$B$.

4. Search for Physics Beyond the Standard Model in Bottomonium Decays

In spite of intensive searches performed at LEP [31], the possibility of a rather light non-standard Higgs boson has not been ruled out in several scenarios beyond the Standard Model [32, 33, 34], due to the fact that a new scalar may be uncharged under the gauge symmetries, similar to a sterile neutrino in the fermion case. These studies indicate that its mass could be less than twice the b mass, placing it within the reach of Super$B$. Moreover, the LHC might not be able to unravel a signal from a light Higgs boson whose mass is below $B\bar{B}$ threshold, since it will be difficult for the soft decay products to pass the LHC triggers. Dark matter may also be light, evading LEP searches if it does not couple strongly to the Z^0 [35, 36, 37, 38]. Super$B$ will be *required* in most of these cases to precisely determine its masses and couplings, and will play an important discovery role.

Light Higgses

A Higgs h with $M_h < M_\Upsilon$ can be produced in $\Upsilon(nS)$ decays via the Wilczek mechanism with a branching ratio approximately given by the leading-order formula [39]

$$\frac{\Gamma(\Upsilon(nS) \to \gamma h)}{\Gamma(\Upsilon(nS) \to \mu\mu)} = \frac{\sqrt{2}G_F m_b^2}{\alpha \pi M_{\Upsilon(nS)}} E_\gamma X_d^2$$

where X_d is a model-dependent quantity containing the coupling of the Higgs to bottom quarks, m_b is the

bottom quark mass, α and G_F are the electroweak parameters, and $E_\gamma = (M_{\Upsilon(nS)}/2)(1 - M_h^2/M_{\Upsilon(nS))}^2)$ is the photon energy.

From a theoretical viewpoint, the existence of a light pseudoscalar Higgs is not unexpected in many extensions of the SM. As an especially appealing example, the Next-to-Minimal Supersymmetric Standard Model (NMSSM) has a gauge singlet added to the MSSM two-doublet Higgs sector (see [40] and references therein for a short summary of other scenarios leading to a light Higgs boson) leading to seven physical Higgs bosons, five of them neutral, including two pseudoscalars.

In the limit of either slightly broken R or Peccei-Quinn (PQ) symmetries, the lightest CP-odd Higgs boson (denoted by A_1) can be much lighter than the other Higgs bosons. Interestingly, the authors of [32] interpret the excess of Z^0+b-jet events found at LEP as a signal, in this formalism, of a Standard Model-like Higgs decaying partly into $b\bar{b}$, but dominantly into τ's via two light pseudoscalars.

Let us write the physical Higgs boson A_1 as a mixture of singlet (A_s) and non-singlet (A_{MSSM}) fractions parametrized by the angle θ_A, according to

$$A_1 = \cos\theta_A A_{MSSM} + \sin\theta_A A_s$$

The A_1 coupling to down-type fermions turns out to be proportional to $X_d = \cos\theta_A \tan\beta$, where $\tan\beta$ denotes the ratio of the vevs of the up- and down-type Higgs bosons. For $\cos\theta_A$ close to zero, the A_1 almost completely decouples from flavor physics. However, if $\cos\theta_A \sim 0.1 - 0.5$, present LEP and B physics bounds can be simultaneously satisfied [41], while a light Higgs could still show up in Υ radiative decays into tauonic pairs:

$$\Upsilon(nS) \to \gamma A_1(\to \tau^+\tau^-) ; \quad n = 1, 2, 3.$$

As this light Higgs acquires its couplings to Standard Model fermions via mixing with the Standard Model Higgs, it therefore couples to mass, and will decay to the heaviest available Standard Model fermion. In the region $M_{A_1} > 2M_\tau$, there are two measurements which have sensitivity: lepton universality of Υ decays, and searches for a monochromatic photon peak in tauonic Υ decays.

The measurement of lepton universality compares the branching ratios of Υ to e^+e^-, $\mu^+\mu^-$ and $\tau^+\tau^-$ [42, 43], which should all be identical up to kinematic factors in the Standard Model, due to the gauge symmetry. It is relevant especially when the A_1 mass is within about 500 MeV of an Υ mass, so that the monochromatic photon signal is buried under backgrounds. It is also the best measurement when $M_{A_1} > M_\Upsilon$, which causes there to be a photon spectrum, rather than monochromatic line.
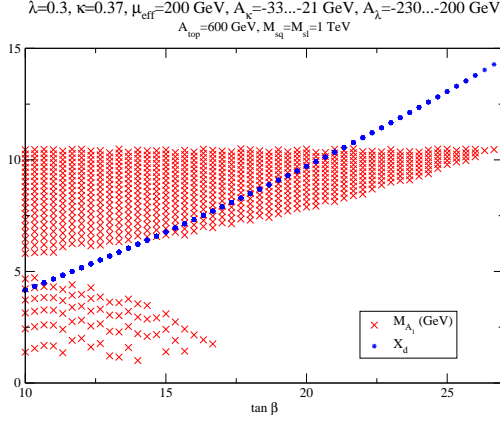
FIG. 22: Plot of $X_d = \cos\theta_A \tan\beta$ (blue points) and A_1 mass in GeV (red crosses) versus $\tan\beta$. All points were generated using the NMHDECAY code [44] satisfying both LEP and B physics constraints using a particular set of NMSSM parameters [45].

FIG. 23: Plot of the 5σ discovery potential of Super$B$ with $\Upsilon(3S)$ data, in the mode $\Upsilon(3S) \rightarrow \pi^+\pi^-\Upsilon(1S) \rightarrow \pi^+\pi^-\tau^+\tau^-\gamma$ (solid black) and $\Upsilon(3S) \rightarrow \tau^+\tau^-\gamma$ (dashed red). An integrated luminosity of 1 ab^{-1} was assumed.

Using the NMHDECAY code [44], we have randomly generated masses and couplings for the A_1 Higgs below the $B\bar{B}$ threshold, under the condition of passing all current LEP and B physics bounds built into the NMHDECAY [41]. We actually chose a physically-motivated set of NMSSM parameters favoring the existence of a scenario with of a light A_1 [34, 45].

In Fig. 22 we plot the resulting points of our scan for the A_1 mass and X_d values as a function of $\tan\beta$. Let us stress that, in view of the available large X_d values, such a light CP-odd Higgs could provide a signal in Υ leptonic decays, whose first hint would be an apparent breaking of lepton universality, *e.g.* at the few percent level. Indeed, the tauonic mode would be (slightly) enhanced by the New Physics channel with respect to the electronic and muonic modes, because of the large leptonic mass difference [40, 42, 43]. The degree of enhancement of the tauonic channel (*i.e.*, of the New Physics contribution) obviously depends on the assumed set of the NMSSM parameters (notably $\tan\beta$) but seems sizeable for reasonable values of them, as can be seen from Fig. 22.

Moreover, the observation (non-observation) of a monochromatic photon from the radiative process would become the smoking gun pointing out (excluding) the existence of such a light non-standard Higgs boson.

In the search for monochromatic photons the first relevant decay mode is $\Upsilon(3S) \rightarrow \Upsilon(1S)\pi^+\pi^-$ first, followed by $\Upsilon(1S) \rightarrow \gamma\tau^+\tau^-$, which has only a 4.5% branching fraction, but has low background. The second decay mode is $\U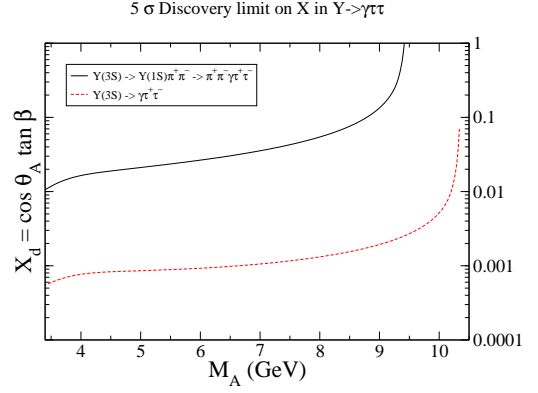psilon(3S) \rightarrow \gamma\tau^+\tau^-$, which suffers from much worse backgrounds from $e^+e^- \rightarrow \tau^+\tau^-\gamma$ events, but also has a rate that is more than a factor of ten higher. The corresponding exclusion plots are in Fig. 23.

Invisible decays and light dark matter

Finally, if Dark Matter is lighter than 5 GeV, it will require a Super B Factory to determine its properties. Generally, in this mass region one needs two particles, the dark matter particle χ, and a boson that couples it to the Standard Model U. The most promising searches are in invisible and radiative decays of the Υ, which can be measured in the mode $\Upsilon(3S) \rightarrow \pi^+\pi^-\Upsilon(1S) \rightarrow \pi^+\pi^- + invisible$, which is sensitive to a vector U. However, to substantially improve on existing measurements from Belle and CLEO, far-forward tagging must be incorporated into the design of the detector. This is needed to veto events in which the $\Upsilon(1S)$ decays to a two-body state, with decay products that disappear down the beampipe [37].

The second most promising signature is radiative decays $\Upsilon \rightarrow \gamma + invisible$. This is probably the most favored mode theoretically, and is sensitive to a scalar or pseudoscalar U. The mediator coupling the Standard Model particles to final-state χ's can be a pseudoscalar Higgs, $U = A_1$, which can be naturally light, and would appear in this mode [38]. In such models the Dark Matter can be naturally be a bino-like neutralino.

5. Summary

SuperB will open a unique window on this physics because it allows a high statistics study of the current hints of new aggregations of quarks and gluons. Besides the physics one can study in running at the $\Upsilon(4S)$ resonance, the following alternative energies are of interest: $\Upsilon(3S)$ (at least 0.3 ab^{-1}) and a high luminosity scan between 4-5 GeV (5 MeV steps of 0.2 fb^{-1} each would require a total of 40 fb^{-1}) [46]. While this is not huge statistics, this scan is only feasible with SuperB. The only possible competitor, BES-III, is not planning to scan above 4 GeV, since their data sample would, in any case, be lower than that of the B Factories alone.

Finally, the search for exotic particles among the decay products of the bottomonia can probe regions of the parameters space of non-minimal supersymmetric models that cannot be otherwise explored directly, for instance at LHC. These studies are particularly efficient when producing $\Upsilon(nS)$ mesons with $n < 4$.

The superiority of SuperB with respect to the planned upgrade of Belle lies both in the ten times higher statistics, which broadens the range of cross sections the experiment is sensitive to, but also in the flexibility to change center of mass energy.

----

[1] M. Gell-Mann, Phys. Lett. 8, 214 (1964)

[2] D. D. Dietrich, F. Sannino and K. Tuominen, Phys. Rev. D **72**, 055001 (2005) [arXiv:hep-ph/0505059]; R. Contino, T. Kramer, M. Son and R. Sundrum, JHEP **0705**, 074 (2007) [arXiv:hep-ph/0612180] *and references therein.*

[3] E. Kou and O. Pene, Phys. Lett. B **631**, 164 (2005) [arXiv:hep-ph/0507119]; F. E. Close and P. R. Page, Phys. Lett. B **628**, 215 (2005) [arXiv:hep-ph/0507199].

[4] E. Braaten and M. Kusunoki, Phys. Rev. D **69**, 074005 (2004) [arXiv:hep-ph/0311147]; F. E. Close and P. R. Page, Phys. Lett. B **578**, 119 (2004) [arXiv:hep-ph/0309253]; N. A. Tornqvist, Phys. Lett. B **590**, 209 (2004) [arXiv:hep-ph/0402237]; E. S. Swanson, Phys. Rept. **429**, 243 (2006) [arXiv:hep-ph/0601110]; M. B. Voloshin, *In the Proceedings of 4th Flavor Physics and CP Violation Conference (FPCP 2006), Vancouver, British Columbia, Canada, 9-12 Apr 2006, pp 014* [arXiv:hep-ph/0605063]; S. Fleming, M. Kusunoki, T. Mehen and U. van Kolck, Phys. Rev. D **76**, 034006 (2007) [arXiv:hep-ph/0703168]; E. Braaten and M. Lu, Phys. Rev. D **76**, 094028 (2007) [arXiv:0709.2697 [hep-ph]]; E. Braaten and M. Lu, arXiv:0710.5482 [hep-ph];

[5] L. Maiani, F. Piccinini, A. D. Polosa and V. Riquer, Phys. Rev. D **71**, 014028 (2005) [arXiv:hep-ph/0412098].

[6] M. Gell-Mann and M. Levy, Nuovo Cim. **16**, 705 (1960).

[7] N. A. Tornqvist and M. Roos, Phys. Rev. Lett. **76**, 1575 (1996) [arXiv:hep-ph/9511210].

[8] I. Caprini, G. Colangelo and H. Leutwyler, Phys. Rev. Lett. **96**, 132001 (2006) [arXiv:hep-ph/0512364]; S. Descotes-Genon and B. Moussallam, Eur. Phys. J. C **48**, 553 (2006) [arXiv:hep-ph/0607133].

[9] E. M. Aitala *et al.* [E791 Collaboration], Phys. Rev. Lett. **86**, 770 (2001) [arXiv:hep-ex/0007028].

[10] R. Gatto, G. Nardulli, A. D. Polosa and N. A. Tornqvist, Phys. Lett. B **494**, 168 (2000) [arXiv:hep-ph/0007207]; N. A. Tornqvist and A. D. Polosa, Frascati Phys. Ser. **20**, 385 (2000) [arXiv:hep-ph/0011107]; N. A. Tornqvist and A. D. Polosa, Nucl. Phys. A **692**, 259 (2001) [arXiv:hep-ph/0011109]; A. Deandrea, R. Gatto, G. Nardulli, A. D. Polosa and N. A. Tornqvist, Phys. Lett. B **502**, 79 (2001) [arXiv:hep-ph/0012120].

[11] A. Deandrea and A. D. Polosa, Phys. Rev. Lett. **86**, 216 (2001) [arXiv:hep-ph/0008084]; S. Gardner and U. G. Meissner, Phys. Rev. D **65**, 094004 (2002) [arXiv:hep-ph/0112281]. I. Bigi, L. Maiani, F. Piccinini, A. D. Polosa and V. Riquer, "Four-quark mesons in non-leptonic B decays: Could they resolve some old puzzles?," Phys. Rev. D **72**, 114016 (2005) [arXiv:hep-ph/0510307].

[12] F. E. Close, Y. L. Dokshitzer, V. N. Gribov, V. A. Khoze and M. G. Ryskin, Phys. Lett. B **319**, 291 (1993).

[13] R. L. Jaffe, Phys. Rev. D **15**, 267 (1977); Phys. Rev. D **15**, 281 (1977); Phys. Rept. **409**, 1 (2005) [Nucl. Phys. Proc. Suppl. **142**, 343 (2005)] [arXiv:hep-ph/0409065].

[14] R. L. Jaffe and F. Wilczek, Phys. Rev. Lett. **91**, 232003 (2003) [arXiv:hep-ph/0307341].

[15] L. Maiani, F. Piccinini, A. D. Polosa and V. Riquer, Phys. Rev. Lett. **93**, 212002 (2004) [arXiv:hep-ph/0407017].

[16] G. 't Hooft, G. Isidori, L. Maiani, A. D. Polosa and V. Riquer, arXiv:0801.2288 [hep-ph].

[17] The six-fermion interaction (36) expands to terms of the form: $(\bar{u}^{\alpha}(1 - \gamma_5)u_{\alpha})(\bar{d}^{\alpha}(1 - \gamma_5)d_{\alpha})(\bar{s}^{\alpha}(1 - \gamma_5)s_{\alpha})$. Upon appropriate Fierz rearrangement of, *e.g.*, $(\bar{d}^{\alpha}(1-\gamma_5)d_{\alpha})(\bar{s}^{\alpha}(1-\gamma_5)s_{\alpha})$, one obtains: $C \times (\bar{u}^{\alpha}(1-\gamma_5)u_{\alpha})\mathsf{q}^{1\gamma}\bar{\mathsf{q}}_{1\gamma}$, C being a constant factor.

[18] R. Escribano and J. M. Frere, JHEP **0506** (2005) 029 [arXiv:hep-ph/0501072]; J. M. Gerard and E. Kou, Phys. Lett. B **616** (2005) 85 [arXiv:hep-ph/0411292].

[19] B. Aubert *et al.* [BABAR Collaboration], Phys. Rev. D **74**, 091103 (2006) [arXiv:hep-ex/0610018].

[20] Belle, S. K. Choi *et al.*, Phys. Rev. Lett. **91**, 262001 (2003), [hep-ex/0309032].

[21] CDF, A. Abulencia *et al.*, Phys. Rev. Lett. **98**, 132002 (2007), [hep-ex/0612053].

[22] Belle, K. Abe *et al.*,hep-ex/0505038.

[23] BABAR Collaboration, B. Aubert *et al.*,arXiv:0708.1565 [hep-ex].

[24] BABAR Collaboration, B. Aubert *et al.*, Phys. Rev. Lett. **95**, 142001 (2005), [hep-ex/0506081].

[25] BABAR Collaboration, B. Aubert *et al.*, Phys. Rev. Lett. **98**, 212001 (2007), [hep-ex/0610057].

[26] Belle, X. L. Wang *et al.*, arXiv:0707.3699 [hep-ex].

[27] BABAR Collaboration, B. Aubert, arXiv:0710.1371 [hep-ex].

[28] Belle, K. Abe *et al.*, arXiv:0708.1790.

[29] L. Maiani, A. D. Polosa and V. Riquer, Phys. Rev.

Lett. **99**, 182003 (2007) [arXiv:0707.3354 [hep-ph]].

[30] K. F. Chen *et al.* [Belle Collaboration], arXiv:0710.2577 [hep-ex].

[31] S. Schael *et al.* [ALEPH Collaboration], Eur. Phys. J. C **47** (2006) 547.

[32] R. Dermisek and J. F. Gunion, and Phys. Rev. D **73** (2006) 111701.

[33] R. Dermisek, J. F. Gunion and B. McElrath, Phys. Rev. D **76** (2007) 051105 [arXiv:hep-ph/0612031].

[34] M. A. Sanchis-Lozano, arXiv:0709.3647 [hep-ph].

[35] P. Fayet, and Phys. Rev. D **75**, 115017 (2007) [arXiv:hep-ph/0702176]; P. Fayet, pi0, Phys. Rev. D **74**, 054034 (2006) [arXiv:hep-ph/0607318].

[36] C. Bird, R. Kowalewski and M. Pospelov, Mod. Phys. Lett. A **21**, 457 (2006) [arXiv:hep-ph/0601090].

[37] B. McElrath, Phys. Rev. D **72**, 103508 (2005).

[38] J. F. Gunion, D. Hooper and B. McElrath, Phys. Rev.

D **73**, 015011 (2006) [arXiv:hep-ph/0509024].

[39] F. Wilczek, Phys. Rev. Lett. **39**, 1304 (1977).

[40] E. Fullana and M. A. Sanchis-Lozano, decay Phys. Lett. B **653** (2007) 67 [arXiv:hep-ph/0702190].

[41] F. Domingo and U. Ellwanger, JHEP **0712** (2007) 090 [arXiv:0710.3714 [hep-ph]].

[42] M. A. Sanchis-Lozano, Int. J. Mod. Phys. A **19** (2004) 2183 [arXiv:hep-ph/0307313]..

[43] M. A. Sanchis-Lozano, B-factory J. Phys. Soc. Jap. **76** (2007) 044101 [arXiv:hep-ph/0610046].

[44] U. Ellwanger and C. Hugonie, Comput. Phys. Commun. **175** (2006) 290 [arXiv:hep-ph/0508022].

[45] M. A. Sanchis-Lozano, in preparation.

[46] We assumed $\sigma(e^+e^- \rightarrow Y) * \mathcal{B}$ 50pb as measured for the $Y(4320)$ in Ref. [25] and require at least ten thousand events per resonance.

Appendix: Physics Tools

We describe herein the tools used to simulate physics events and evaluate detector performance at the Super$B$ flavor factory. The simulation should meet two main requirements. First, since the design of the subsystems is evolving, the user should be able to perform optimization studies and modify the detector description in a simple way. Second, the program should be very fast, to simulate very large numbers of physics events. Table XIII shows the event rate expected at a luminosity of 1.0×10^{36} cm$^{-2}s^{-1}$. Over one year it translates to 1.1×10^{10} $\Upsilon(4S)$ decays and a total of about 5.4×10^{10} $e^+e^- \to q\bar{q}$ ($q = u, d, s, c, b$) and $\tau^+\tau^-$ decays.

TABLE XIII: Physics rates at 1.0×10^{36} cm$^{-2}s^{-1}$.

Process	Rate at $\mathcal{L} = 1 \times 10^{36}$ cm$^{-2}s^{-1}$ (kHz)
$\Upsilon(4S) \to B\bar{B}$	1.1
$udsc$ continuum	3.4
$\tau^+\tau^-$	0.94
$\mu^+\mu^-$	1.16
e^+e^- for $\|\cos\theta_{\mathrm{Lab}}\| < 0.95$	30

At this stage, a single tool cannot fulfill completely both requirements. Therefore the development of the simulation tools moves along parallel paths. A very fast and relatively simple simulation program has been already developed and is operational. It can simulate large amounts of both hadronic and $\tau^+\tau^-$ events while allowing to some extent the modification of the detector configuration. An upgrade schedule has been defined to increase the accuracy of the simulation without sacrificing the speed. More details are provided in the next section.

In parallel, a project is planned where the detailed description of both the detector and the interaction region are done within the Geant4 [1] framework.

Finally, the BABAR simulation and reconstruction packages are being used to perform Super$B$ subdetector optimization studies. Although some aspects of the BABAR simulation make its evolution towards Super$B$ not attractive, there are good reasons why the possibility of exploring it for Super$B$ can continue to be particularly important. Detailed performance evaluations for Super$B$ can in fact be carried out by introducing minor modifications to the BABAR detector. This will represent for a while the main option available to extract the parameters needed as input by the Super$B$ fast simulation. Negotiations with BABAR management are currently underway to extend access to non-BABAR members.

The parametric fast simulation

The simplest fast simulation program we have, named PravdaMC [2], is a very fast Monte Carlo which uses parametrization to simulate the detector response. The radius, thickness and material of the beam pipe is configurable. The tracking system can be modified by changing the number of active layers of the silicon detector, the intrinsic spatial resolutions and the amount of interaction length, as well as the number and dimension of the drift chamber cells and their spatial resolutions. The current tracking algorithm is TRACKERR [3] which starts from the truth Monte Carlo charged particle to produce the track and evaluate the error matrix of its parameters taking into account the energy loss and the multiple scattering. The main limitation is that the trajectory is not modified by the energy loss and therefore it is a perfect helix. This approximation is poor for very low momentum tracks, like soft pions from $D^{*\pm}$.

The response of the electromagnetic calorimeter is analytic. In the current version of the program, the response of the DIRC and IFR to the passage of a charged particle is implemented as an efficiency map of a particle identification algorithm provided externally.

PravdaMC uses the same generators-framework interface as used by the BABAR simulation code. In particular it can generate both hadronic $e^+e^- \to q\bar{q}$ events (including obviously $e^+e^- \to \Upsilon(4S)$) and $e^+e^- \to \tau^+\tau^-$ events. In the latter case it is possible to generate events where the e^- or e^+ beams are polarized, which is a unique and important aspect of the τ physics program at the Super$B$ flavor factory.

Activity is ongoing to develop an improved fast simulation. It uses PravdaMC as a basis but eventually it will become a completely different program. First, TRACKERR is replaced by a more accurate track fitting algorithm based on the BABAR track reconstruction and taking into account all the effects of the interaction between particles and materials. Second, the response of the DIRC, EMC and IFR is simulated through the parametrization of the physics quantities measured by each subsystem and used to perform the analysis of the physics events. Several sources can be used to tune the parametrization of the detectors output: the real data collected by the BABAR detector,

the Geant4 simulation of the *BABAR* detector and the standalone detailed simulation of the Super*B* subsystems.

Readout and analysis of simulated data

The analysis of simulated events requires several specific tools. Composition and vertexing algorithms for the reconstruction of the signal decay trees, the algorithms to determine the flavor and vertex position of the recoil *B*, and an extensive set of utilities for signal/background separation are inherited from the *BABAR* experiment and therefore are mature and fully functional. The output of the simulation with the information of the simulated tracks and neutral clusters together with the reconstructed composite particles are stored in ROOT files [4]. Effort is ongoing to make the existing tools independent of the *BABAR* framework.

Simulation with Geant4

A medium-term plan for the development of a detailed simulation of the Super*B* detector has been defined. The simulation of the machine-induced backgrounds is at present accomplished with a Geant4 application that incorporates a preliminary description of the Super*B* detector volumes. This initial effort of describing the Super*B* detector in Geant4 can represent the basis for the future development of a detailed detector simulation. At present some work is needed to improve the usability and maintainability of the tool for background studies. The most important improvement consists in decoupling the geometry description from the code. The "technology" is available, since using a markup language to allow definition of geometry data in XML format is now implemented in Geant4 through GDML files. Input from the subdetectors is needed to refine the current initial models. When the detailed simulation of the Super*B* detector will be available, it will be used to tune the output of the fast simulation including the effects of the machine backgrounds.

Simulation of tau pair production with polarized beams

The Super*B* project includes the ability to operate with an 85% longitudinally polarized electron beam, which is especially relevant for tau physics studies. For this document, tau pairs produced with polarized beams have been simulated with the KK generator [5] and Tauola [5]. That simulation framework includes all QED effects up to the second order. Tau decays are simulated taking into account spin polarization effects as well., and the complete spin correlations density matrix of the initial-state beams and final state is incorporated in an exact manner.

---

[1] Geant4 Collaboration, Nucl. Instrum. Methods A**506**, 250 (2003).
[2] Originally developed by N. Kuznetsova and A. Ryd for the *BABAR* experiment.
[3] *BABAR* Note 121.
[4] ROOT, An Object-Oriented Data Analysis Framework. http://root.cern.ch/
[5] S. Jadach, B.F.L. Ward, and Z. Was, Comput. Phys. Commun. **130**, 260 (2000), arXiv:hep-ph/9912214.